This is a repository copy of *Search for heavy particles decaying into top-quark pairs using lepton-plus-jets events in proton-proton collisions at root s=13 TeV with the ATLAS detector*.

White Rose Research Online URL for this paper:
http://eprints.whiterose.ac.uk/138005/

Version: Published Version

Article:
Aaboud, M, Aad, G, Abbott, B et al. (2882 more authors) (2018) Search for heavy particles decaying into top-quark pairs using lepton-plus-jets events in proton-proton collisions at root s=13 TeV with the ATLAS detector. European Physical Journal C, 78 (7). 565. ISSN 1434-6044

https://doi.org/10.1140/epjc/s10052-018-5995-6

Reuse
This article is distributed under the terms of the Creative Commons Attribution (CC BY) licence. This licence allows you to distribute, remix, tweak, and build upon the work, even commercially, as long as you credit the authors for the original work. More information and the full terms of the licence here: https://creativecommons.org/licenses/

Takedown
If you consider content in White Rose Research Online to be in breach of UK law, please notify us by emailing eprints@whiterose.ac.uk including the URL of the record and the reason for the withdrawal request.

eprints@whiterose.ac.uk
https://eprints.whiterose.ac.uk/

Eur. Phys. J. C (2018) 78:565
https://doi.org/10.1140/epjc/s10052-018-5995-6

THE EUROPEAN PHYSICAL JOURNAL C

CrossMark

Regular Article - Experimental Physics

Search for heavy particles decaying into top-quark pairs using lepton-plus-jets events in proton–proton collisions at $\sqrt{s} = 13$ TeV with the ATLAS detector

ATLAS Collaboration[⋆]

CERN, 1211 Geneva 23, Switzerland

Received: 1 May 2018 / Accepted: 14 June 2018 / Published online: 9 July 2018
© CERN for the benefit of the ATLAS collaboration 2018

Abstract A search for new heavy particles that decay into top-quark pairs is performed using data collected from proton–proton collisions at a centre-of-mass energy of 13 TeV by the ATLAS detector at the Large Hadron Collider. The integrated luminosity of the data sample is 36.1 fb^{-1}. Events consistent with top-quark pair production are selected by requiring a single isolated charged lepton, missing transverse momentum and jet activity compatible with a hadronic top-quark decay. Jets identified as likely to contain b-hadrons are required to reduce the background from other Standard Model processes. The invariant mass spectrum of the candidate top-quark pairs is examined for local excesses above the background expectation. No significant deviations from the Standard Model predictions are found. Exclusion limits are set on the production cross-section times branching ratio for hypothetical Z' bosons, Kaluza–Kein gluons and Kaluza–Klein gravitons that decay into top-quark pairs.

1 Introduction

This paper presents a search for new particles in the top-quark pair ($t\bar{t}$) final state. The signature is a deviation from the $t\bar{t}$ invariant mass ($m_{t\bar{t}}^{\text{reco}}$) spectrum predicted by the Standard Model (SM). The search uses a data sample with an integrated luminosity of 36.1 fb^{-1} collected by the ATLAS detector from the Large Hadron Collider (LHC) proton–proton collisions at $\sqrt{s} = 13$ TeV in 2015 and 2016. Previous searches for this signature with 8 TeV data at the LHC were performed by the ATLAS [1] and CMS [2] collaborations. The CMS Collaboration also searched in 13 TeV LHC data using a smaller sample of 2.6 fb^{-1} [3].

The analysis selects events consistent with $t\bar{t}$ production followed by subsequent decay into the *lepton-plus-jets* topology. In this topology, most of the top quarks decay into a bottom quark plus a W boson, $t \to Wb$, and one of the W bosons decays into an electron or muon plus a neutrino while the other decays into quarks. If the W boson decays into a τ-lepton and a neutrino, and the τ-lepton subsequently decays into an electron or a muon, and neutrinos, these decays are included in the search. No attempt is made to identify hadronically decaying τ-leptons. Approximately 30% of $t\bar{t}$ pairs decay this way, and the non-$t\bar{t}$ background is much smaller than in the all-hadronic topology. The selection requires a single isolated electron or muon, large missing transverse momentum, and hadronic jets. At least one of the jets must be identified as likely to contain a b-hadron (b-jet).

The $m_{t\bar{t}}^{\text{reco}}$ variable is reconstructed using the jets, charged leptons and missing transverse momentum in the events. The $m_{t\bar{t}}^{\text{reco}}$ distribution is then examined for deviations from the SM predictions. In the absence of significant deviations, upper limits are set on the cross-section for the possible production of new heavy particles that decay into $t\bar{t}$. For comparison with other searches, these limits are transformed to lower limits on the allowed mass within particular *benchmark* models. The sensitivity of the search is tested for new colour-singlet and colour-octet bosons with spin 1 or spin 2 and masses from 0.4 to 5 TeV. The resonance widths for the specific models vary from very narrow (1% of the heavy particle mass) to a value (30% of the heavy particle mass) larger than that of the experimental resolution.

The paper is organised as follows. Details of the potential signals tested in this search are given in Sect. 2. The ATLAS detector is introduced in Sect. 3 and the data samples used for the analysis are described in Sect. 4. The event selection and reconstruction of the $t\bar{t}$ system are described in Sect. 5 and the estimation of background contributions using data is described in Sect. 6. The systematic uncertainties affecting the analysis are detailed in Sect. 7 and the expected background contributions are compared with data in Sect. 8. The results are presented in Sect. 9 and the paper is summarised in Sect. 10.

⋆ e-mail: atlas.publications@cern.ch

2 Signal models tested

The details of potential signals considered in this search are reviewed below. Interference between the signal processes and SM $t\bar{t}$ production is not considered here since these signals are not expected to interfere strongly with the dominant component of the SM $t\bar{t}$ background. The effect of interference is particularly important for new heavy scalar particles produced via gluon–gluon fusion, and was studied by ATLAS using 8 TeV data [4]; such signals are not considered in this search.

2.1 Spin-1 colour singlet

Spin-1 colour singlets that decay into $t\bar{t}$ are predicted in many SM extensions. Three different types of Z' bosons are explored in this study: one arising in topcolor-assisted-technicolor (TC2) models [5,6] and two others arising in simplified models of dark matter [7]. The primary production mode is $q\bar{q}$ annihilation as shown in Fig. 1a.

The TC2 benchmark model chosen for this search produces a Z' boson, denoted Z'_{TC2}. This is a leptophobic boson, with couplings only to first- and third-generation quarks, referred to as Model IV [8]. The properties of the boson are controlled by three parameters: the topcolour tilting parameter, $\cot\theta_{\mathrm{H}}$, which controls the width and the production cross-section, and f_1 and f_2, which are related to the coupling to up-type and down-type quarks, respectively. Here $f_1 = 1$ and $f_2 = 0$, which maximises the fraction of Z'_{TC2} bosons that decay into $t\bar{t}$. The parameter $\cot\theta_{\mathrm{H}}$ is tuned[1] for each mass point such that the resonance has a width of 1% of its mass [9]. Previous searches by the ATLAS [1] and CMS [2,3] collaborations set lower limits of $m(Z'_{\mathrm{TC2}}) > 1.8\,\mathrm{TeV}$ and $m(Z'_{\mathrm{TC2}}) > 2.5\,\mathrm{TeV}$, respectively, on the allowed mass for such bosons. As the detector resolution is not sufficient to resolve the resonance width for the Z'_{TC2} model, limits are also quoted assuming a 3% width. A previous search by the ATLAS Collaboration [1] set a lower limit of $m(Z'_{\mathrm{TC2}}) > 2.3\,\mathrm{TeV}$ on the mass for such bosons.

Interactions between dark matter and normal matter may be mediated by weakly coupled TeV-scale particles. This search considers an axial-vector mediator, $Z'_{\mathrm{DM,ax}}$ and a vector mediator, $Z'_{\mathrm{DM,vec}}$, within a framework of simplified models proposed by the LHC Dark Matter Working group [7]. There are five free parameters for these mediators: the coupling to quarks (g_q), the coupling to leptons (g_ℓ), the coupling to dark matter (g_{DM}), the dark-matter mass (m_{DM}) and the mediator mass. The mediator mass is varied between 0.5 TeV and 5 TeV with the other parameters set to $g_q = 0.25$, $g_\ell = 0$, $g_{\mathrm{DM}} = 1$, and $m_{\mathrm{DM}} = 10\,\mathrm{GeV}$ following the benchmarks A1 and V1 defined in Ref. [7]. The width of $Z'_{\mathrm{DM,ax}}$ and $Z'_{\mathrm{DM,vec}}$ are 5.6% of their masses, with the $Z'_{\mathrm{DM,ax}}$ width kinematically limited to 5.3% at 0.5 TeV.

2.2 Spin-2 colour singlet

Spin-2 colour-singlet bosons are produced in models that postulate extra dimensions of space leading to Kaluza–Klein excitations of the graviton. This search considers a Randall–Sundrum (RS) model with an extra dimension where the SM fields are in the warped bulk and the fermions are localised appropriately to explain the flavour structure of the SM [10–12]. This kind of graviton (G_{KK}) is commonly referred to as a 'Bulk' RS graviton and is characterised by a dimensionless coupling constant $k/\bar{M}_{\mathrm{Pl}} \sim 1$, where k is the curvature of the warped extra dimension and $\bar{M}_{\mathrm{Pl}} = M_{\mathrm{Pl}}/\sqrt{8\pi}$ is the reduced Planck mass. For these gravitons, decays into light fermions are suppressed and the branching ratio to photons is negligible. The primary production mode is gluon–gluon fusion as shown in Fig. 1b. The branching ratios to $t\bar{t}$, WW, ZZ and HH are significant. In this particular model, $k/\bar{M}_{\mathrm{Pl}}$ is chosen to be 1, and the G_{KK} width varies from 3% to 6% in the mass range 0.4–3 TeV. The branching ratio of the G_{KK} decay into a $t\bar{t}$ pair increases rapidly from 18% to 50% for masses between 400 and 600 GeV, plateauing at 68% for masses larger than 1 TeV. The ATLAS Collaboration's search for such gravitons in $\sqrt{s} = 8$ TeV data in the $t\bar{t}$ decay channel set cross-section limits but did not exclude any graviton masses [1], while the search for the same model in the $G_{\mathrm{KK}} \to ZZ$ channel [13] excluded a Bulk RS G_{KK} with mass less than 740 GeV. The CMS Collaboration performed searches in the $G_{\mathrm{KK}} \to ZZ$ and $G_{\mathrm{KK}} \to WW$ decay channels [14,15] excluding such RS gravitons with masses less than 1.3 TeV.

2.3 Spin-1 colour octet

Spin-1 colour-octet bosons are produced in models that postulate extra dimensions of space leading to Kaluza–Klein excitations of the gluon. This search considers heavy Kaluza–Klein gluons, g_{KK}, as produced in RS models with a single warped extra dimension [16,17], with widths varying between 10% and 40% of the g_{KK} mass. The primary production mode in both cases is $q\bar{q}$ annhilation as shown in Fig. 1c. The strong coupling of these gluon excitations to light quarks is set to $g_q = -0.2g_{\mathrm{s}}$, where g_{s} is the SM gluon coupling.[2] The left-handed coupling to the top quark is fixed at $g_{\mathrm{L}^{(t)}} = g_{\mathrm{s}}$, and the right-handed coupling to the top quark, $g_{\mathrm{R}^{(t)}}$, is varied to obtain the desired width. A previous search using $\sqrt{s} = 8$ TeV ATLAS data [18] excludes a similar g_{KK}

[1] There is a one-to-one mapping between $\cot\theta_{\mathrm{H}}$ and the width, given a fixed mass, as shown in Eq. (6) of Ref. [9].

[2] The couplings used here correspond to the configuration mentioned in Eq. (2.3) of Ref. [16].

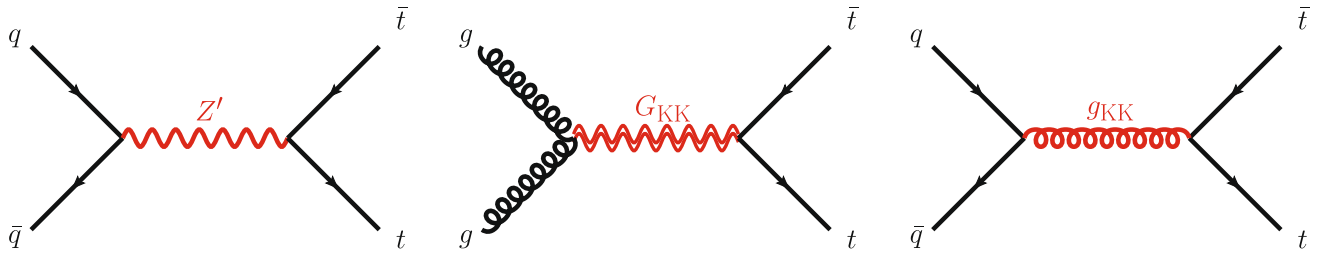

(a) $Z' \to t\bar{t}$ **(b)** $G_{KK} \to t\bar{t}$ **(c)** $g_{KK} \to t\bar{t}$

Fig. 1 Leading-order Feynman diagrams for the signal processes studied in this search. The Z' (**a**) and Kaluza–Klein gluons (g_{KK}) have spin 1 (**b**), while the Kaluza–Klein graviton (G_{KK}) has spin 2 (**c**)

(15% width) with a mass less than 2.2 TeV. The CMS Collaboration searched for similar resonances [3], using a slightly different benchmark model [19]. The CMS choice leads to a natural width of 20% and a larger production cross-section, and, for such a scenario, CMS excludes the existence of g_{KK} with masses less than 3.3 TeV.

3 ATLAS detector

The ATLAS detector [20] at the LHC covers nearly the entire solid angle around the collision point. It consists of an inner tracking detector surrounded by a thin superconducting solenoid, electromagnetic and hadronic calorimeters and a muon spectrometer incorporating three large superconducting toroid magnets.

A high-granularity silicon pixel detector covers the vertex region and typically provides four measurements per track. The innermost layer, known as the insertable B-Layer [21], was added in 2014 and provides high-resolution hits at small radius to improve the tracking performance. The silicon pixel detector is followed by a silicon microstrip tracker that typically provides four measurements from four strip double layers. These silicon detectors are complemented by a transition radiation tracker (TRT), which enables radially extended track reconstruction up to $|\eta| = 2.0$.[3] The TRT also provides electron identification information based on the fraction of hits (typically 30 in total) above a higher energy-deposit threshold corresponding to transition radiation. The inner-detector system (ID) is immersed in a 2 T axial magnetic field and provides charged-particle tracking in the pseudorapidity range $|\eta| < 2.5$.

The calorimeter system covers the pseudorapidity range $|\eta| < 4.9$. Within the region $|\eta| < 3.2$, electromagnetic calorimetry is provided by barrel and endcap high-granularity lead/liquid-argon (LAr) electromagnetic calorimeters, with an additional thin LAr presampler covering $|\eta| < 1.8$ to correct for energy loss in material upstream of the calorimeters. Hadronic calorimetry is provided by a steel/scintillator-tile calorimeter, segmented into three barrel structures within $|\eta| < 1.7$, and two copper/LAr hadronic endcap calorimeters. The solid angle coverage is completed with forward copper/LAr and tungsten/LAr calorimeter modules optimised for electromagnetic and hadronic measurements, respectively.

The muon spectrometer comprises separate trigger and high-precision tracking chambers measuring the deflection of muons in a magnetic field generated by superconducting air-core toroids. The precision chamber system covers the region $|\eta| < 2.7$ with three layers of monitored drift tubes, complemented by cathode strip chambers in the forward region, where the background is highest. The muon trigger system covers the range $|\eta| < 2.4$ with resistive plate chambers in the barrel and thin gap chambers in the endcap regions.

A two-level trigger system [22,23] is used to select interesting events. The first level of the trigger is implemented in hardware and uses a subset of detector information to reduce the event rate to a design value of at most 100 kHz. This is followed by a software-based trigger that reduces the event rate to a maximum of around 1 kHz for offline storage.

4 Data and Monte Carlo samples

This search is performed using data from $\sqrt{s} = 13$ TeV proton–proton collisions recorded by the ATLAS detector in 2015 and 2016. Only data recorded during stable beam conditions and with all relevant subdetector systems opera-

[3] ATLAS uses a right-handed coordinate system with its origin at the nominal interaction point (IP) in the centre of the detector and the z-axis along the beam pipe. The x-axis points from the IP to the centre of the LHC ring, and the y-axis points upwards. Cylindrical coordinates (r, ϕ) are used in the transverse plane, ϕ being the azimuthal angle around the z-axis. The pseudorapidity is defined in terms of the polar angle θ as $\eta = -\ln\tan(\theta/2)$. Angular distance is measured in units of $\Delta R \equiv \sqrt{(\Delta\eta)^2 + (\Delta\phi)^2}$.

tional are used. The integrated luminosity of the data sample is 36.1 fb^{-1}. Lepton-plus-jets events were collected using single-electron and single-muon triggers.

The SM background processes are, in order of decreasing importance: the production of $t\bar{t}$, a W or Z boson in association with additional jets (W/Z + jets), a single top quark, multi-jets and dibosons. Simulated Monte Carlo (MC) data samples are used for signal processes, as well as for background processes that produce jets and prompt leptons. The MC samples are used to optimise the event selection, provide SM background estimates, and evaluate signal efficiencies. The multi-jet background is evaluated directly from data as described in Sect. 6.

For the generation of SM $t\bar{t}$ events [24] and single-top-quark events in the Wt- [25] and s-channels [26], the POWHEG v2 [27–29] generator with the CT10 [30,31] parton distribution function (PDF) set was used. The overlap between $t\bar{t}$ and Wt production was treated within the diagram removal (DR) scheme [32]. Electroweak t-channel single-top-quark events were generated using POWHEG-BOX v1 [33]. This generator uses the four-flavour scheme for the next-to-leading-order (NLO) matrix element calculations together with the four-flavour PDF set CT10f4. For this process, the top-quark decays were simulated using MADSPIN [34], preserving all spin correlations. For all SM top-quark processes the parton shower, fragmentation and the underlying event were simulated using PYTHIA v6.428 [35] with the CTEQ6L1 [36] PDF set and the corresponding Perugia 2012 (P2012) set of tuned parameters [37]. The top quark's mass was set to 172.5 GeV. The EVTGEN v1.2.0 program [38] was used to model the decays of heavy-flavour hadrons. For the generation of $t\bar{t}$ events, the h_{damp} parameter, which controls the transverse momentum of the first additional emission beyond the Born configuration, was set to the mass of the top quark. The main effect of this parameter is to regulate the high transverse momentum emission against which the $t\bar{t}$ system recoils. The top-quark kinematics in all SM $t\bar{t}$ samples were corrected to account for higher-order electroweak (EW) effects [39]. This correction to the generated samples was made by applying a weight that depends on the flavour and energy of the initial partons in the centre-of-mass frame, and on the decay angle of the top quarks in the same frame. The value of the correction factor decreases with the invariant mass of the $t\bar{t}$ system from 0.98 at a mass of 0.4 TeV to 0.87 at a mass of 3.5 TeV.

Samples of W/Z + jets events were simulated using the SHERPA 2.2.1 [40] generator. Matrix elements were calculated for up to two partons at NLO in QCD and four partons at leading order (LO) using the COMIX [41] and OPENLOOPS [42] matrix element generators and merged with the SHERPA parton shower [43] using the ME+PS@NLO prescription [44]. The NNPDF3.0 NLO PDF set [45] was used in conjunction with dedicated parton shower tuning developed by the authors of SHERPA. The W/Z + jets events were normalised to the next-to-next-to-leading-order (NNLO) cross-sections [46].

Diboson (WW, WZ, ZZ) production processes with four charged leptons (4ℓ), three charged leptons and one neutrino ($3\ell+\nu$), two charged leptons and two neutrinos ($2\ell+2\nu$), or one charged lepton and one neutrino plus jets ($\ell\nu q\bar{q}'$) were simulated using the SHERPA 2.1.1 generator. The matrix elements contain all diagrams with four EW vertices. They were calculated for zero ($3\ell+\nu$, $\ell\nu q\bar{q}'$) or up to one (4ℓ, $2\ell+2\nu$) additional partons at NLO in QCD and up to three partons at LO using the COMIX and OPENLOOPS matrix element generators and were merged with the SHERPA parton shower using the ME+PS@NLO prescription. The CT10 PDF set was used with the dedicated parton shower tuning developed by the SHERPA authors. The cross-sections from the generator were used for sample normalisation.

Production of a new spin-1 colour-singlet particle that decays into $t\bar{t}$ was modelled using the $Z' \rightarrow t\bar{t}$ process from PYTHIA v8.165 [47] with the NNPDF2.3 LO [48] PDF set and the A14 [49] set of tuned parameters. This search uses topcolour-assisted technicolour Z'_{TC2} [6,8,9] as a benchmark. To account for higher-order contributions to the cross-section, the samples were normalised to cross-section calculations performed at NLO in QCD [50] using the PDF4LHC2015 PDF set [51]. The same sample, reweighted to have the appropriate resonance width as simulated in MADGRAPH5_aMC@NLO [52], was used to model $Z'_{\text{DM,ax}}$ and $Z'_{\text{DM,vec}}$ with the cross-sections normalised to LO QCD calculations using the NNPDF2.3 LO PDF set. No corrections for higher-order EW effects were applied to these signal samples.

Production of a spin-1 colour-octet particle that decays into $t\bar{t}$ was modelled using the $g_{\text{KK}} \rightarrow t\bar{t}$ process from PYTHIA 8.165 at leading order with the NNPDF2.3 LO PDF set and the A14 set of tuned parameters.

The case of a spin-2 colour-singlet signal was modelled using MADGRAPH5_aMC@NLO with the NNPDF2.3 LO PDF set, with parton showering performed by PYTHIA v8.165 with the A14 set of tuned parameters.

The MC samples were processed through the full ATLAS detector simulation [53] based on GEANT 4 [54] or through a faster simulation making use of parameterised showers in the calorimeters [55]. The $t\bar{t}$ parton shower uncertainty is estimated using samples passed through the ATLAS fast simulation. Additional simulated proton–proton collisions generated using PYTHIA v8.165 with the A2 set of tuned parameters [56] and the MSTW2008LO PDF set [57] were overlaid to simulate the effects of additional collisions from the same and nearby bunch crossings (pile-up). All simulated events were then processed using the same reconstruction algorithms and analysis chain as used for real data.

5 Event selection and $t\bar{t}$ reconstruction

This section describes the selection of events containing a single charged lepton, hadronic jets, and large missing transverse momentum. The construction of an observable that approximates the mass of the $t\bar{t}$ system and the categorisation of the events are also described.

5.1 Event selection

The event selection criteria are applied to the following physics objects:

Hadronic jets defined in three different ways are used in this analysis.

Small-R jets are built from three-dimensional topological clusters [58] of energy in the calorimeters, calibrated at the electromagnetic (EM) energy scale, using the anti-k_t algorithm [59] with a radius parameter $R = 0.4$. The jet energy is calibrated using a correction that relates the reconstructed jet energy to the true jet energy when reconstructed from stable particles with a lifetime of at least 30 ps (excluding muons and neutrinos) [60]. The correction depends on the transverse momentum and pseudorapidity of each jet, and accounts for pile-up effects [61]. They are required to have transverse momentum, p_{T}, greater than 25 GeV and $|\eta| < 2.5$. For jets with $p_{\mathrm{T}} < 60$ GeV and $|\eta| < 2.4$, a jet-vertex-tagger requirement corresponding to a 92% efficiency while rejecting 98% of jets from pile-up and noise is imposed [62].

Large-R jets are built from three-dimensional topological clusters of energy in the calorimeters, calibrated with the local cluster weighting (LCW) procedure [63], using the anti-k_t algorithm with a radius parameter $R = 1.0$. In the LCW calibration procedure, corrections for the non-compensating response of the calorimeter and for the energy lost in dead material and from out-of-cluster leakage are applied to the cluster energy before applying the jet algorithm. These corrections are obtained from simulations of charged and neutral particles. These jets are further *trimmed* [64], which mitigates the effects of pile-up [65]. In trimming, the constituents of a jet are reclustered into subjets according to the k_t algorithm [66–68] with a radius parameter R_{sub}. Subjets with a transverse momentum smaller than a fraction f_{cut} of the parent jet's transverse momentum are then discarded. The surviving subjets are recombined to produce the final trimmed jet. Based on a study of sensitivity to pile-up, the trimming parameters used are $R_{\mathrm{sub}} = 0.2$ and $f_{\mathrm{cut}} = 0.05$ [69]. The jets are calibrated using corrections that relate the reconstructed jet to its true jet when clustered from stable particles with a lifetime of at least 30 ps (excluding muons and neutrinos) [60,70]. The resultant jets are required to have $p_{\mathrm{T}} > 300$ GeV and $|\eta| < 2.0$. Large-R jets consistent with the decay products of a hadronically decaying top quark are identified (*top-tagged*) using an algorithm [71] based on the invariant mass of the jet and the N-subjettiness ratio τ_{32} [72,73]. This algorithm has an efficiency of approximately 80% for selecting top-quark jets with $p_{\mathrm{T}} > 300$ GeV and $|\eta| < 2.0$ in simulated SM $t\bar{t}$ events.

Track-jets are built from charged-particle tracks using the anti-k_t algorithm with a radius parameter $R = 0.2$. These jets are required to have $p_{\mathrm{T}} > 10$ GeV and $|\eta| < 2.5$ and at least two constituent charged-particle tracks. The charged-particle tracks used to build the jets must themselves have $p_{\mathrm{T}} > 0.4$ GeV and $|\eta| < 2.5$, and pass quality requirements that test the number of hits used to reconstruct the track and the matching to the primary vertex [74]. Track-jets consistent with including the decay products of a b-hadron are identified (*b-tagged*) using the MV2c20 algorithm [75]. The b-tagging working point chosen has approximately 70% efficiency for such jets to contain a b-hadron in simulated SM $t\bar{t}$ events. The track-jets are used in this analysis for the identification of the b-tagged small-R calorimeter-measured jets. Small-R calorimeter-measured jets, j_{calo}, are identified as b-jets if a track-jet that passes the b-tagging selection, j_{track}, satisfies the $\Delta R(j_{\mathrm{calo}}, j_{\mathrm{track}}) < 0.4$ requirement.

The anti-k_t and k_t algorithms are applied through their implementation in FastJet [76,77].

Muon candidates are reconstructed by combining tracks found in the ID with tracks found in the muon spectrometer that satisfy $p_{\mathrm{T}} > 25$ GeV and $|\eta| < 2.5$. Muons are required to be isolated using the requirement that the sum of the p_{T} of the tracks in a variable-size cone around the muon direction (excluding the track identified as the muon) be less than 6% of the transverse momentum of the muon. The track isolation cone size is given by the minimum of $\Delta R = 10\ \mathrm{GeV}/p_{\mathrm{T}}^{\mu}$ and $\Delta R = 0.3$, where p_{T}^{μ} is the muon p_{T}. Thus, the cone radius increases with decreasing p_{T} up to a maximum of 0.3. To reduce the background contributions due to muons from heavy-flavour decays inside jets, muons are removed if they are separated from the nearest jet by $\Delta R < 0.04 + 10\ \mathrm{GeV}/p_{\mathrm{T}}^{\mu}$. However, if the jet has fewer than three associated tracks, the muon is kept and the jet is removed instead; this avoids an inefficiency for high-

energy muons undergoing significant energy loss in the calorimeter.

Electron candidates are reconstructed from an isolated energy deposit in the electromagnetic calorimeter matched to an ID track, within the fiducial region of transverse energy $E_{\mathrm{T}} > 25$ GeV and $|\eta| < 2.47$. Candidates within the transition region between the barrel and endcap electromagnetic calorimeters, $1.37 < |\eta| < 1.52$, are removed. A tight likelihood-based requirement [78] is used to further suppress the background from multi-jet production. Electrons are also required to be isolated, using the same track-based variable as for muons, except that the maximum ΔR in this case is 0.2. Electrons sharing the same track with a muon candidate are assumed to be bremsstrahlung photon and are rejected as electron candidates. To prevent double-counting of electron energy deposits as jets, the closest small-R jet within $\Delta R = 0.2$ of a reconstructed electron is removed. Finally, if the nearest small-R jet surviving this selection is within $\Delta R = 0.4$ of the electron, the electron is discarded, to ensure it is sufficiently separated from nearby jet activity. This procedure is referred to as "overlap removal".

The **Missing transverse momentum**, $E_{\mathrm{T}}^{\mathrm{miss}}$, is defined as the magnitude of $\overrightarrow{E}_{T}^{\mathrm{miss}}$, which is the negative of the total vector sum p_{T} of all selected physics objects (electrons, muons, small-R jets) as well as specific 'soft terms' considering tracks that do not match the selected physics objects. In this way, the missing transverse momentum is adjusted to take into account the best calibration of the identified physics objects [79].

In addition:

The **primary vertex** is defined as the vertex with the highest sum of squared transverse momentum of the tracks associated with it.

Following the initial selection by the triggers described in Sect. 4, the event selection proceeds with the following steps:

1. **Event cleaning requirement:** Events are required to have been recorded when all subsystems of the ATLAS detector were working acceptably. Events are also required to have at least two tracks associated with the primary vertex.
2. **Charged-lepton selection:** Exactly one charged-lepton candidate (electron or muon) is required with a minimum p_{T} of 30 GeV. The lepton candidates must geometrically match the candidate that triggered the event. Events containing a second charged lepton with a transverse momentum larger than 25 GeV are rejected.
3. **Leptonic-W selection:** The event is required to have a charged lepton and missing transverse momentum consistent with the leptonic decay of a W boson. This is achieved by requiring that the event satisfies two criteria. Firstly, the $E_{\mathrm{T}}^{\mathrm{miss}}$ is required to be greater than 20 GeV. Secondly, the transverse mass of the selected lepton, ℓ, and $\mathbf{E}_{\mathrm{T}}^{\mathrm{miss}}$, $m_{\mathrm{T}}^{W} = \sqrt{2p_{\mathrm{T}}^{\ell}E_{\mathrm{T}}^{\mathrm{miss}}(1-\cos\Delta\phi(\ell,\mathbf{E}_{\mathrm{T}}^{\mathrm{miss}}))}$, is required to satisfy $E_{\mathrm{T}}^{\mathrm{miss}} + m_{\mathrm{T}}^{W} > 60$ GeV.
4. **b-tagging:** The event is required to contain at least one b-tagged track-jet. The b-tagged track-jets are used to categorise the accepted events into several channels. More information about this is given at the end of this section.
5. **Classification into Boosted or Resolved selection:** Based on the hadronic activity, the event is classified as *Boosted* or *Resolved* as described below.

An event passes the boosted selection if it meets the following criteria:

1. **Leptonic-top b-jet:** Events are required to contain at least one small-R jet with $\Delta R(\text{jet, lepton}) < 1.5$. If multiple jets satisfy this condition, the one with the highest p_{T} is chosen and subsequently referred to as the *selected jet*, j_{sel}. This is identified with the expected b-jet from the leptonic top-quark decay, although no b-tagging requirement is enforced on it. This definition is found to yield better resolution for the invariant mass of the $t\bar{t}$ system than others based on b-tagging or information about the top-quark candidate's mass.
2. **Hadronic-top jet:** Events are required to contain at least one large-R jet, j_{top}, passing the top-tagging requirements. The jet is further required to be well separated from the leptonically decaying top quark by requiring differences in azimuthal angle between it and the charged lepton $\Delta\phi(j_{\mathrm{top}}, \text{lepton}) > 2.3$ and $\Delta R(j_{\mathrm{top}}, j_{\mathrm{sel}}) > 1.5$. The highest-$p_{\mathrm{T}}$ jet passing all of these requirements is referred to as the hadronic-top jet.

Events that fail any of these boosted selection requirements are classified as passing the resolved selection if there are at least four small-R jets with $p_{\mathrm{T}} > 25$ GeV and if the χ^2 algorithm for reconstructing the $t\bar{t}$ system (described in Sect. 5.2) yields a value of $\log_{10}(\chi^2) < 0.9$. This selection requirement has been found to effectively reject $t\bar{t}$ events not correctly reconstructed and a fair fraction of the other background, while improving the actual resolution on the ttbar mass system.

The acceptance times efficiency ($A \times \epsilon$) including the branching ratio for simulated beyond-the-SM (BSM) particles decaying into $t\bar{t}$ is given in Fig. 2. For reference, the branching ratio for $t\bar{t}$ to electron- or muon-plus-jets is about 17% for each lepton flavour, taking into account leptonic

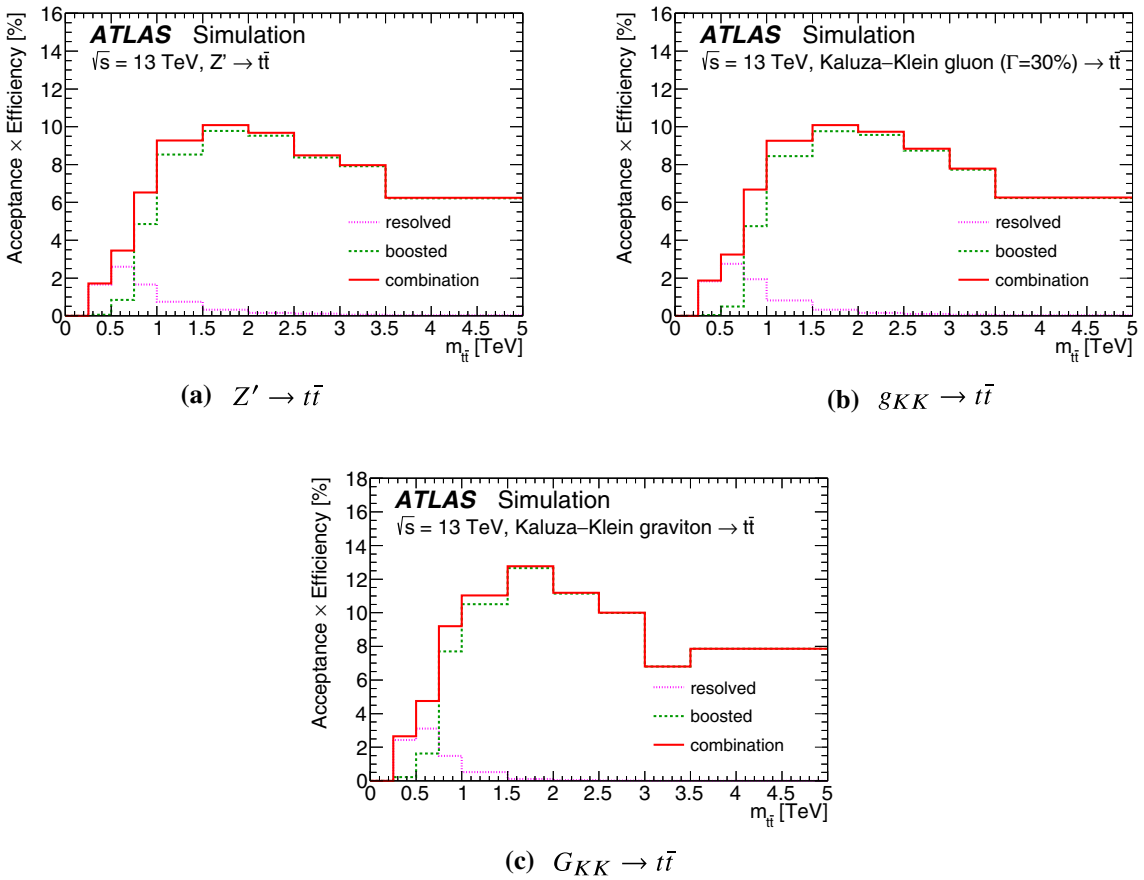

Fig. 2 Acceptance times efficiency ($A \times \epsilon$), including the branching ratio for MC simulated BSM particles decaying into $t\bar{t}$, as a function of the $t\bar{t}$ invariant mass $m_{t\bar{t}}$ (computed before parton radiation) for simulated signal events. The signal samples shown here include events from generated masses ranging from 0.4 to 5 TeV. All $t\bar{t}$ decay modes are simulated. The e and μ channel efficiencies are combined

τ-lepton decays [80]. There are efficiency losses from the large-R jet requirements and the b-tagging requirement, as well as the four-jet and χ^2 kinematic fit requirement in the resolved channel. The value of $A \times \epsilon$ is smaller for e+jets events than μ+jets for resonance masses above 1.5 TeV, due to the inefficiency of the electron identification and overlap removal in an environment with highly boosted top quarks. For the Z' and g_{KK} signals, the $A \times \epsilon$ values are very similar to each other, whereas the total G_{KK} $A \times \epsilon$ is about two percentage points higher than the other signals for masses greater than 0.8 TeV, because the G_{KK} produces top quarks that are more central than those produced by g_{KK}.

5.2 Mass reconstruction and event categorisation

Following the event selection, an observable $m_{t\bar{t}}^{\mathrm{reco}}$ is constructed from the physics objects described above to approximate the invariant mass of the $t\bar{t}$ system. The construction of the variable in the boosted and resolved selections uses different physics objects.

For events passing the boosted selection, the four-momentum of the hadronic-top jet is used for the *hadronic-top candidate*. The *leptonic-top candidate* is constructed by summing the four-momenta of the charged lepton, the neutrino candidate, and j_{sel}. The neutrino candidate's transverse momentum is taken equal to $\overrightarrow{E}_T^{\mathrm{miss}}$. The z component of its momentum, p_z, is estimated by assuming that the neutrino and the lepton come from an on-shell W boson decay and imposing a W mass constraint on the neutrino–lepton system [1]. If no real solution is found for the neutrino's p_z, it is assumed that a mismeasurement of the $\overrightarrow{E}_T^{\mathrm{miss}}$ leads to this effect, in which case the $\overrightarrow{E}_T^{\mathrm{miss}}$ is rescaled and rotated by the minimal amount until a real solution is found. If more than one solution is available, the solution with smallest absolute value of the neutrino's p_z is taken. The value of $m_{t\bar{t}}^{\mathrm{reco}}$ is then the mass of the summed four-momenta of the leptonic- and hadronic-top candidates.

For events passing the resolved selection, following the approach of previous ATLAS searches [1], a χ^2 algorithm is employed to find the best assignment of jets to the leptonic-

top candidate and hadronic-top candidate. Using the four-momenta of the neutrino, lepton, and all small-R jets in the event, a χ^2 is defined using the expected top-quark and W boson masses:

$$\chi^2 = \left[\frac{m_{jj} - m_{W_\mathrm{h}}}{\sigma_{W_\mathrm{h}}}\right]^2 + \left[\frac{m_{jjb} - m_{jj} - m_{t_\mathrm{h}-W_\mathrm{h}}}{\sigma_{t_\mathrm{h}-W_\mathrm{h}}}\right]^2 + \left[\frac{m_{b\ell\nu} - m_{t_\ell}}{\sigma_{t_\ell}}\right]^2 + \left[\frac{(p_{\mathrm{T},jjb} - p_{\mathrm{T},b\ell\nu}) - (p_{\mathrm{T},t_\mathrm{h}} - p_{\mathrm{T},t_\ell})}{\sigma_{p_{\mathrm{T},t_\mathrm{h}}-p_{\mathrm{T},t_\ell}}}\right]^2.$$

The first term is a constraint using the mass of the hadronically decaying W boson. The second term is a constraint using the mass difference between the hadronically decaying top quark and the hadronically decaying W boson. Since the mass of the hadronically decaying W boson, m_{jj}, and the mass of the hadronically decaying top quark, m_{jjb}, are highly correlated, the mass of the hadronically decaying W boson is subtracted from the second term to decouple it from the first term. The third term is a constraint using the mass of the semileptonically decaying top quark. The last term arises as a constraint on the expected transverse momentum balance between the two decaying top quarks. In the χ^2 definition above, t_h and t_ℓ refer to the hadronically and semileptonically decaying top quarks. Only arrangements in which b-quarks are assigned to b-tagged jets are considered.[4] The values of the χ^2 central-value parameters m_{W_h}, $m_{t_\mathrm{h}-W_\mathrm{h}}$, m_{t_ℓ}, and $p_{\mathrm{T},t_\mathrm{h}} - p_{\mathrm{T},t_\ell}$, and the values of the width parameters σ_{W_h}, $\sigma_{t_\mathrm{h}-W_\mathrm{h}}$, σ_{t_ℓ}, and $\sigma_{p_{\mathrm{T},t_\mathrm{h}}-p_{\mathrm{T},t_\ell}}$ are obtained from Gaussian fits to the distributions of relevant reconstructed variables, using MC events for which the reconstructed objects are matched to partons, from Z' samples with masses from 0.5 to 2.0 TeV. As in the case of the boosted reconstruction, the neutrino candidate's transverse momentum is taken to be the $\overrightarrow{E}_T^{\mathrm{miss}}$ and the neutrino z component is estimated by assuming that the neutrino and the lepton come from an on-shell W boson decay. All possible neutrino p_z solutions and jet permutations are considered, and the one with the lowest χ^2 value is selected. The $m_{t\bar{t}}^{\mathrm{reco}}$ observable is estimated as the mass of the four-momentum obtained by summing the four-momenta of the objects that minimise the χ^2 value.

The resulting $m_{t\bar{t}}^{\mathrm{reco}}$ distributions for several signal masses are shown in Fig. 3. For this figure, all events satisfying the selection criteria are used. The low-mass tails arise from two effects: first, the $t\bar{t}$ system may emit radiation that is not included in the reconstruction, thus shifting $m_{t\bar{t}}^{\mathrm{reco}}$ to lower values; second, before reconstruction the Breit–Wigner signal shape in $m_{t\bar{t}}$ has a tail at lower values due to the steep fall in parton luminosity with increasing partonic centre-of-mass energy. The former is particularly true for high-mass resonances, such as the benchmark processes used in this analysis, while the latter has a larger effect on broad resonances. Figure 3a–c show the $m_{t\bar{t}}^{\mathrm{reco}}$ distributions in the resolved channel before and after the requirement that the events fail the boosted selection ('boosted channel-veto') is imposed.

Following this reconstruction, events are placed into one of four b-tagging categories:

Category 0: there is no b-tagged jet matching the hadronic- nor leptonic-top candidates
Category 1: only the leptonic-top candidate has a matching b-tagged jet
Category 2: only the hadronic-top candidate has a matching b-tagged jet
Category 3: the hadronic-top candidate and the leptonic-top candidate both have a matching b-tagged jet.

The matching requirement for the leptonic top candidate in the boosted channel is that at least one b-tagged track-jet must be within $\Delta R = 0.4$ of the small-R jet used for the leptonic top candidate reconstruction. The criterion used to reconstruct the hadronic top candidate is that at least one b-tagged track-jet is within $\Delta R = 1.0$ of the large-R jet used to reconstruct the hadronic top candidate. In the resolved channel, this matching must be to one small-R jet assigned as a b-quark jet by the χ^2 algorithm. Events in Category 0 are rejected.

6 Estimation of background contributions using data

SM $t\bar{t}$ production is the dominant source of background, followed by W+jets and multi-jet production. The SM $t\bar{t}$ background is estimated using MC samples and fixed-order theory calculations as described in Sect. 4. The background contributions from multi-jet and W+jets production are estimated using data, as described in this section.

6.1 Multi-jet background

The multi-jet background consists mainly of events that have a jet that is misreconstructed as a lepton. The normalisation, kinematic distributions, and statistical and systematic uncertainties associated with the multi-jet background are estimated from data using a technique known as a *matrix method*. The particular matrix method used in this search is a variation of the one used in the previous ATLAS $t\bar{t}$ resonance searches analyses described in detail in Ref. [81].

[4] If there is only one b-tagged jet in the event, then only arrangements in which it is assigned to a b-quark in the χ^2 kinematic fit are considered and one of the top quark candidates is allowed not to have a b-quark candidate associated with it.

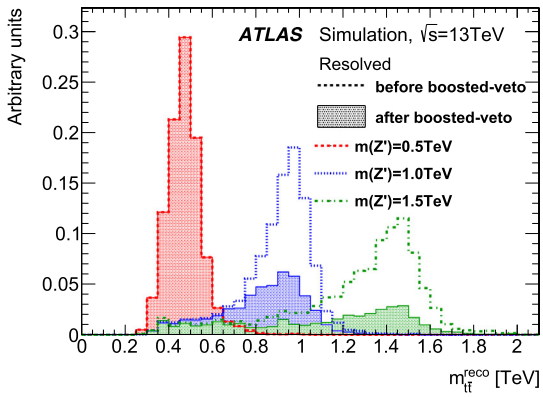

(a) $Z' \to t\bar{t}$, resolved selection

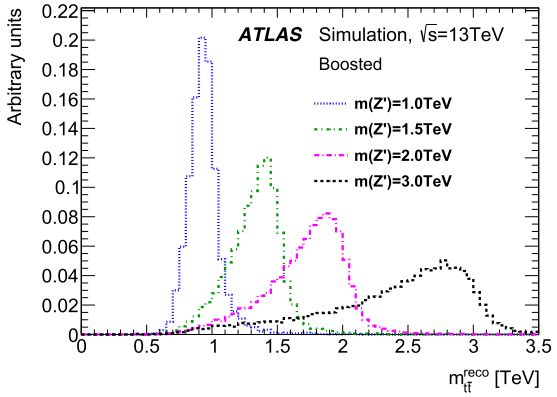

(b) $Z' \to t\bar{t}$, boosted selection

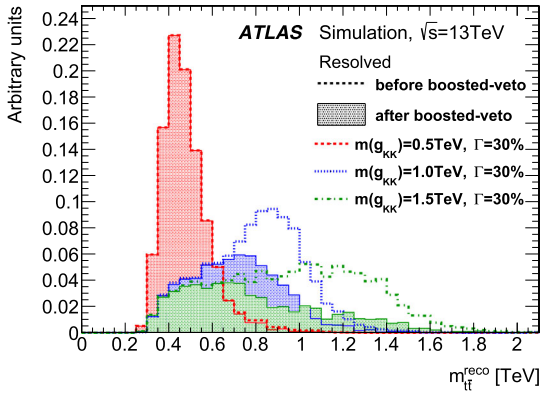

(c) g_{KK}, resolved selection

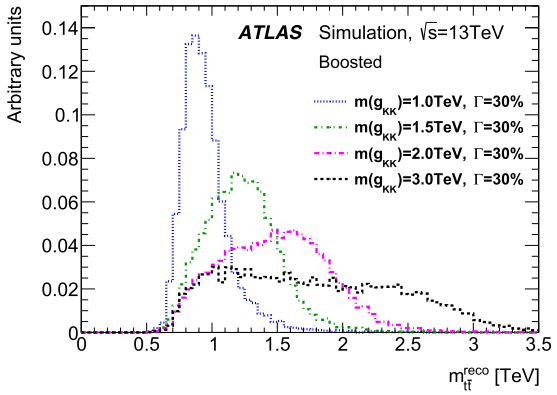

(d) g_{KK}, boosted selection

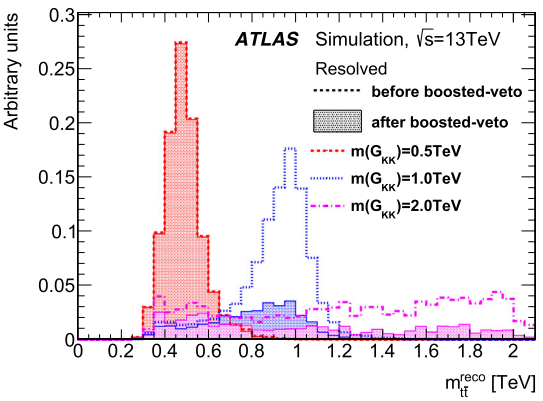

(e) G_{KK}, resolved selection

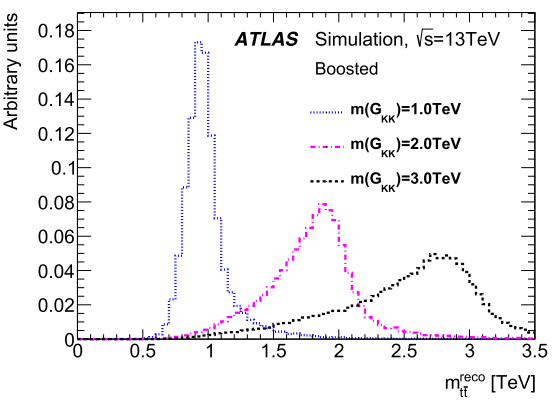

(f) G_{KK}, boosted selection

Fig. 3 Reconstructed top-quark pairs invariant mass, $m_{t\bar{t}}^{\mathrm{reco}}$, for simulated signal events satisfying the selection criteria. The Z' in the simulated samples used here has a width of 3% of its mass. The g_{KK} shown here has a width of 30% of its mass and the width of the G_{KK} width varies between 3 and 6% of its mass. The figure shows the distribution including events that may satisfy both the boosted and resolved selections in the line marked as "before boosted-veto". The line marked as "after boosted-veto" excludes events which satisfy both the boosted and resolved selections from the resolved selection

The matrix method uses lepton misidentification probabilities and lepton identification efficiencies to estimate the multi-jet background. The efficiency f, which is also referred to as the 'fake rate', is defined as the probability that a jet from multi-jet production that satisfies a looser set of lepton identification criteria, in particular without an isolation

requirement, also satisfies the tight lepton identification criteria. It is estimated from a control region with the same selection as the resolved signal, but with the missing transverse momentum and transverse mass requirements inverted. In this control region, which is enriched in multi-jet events, the subtraction of prompt-lepton contributions is based on MC simulation. The efficiency ϵ is defined as the probability that a prompt lepton (from a W or Z boson) that satisfies the loose lepton identification criteria also satisfies the tight identification criteria. It is determined using SM $t\bar{t}$ MC samples, corrected using comparisons of MC and data $Z \to \ell\ell$ events.

The number of multi-jet background events satisfying the selection criteria is estimated using data events that satisfy all criteria, except that the loose lepton identification criteria are used.

The number of events with leptons satisfying the loose identification criteria, N_{L}, is defined as

$$N_{\mathrm{L}} = N_{\text{prompt}} + N_{\text{multi-jet}}$$

where N_{prompt} and $N_{\text{multi-jet}}$ are the numbers of events satisfying those criteria with prompt leptons and with leptons from other sources, respectively. The number of events satisfying the tight identification criteria, N_{T}, is then

$$N_{\mathrm{T}} = \epsilon \times N_{\text{prompt}} + f \times N_{\text{multi-jet}}.$$

Solving these two equations for N_{prompt} and $N_{\text{multi-jet}}$ gives the multi-jet contribution from events satisfying all the selection criteria. A large uncertainty is associated with this background, which was obtained by testing its modelling in a validation region, as described below.

Good modelling of the shape of kinematic distributions is achieved by parameterising the efficiencies as functions of relevant kinematic variables. For electrons, the efficiencies are parameterised as a two-dimensional function of the transverse momentum of the lepton and a calorimeter-based isolation variable. For muons, in addition to the transverse momentum and the calorimeter-based isolation variable, the angular separation between the lepton and the closest jet is also used. The modelling is validated in separate dedicated validation regions, where only one of the $E_{\mathrm{T}}^{\text{miss}}$ cut or the $E_{\mathrm{T}}^{\text{miss}} + m_{\mathrm{T}}^{W}$ cut is inverted. Such validation regions contain a more similar mixture of contributions to the signal region samples' contributions, but still have an enhanced multi-jet contribution.

The fake rates for electrons vary from 18 to 92%, with the largest values occurring at high lepton p_{T}, with low nearby calorimeter activity. This behaviour is explained by the track-based lepton isolation criterion that uses a p_{T}-dependent cone and leads to a looser isolation requirement at higher p_{T}. The fake rates for muons vary from 4 to 94%, with the largest values occurring in conditions similar to the electron case. Such variations are parameterised, as mentioned previously, using the lepton transverse momentum, the ΔR between the lepton and the closest jet, as well as a calorimeter-based isolation requirement around the lepton.

6.2 W+jets background

For the W+jets background, data are used to derive scale factors that are applied to correct the normalisation given by SHERPA MC simulations of this background for possible mismodelling of the cross-section times acceptance. Furthermore, the data are used to correct the fractions of the different quark-flavour components of the W+jets background. The procedure used is implemented separately for the electron and muon channels, as the different lepton selections can lead to differences between the correction factors.

The scale factors that correct the normalisation are determined by comparing the measured W boson charge asymmetry in data [82,83] with that predicted by the simulation. A relaxed set of selection criteria that does not include a b-tagging requirement is used, so that the W+jets purity of the control region is increased, while also reducing the statistical uncertainty in the scale factors used for this procedure. Any bias induced by relaxing the selection criteria is found to be negligible compared to the statistical uncertainty in the scale factor determination. The total number of W+jets events in data, $N_{W^+} + N_{W^-}$, is given by:

$$N_{W^+} + N_{W^-} = \left(\frac{r_{\mathrm{MC}} + 1}{r_{\mathrm{MC}} - 1}\right)(D_{\mathrm{corr}+} - D_{\mathrm{corr}-}), \tag{1}$$

where r_{MC} is the ratio given by MC simulation of the number of W+jets events with a positively charged lepton to that with a negatively charged lepton and $D_{\mathrm{corr}+(-)}$ is the number of observed events with a positively (negatively) charged lepton. Contributions to $D_{\mathrm{corr}+(-)}$ from charge-asymmetric processes such as single top, WZ and $t\bar{t}$+W production are estimated from MC simulation and are subtracted. Contributions from charge-symmetric processes such as $t\bar{t}$ production cancel out in the difference on the right-hand side of Eq. (1). A scale factor, C_{A}, applied to the MC simulated samples of W + jets events, is then calculated as the ratio of $N_{W^+} + N_{W^-}$ evaluated from data to that predicted from MC simulation. This evaluation is performed separately for four jet multiplicity bins; $n_{\text{jet}} = 2$, $n_{\text{jet}} = 3$, $n_{\text{jet}} = 4$, and $n_{\text{jet}} \geq 5$.

The flavour fractions $f_{\text{flavour}} = N_{\mathrm{MC},W}^{\text{flavour}} / N_{\mathrm{MC},W}$ are extracted from a W+jets-dominated control region. This control region is selected using criteria identical to the signal event selection except for requirements on the hadronic jet activity: exactly two small-R jets are required. Based on the lepton charge distribution of events with at least one b-tagged

jet, scale factors are derived for the flavour components $W_{b\bar{b}}$, $W_{c\bar{c}}$, W_c, and W_{light}[5] by solving a system of linear equations:

$$\begin{pmatrix} C_A \cdot (N^{bb}_{\text{MC},W^-} + N^{cc}_{\text{MC},W^-}) & C_A \cdot N^{c}_{\text{MC},W^-} & C_A \cdot N^{\text{light}}_{\text{MC},W^-} & N_{Q^-} \\ (f_{bb} + f_{cc}) & f_c & f_{\text{light}} & 0 \\ 0 & 1 & 0 & 0 \\ C_A \cdot (N^{bb}_{\text{MC},W^+} + N^{cc}_{\text{MC},W^+}) & C_A \cdot N^{c}_{\text{MC},W^+} & C_A \cdot N^{\text{light}}_{\text{MC},W^+} & N_{Q^+} \end{pmatrix} \cdot \begin{pmatrix} K_{bb,cc} \\ K_c \\ K_{\text{light}} \\ K_Q \end{pmatrix} = \begin{pmatrix} D_{W^-} + N_{Q^-} \\ 1.0 \\ 1.0 \\ D_{W^+} + N_{Q^+} \end{pmatrix}$$

where $D_{W^\pm}$ is the expected number of W+jets events with a positively or negatively charged lepton in data after subtracting all non-W+jets MC background contributions and each K_{flavour} is a correction factor extracted by this procedure. The $K_{bb,cc}$ factor refers to both the $W+bb$ and $W+cc$ contributions in the background. The variable K_Q, which is a normalisation factor for the multi-jet background, is also extracted by the procedure. The number of events in the MC simulation with positively charged (negatively charged) leptons for each flavour component is $N^{\text{flavour}}_{\text{MC},W^+}$ ($N^{\text{flavour}}_{\text{MC},W^-}$). The fraction of each flavour predicted by the MC simulation is f_{flavour}. The contributions from multi-jet production in the different lepton charge regions, N_{Q^+} and N_{Q^-}, are estimated using the same matrix method as described in Sect. 6.1.

Solving this system of equations gives corrected heavy-flavour fractions for W+jets events with exactly two jets. Since the predicted charge asymmetry depends on the flavour fractions, the charge-asymmetry normalisation followed by flavour-fraction extraction is iterated until stable results for C_A and K_{flavour} are obtained. The MC predictions of the flavour fractions for higher jet multiplicities are used together with these correction factors to obtain a corrected prediction for the flavour fractions at higher jet multiplicities. The extracted correction factors depend on the selection and the jet multiplicity. The $K_{bb,cc}$ factors are between 1.19 and 1.27 (1.34 and 1.51) in the electron (muon) channel. The K_{light} factor varies from 0.87 to 0.91 (0.78–0.88) in the electron (muon) channel. The K_c factor is found to lie between 0.93 and 1 (0.86 and 1) in the electron (muon) channel. The normalisation factor C_A extracted from the charge asymmetry varies from 0.78 to 1.05 (0.8–1.14) in the electron (muon) channel.

7 Systematic uncertainties

In this section, the systematic uncertainties that affect this search are detailed. These are uncertainties in the normalisation and shape of predicted $m^{\text{reco}}_{t\bar{t}}$ distributions for signal and background.

The uncertainty in the combined 2015 + 2016 integrated luminosity is 2.1%. It is derived, following a methodology similar to that detailed in Ref. [84], from a calibration of the luminosity scale using x–y beam-separation scans performed in August 2015 and May 2016. In addition, a 'pile-up' uncertainty due to the observed disagreement between the instantaneous luminosities in data and simulation is estimated.

The modelling of the electron and muon trigger efficiencies, identification efficiencies, energy scales and resolutions are studied using leptonic Z boson decays in data and simulation at $\sqrt{s} = 13\,\text{TeV}$. Small corrections are applied to the simulation to better model the performance seen in data [85,86]. These corrections have associated uncertainties that are propagated to the estimated signal and background yields. The modelling of the isolation requirements on electrons and muons is studied in 13 TeV data using Z boson decays and parameterised as functions of the lepton p_{T}, η, and the hadronic activity near the lepton. The isolation efficiencies are found to be generally well modelled, and the measurements are extrapolated to the $t\bar{t}$ environment to give an uncertainty of 1% for each electrons or muons.

The small-R jet energy scale (JES) uncertainty is derived using a combination of simulations, test-beam data, and in situ measurements. Additional contributions from jet flavour composition, punch-through, single-particle response, calorimeter response to different jet flavours and pile-up are taken into account, resulting in 19 eigenvector systematic uncertainty subcomponents, including the uncertainties in the jet energy resolution obtained with an in situ measurement of the jet response in di-jet events [87].

Correction factors are applied to the simulated event samples to compensate for differences between data and simulation [88,89] in the b-tagging efficiency for b-, c- and light-jets. The correction for b-jets is derived from $t\bar{t}$ events with final states containing two leptons. The corrections are consistent with unity with uncertainties at the level of a few percent over most of the jet p_{T} range. Uncertainties in the correction factors for the b-tagging identification response are estimated by examining dedicated flavour-enriched samples in the data. An additional term is included to extrapolate the measured uncertainties to the high-p_{T} region of interest. This term is calculated from simulated events by considering variations of quantities affecting the b-tagging performance such as the impact parameter resolution, percentage of poorly measured tracks, description of the detector material and track multiplicity per jet. The dominant effect on the uncertainty when extrapolating to high p_{T} is related to the different tagging efficiency when adjusting the track impact parameters according to the resolution measured in data and simulation.

[5] The flavour components are: $W_{b\bar{b}}$ – W bosons produced in association with a $b\bar{b}$ pair; $W_{c\bar{c}}$ – W bosons produced in association with a $c\bar{c}$ pair; W_c – W bosons produced in association with a single c- or $\bar{c}$-quark; and W_{light} – W bosons produced in association with light quarks.

The large-R jet energy and mass scales and τ_{32} scale are varied in simulation according to the uncertainties derived from $\sqrt{s} = 8$ TeV [90] simulation and in situ calibration, and the uncertainties are extrapolated to $\sqrt{s} = 13$ TeV [71]. The uncertainties in the jet mass and τ_{32} are propagated into uncertainties in the top-tagging efficiency.

Several uncertainties are specific to the dominant SM $t\bar{t}$ background process. The $t\bar{t}$ cross-section for pp collisions at a centre-of-mass energy of $\sqrt{s} = 13$ TeV is $\sigma_{t\bar{t}} = 832^{+46}_{-52}$ pb for a top-quark mass of 172.5 GeV. It was calculated at next-to-next-to-leading order in QCD including resummation of next-to-next-to-leading-logarithm (NNLL) soft gluon terms with Top++2.0 [91–97]. The uncertainties from the PDFs and α_S were calculated using the PDF4LHC prescription [98] with the MSTW2008 68% CL NNLO [57,99], CT10 NNLO [30,31] and NNPDF2.3 5f FFN [48] PDF sets and added in quadrature to the effect of the scale uncertainty. The normalisation of the $t\bar{t}$ background is obtained from a fit to the data in the boosted channels, within the profile likelihood fit method described in Sect. 9. In addition to this normalisation uncertainty, the following top-modelling uncertainties that affect the shape of the $t\bar{t}$ kinematic distributions as well as the normalisation are considered:

Choice of the event generator: this is evaluated by comparing the prediction from a POWHEG+HERWIG $t\bar{t}$ sample [100] with that from an aMC@NLO+HERWIG sample and symmetrising the difference.
Choice of the parton shower model: this is evaluated by comparing the prediction from a POWHEG+PYTHIA $t\bar{t}$ sample with that from a POWHEG+HERWIG 7 sample [101] and symmetrising the difference.
Choice of the parton distribution functions: the uncertainties arising from the choice of the PDF set are evaluated using the PDF4LHC15 PDF set. The version that provides 30 separate uncertainty eigenvectors is used [51].
Modelling of extra QCD radiation: this is evaluated using POWHEG+PYTHIA samples in which the renormalisation and factorisation scales and the h_{damp} parameter are varied within ranges consistent with measurements of $t\bar{t}$ production in association with jets [102–104].
EW corrections: the uncertainty in the EW corrections to $t\bar{t}$ production is 10% of their deviation from unity.
NNLO QCD corrections: sensitivity of the $m_{t\bar{t}}$ distribution to higher-order QCD corrections relative to the MC generators used is accounted for by adding an uncertainty covering the difference between NLO and NNLO QCD calculations of $t\bar{t}$ production. Corrections are derived from recent calculations [105] and applied as a function of top-quark p_{T} and the transverse momentum of the $t\bar{t}$ system, following the recommended scales given in Ref. [105]. The effect of this uncertainty in the $m_{t\bar{t}}$ distribution is very small at low mass, but increases to 7% at masses of 2 TeV in the resolved selection and 20% above 3 TeV in the boosted selection.

The normalisation of the single-top background is varied by $\pm 5.3\%$. This corresponds to the theoretical uncertainty in the dominant Wt-channel contribution at approximate NNLO in QCD [106–108]. An additional shape and normalisation uncertainty is applied to account for differences between the predictions from diagram removal and diagram subtraction approaches [32] to the interference between tW production and $t\bar{t}$. Such uncertainty has an effect of less than 1% in the yields. We have found that other single top modeling uncertainties are negligible.

Systematic uncertainties in the W+jets background are evaluated by varying the extracted correction factors for normalisation and flavour fractions by their associated uncertainties. The correction factors are also separately estimated for each of the systematic variations which affect the correction factor estimation described in this section. A 30% uncertainty is associated with the normalisation of the W+c component of the W+jets background.

Systematic uncertainties in the multi-jet background estimation are evaluated using various definitions of multi-jet control regions that result in slightly different estimates of f. Systematic uncertainties associated with object reconstruction and MC simulation are also considered and a total normalisation uncertainty of 50% is assigned.

Table 1 shows a summary of the systematic uncertainties in the yields for the total background and two signals. The $t\bar{t}$ modelling and jet energy uncertainties provide the largest contributions to the overall uncertainties.

8 Comparison of data with expected background contributions

After all event selection criteria are applied, 35 612 (261 554) boosted (resolved) events remain in the e+jets selection and 31 188 (254 277) events remain in the μ+jets selection. There is a deficit of data compared to expectation for the boosted selections; however, this deficit is consistent with the nominal prediction within the associated systematic uncertainties. In the following figures, the legend 'others' refers to single top, Z+jets, $t\bar{t} + W/Z$ and diboson production.

Figure 4 shows the transverse momentum of the charged lepton in the selected events. The $E_{\text{T}}^{\text{miss}}$ distribution is shown in Fig. 5. The transverse momentum of the selected jet and top-tagged jets are shown in Figs. 6 and 7. Figures 8 and 9 show the reconstructed mass of the leptonic- and hadronic-top candidates. For all of the distributions in the resolved selections, any deviations from expectations are well within the statistical and systematic uncertainties. As some top-quark decays are not fully contained within the large-R jet,

Table 1 The systematic uncertainties in the yields in the background, as well as in the 2 and 3 TeV Z'_{TC2} signal models, in percentages. Only rows with at least one column with an uncertainty larger than 2% are shown individually. Systematic uncertainties associated with the muon and electron trigger, identification, energy scales and resolutions combined are smaller than 2% for all signal regions and are not shown. JES and JER stand for jet energy scale and jet energy resolution

Systematic uncertainty	Background (%)		Z'_{TC2}, 2 TeV (%)		Z'_{TC2}, 3 TeV (%)	
	Resolved	Boosted	Resolved	Boosted	Resolved	Boosted
$t\bar{t}$ extra QCD radiation	4.0	2.4	–	–	–	–
$t\bar{t}$ QCD NNLO	0.8	7.4	–	–	–	–
$t\bar{t}$ cross-section	5.2	–	–	–	–	–
$t\bar{t}$ generator	1.7	3.8	–	–	–	–
$t\bar{t}$ parton shower	0.6	3.2	–	–	–	–
Multi-jet	2.6	2.7	–	–	–	–
Anti-k_t $R = 0.4$ JER	1.1	0.2	3.2	0.2	1.2	0.2
Anti-k_t $R = 0.4$ JES	5.8	0.9	7.0	0.7	3.6	0.6
Anti-k_t $R = 1.0$ JER	0.1	4.0	5.3	3.7	2.0	4.2
Anti-k_t $R = 1.0$ JES	0.3	6.0	3.7	4.7	2.8	6.0
b-tagging efficiency	3.2	1.8	1.8	1.9	2.3	2.7
b-tagging extrapolation	2.4	2.3	2.0	0.6	1.2	1.8
Luminosity	1.9	1.9	2.1	2.1	2.1	2.1
Pile-up	4.4	0.5	4.4	0.8	3.9	0.5
Total	11.6	12.8	11.7	7.1	7.6	8.7

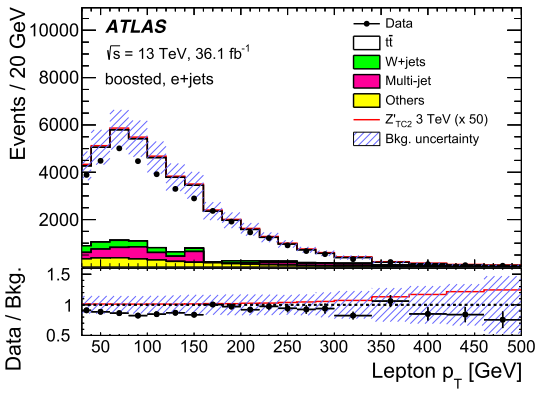

(a) e+jets, boosted selection.

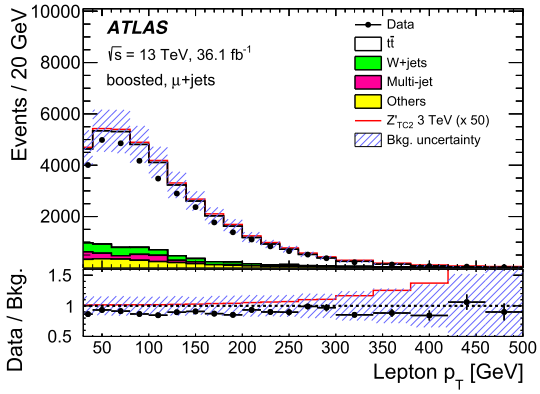

(b) μ+jets, boosted selection.

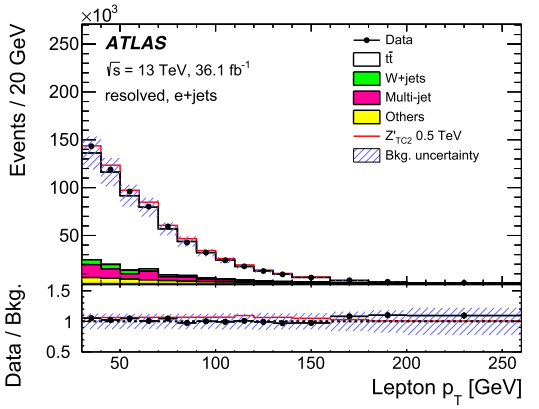

(c) e+jets, resolved selection.

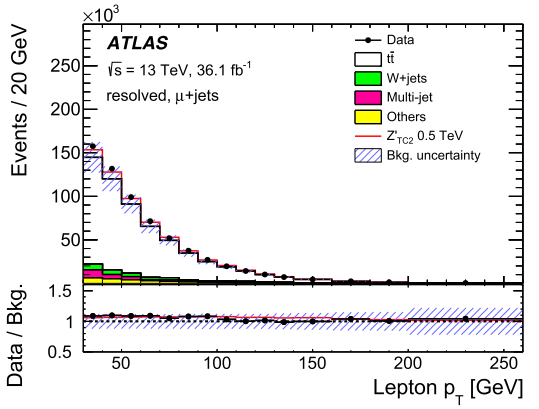

(d) μ+jets, resolved selection.

Fig. 4 The distribution of the transverse momentum of the lepton in the **a** boosted e+jets, **b** boosted μ+jets, **c** resolved e+jets, and **d** resolved μ+jets selections. The SM background components are shown as stacked histograms. The shaded areas indicate the total systematic uncertainties. The lower panels in each plot show the ratio of data (points) and a signal example (line) to the background expectation

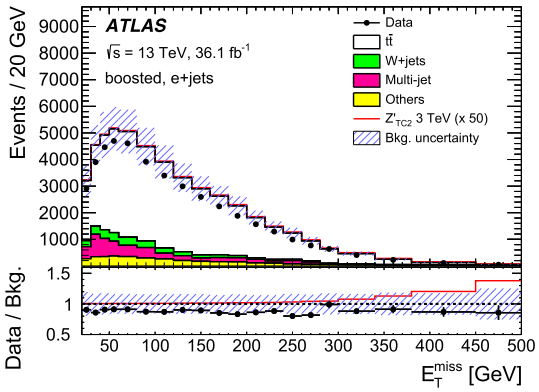

(a) e+jets, boosted selection.

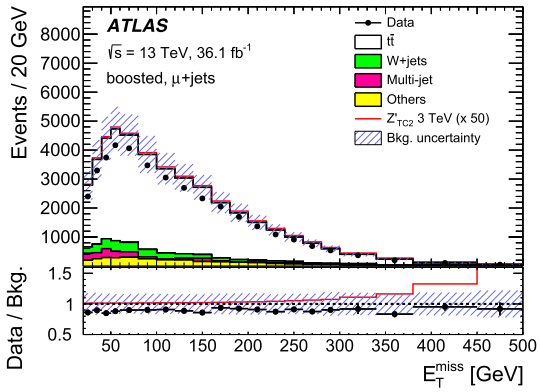

(b) μ+jets, boosted selection.

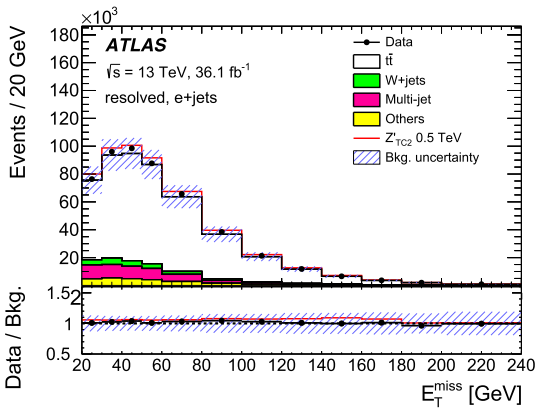

(c) e+jets, resolved selection.

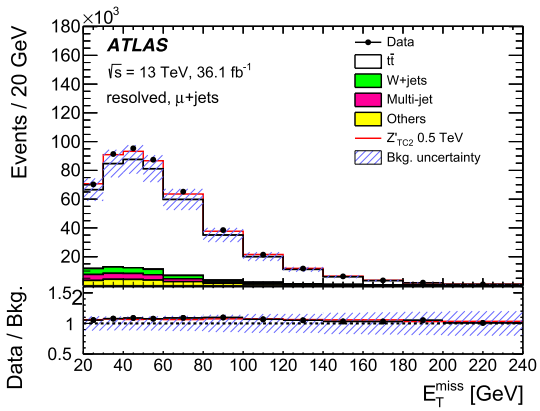

(d) μ+jets, resolved selection.

Fig. 5 The distribution of the $E_{\mathrm{T}}^{\mathrm{miss}}$ in the **a** boosted e+jets, **b** boosted μ+jets, **c** resolved e+jets, and **d** resolved μ+jets selections. The SM background components are shown as stacked histograms. The shaded areas indicate the total systematic uncertainties. The lower panels in each plot show the ratio of data (points) and a signal example (line) to the background expectation

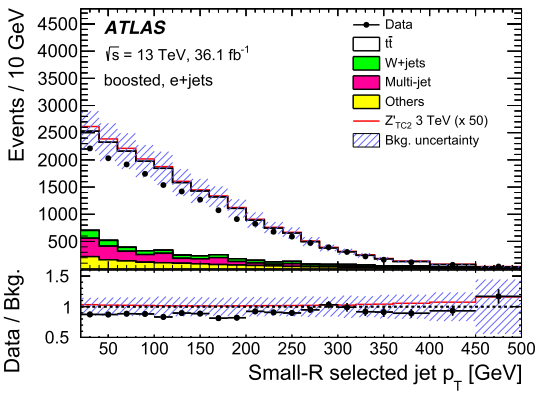

(a) e+jets selection.

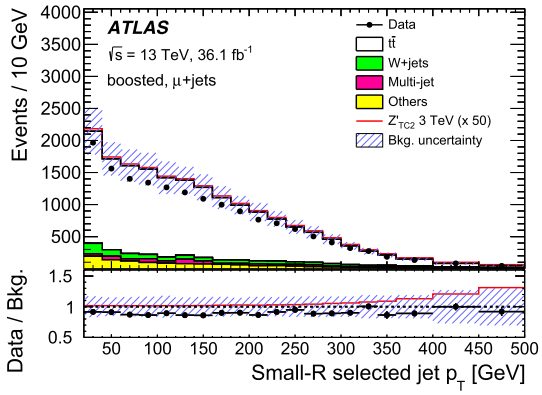

(b) μ+jets selection.

Fig. 6 The distribution of the transverse momentum of the hardest small-R jet with $\Delta R(\ell, \mathrm{jet}) < 1.5$ in the **a** boosted e+jets, and **b** boosted μ+jets selections. The SM background components are shown as stacked histograms. The shaded areas indicate the total systematic uncertainties. The lower panels in each plot show the ratio of data (points) and a signal example (line) to the background expectation

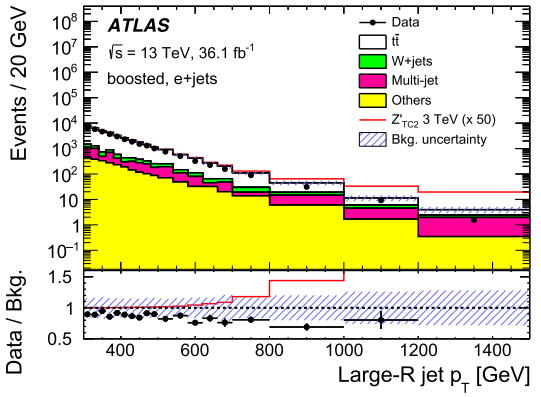

(a) e+jets selection.

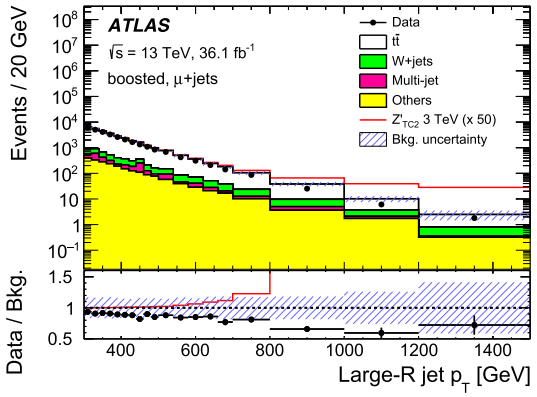

(b) μ+jets selection.

Fig. 7 The distribution of the transverse momentum of the large-R jet in the **a** boosted e+jets, and **b** boosted μ+jets selections. The SM background components are shown as stacked histograms. The shaded areas indicate the total systematic uncertainties. The lower panels in each plot show the ratio of data (points) and a signal example (line) to the background expectation

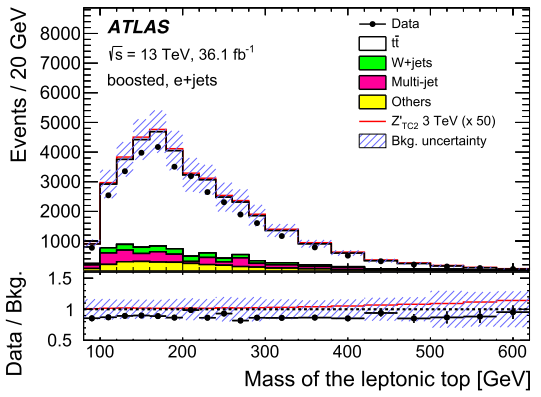

(a) e+jets, boosted selection.

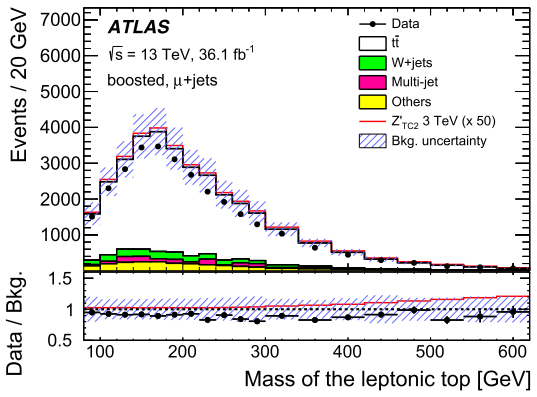

(b) μ+jets, boosted selection.

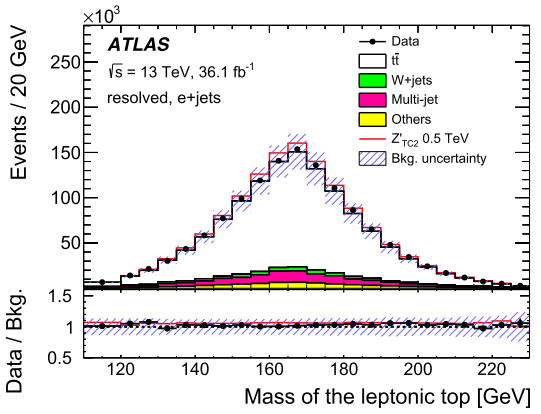

(c) e+jets, resolved selection.

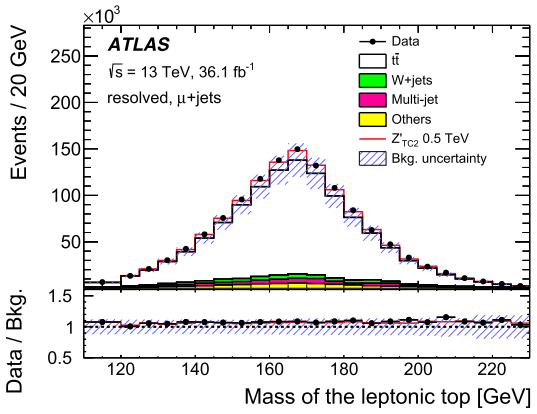

(d) μ+jets, resolved selection.

Fig. 8 The distribution of the reconstructed mass of the leptonic-top candidate in the **a** boosted e+jets, **b** boosted μ+jets, **c** resolved e+jets, and **d** resolved μ+jets selections. The SM background components are shown as stacked histograms. The shaded areas indicate the total systematic uncertainties. The lower panels in each plot show the ratio of data (points) and a signal example (line) to the background expectation

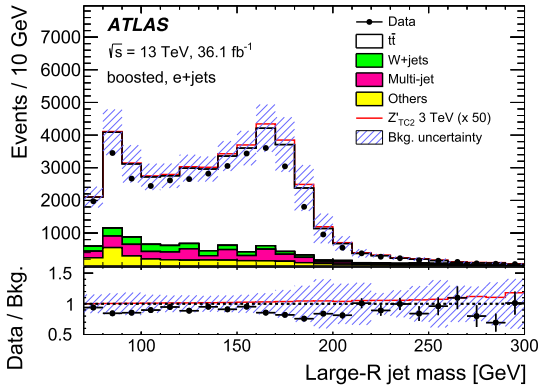

(a) e+jets, boosted selection.

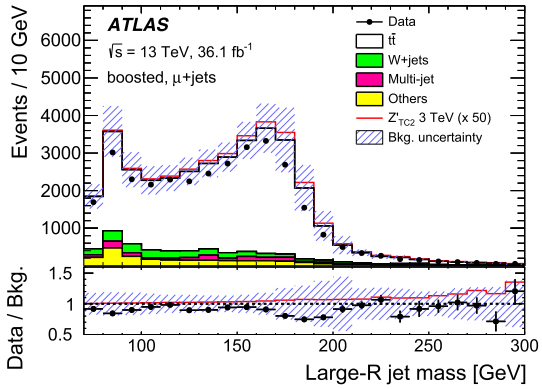

(b) μ+jets, boosted selection.

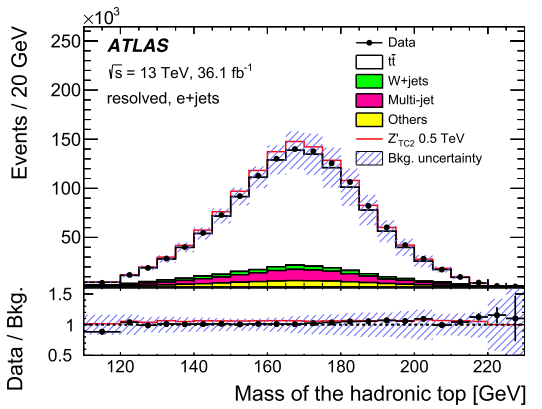

(c) e+jets, resolved selection.

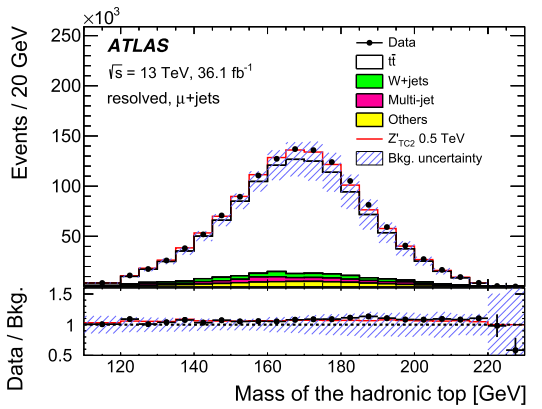

(d) μ+jets, resolved selection.

Fig. 9 The distribution of the mass of the large-R jet in the **a** boosted e+jets, and **b** boosted μ+jets selections. The mass of the hadronic-top candidate in the **c** resolved e+jets, and **d** resolved μ+jets selections. The SM background components are shown as stacked histograms. The shaded areas indicate the total systematic uncertainties. The lower panels in each plot show the ratio of data (points) and a signal example (line) to the background expectation

two peaks in the jet mass distribution are visible in Fig. 9. One close to the W boson mass for the cases in which only the W boson decay products are reconstructed within the large-R jet, and one close to the top-quark mass. There is a tendency for the expectations in the boosted selections to be 10–20% below the data while exhibiting a similar shape.

The reconstructed $t\bar{t}$ invariant mass spectra for the electron and muon selections are shown in Figs. 10 and 11. The data generally agree with the expected background with slight shape differences seen especially in the high-mass and low-mass regions. These deviations are consistent with the nominal predictions within the associated uncertainties.

The fraction of the SM W+jets background increases as a function of $m_{t\bar{t}}^{\text{reco}}$ in the boosted channel, with a higher fraction in the boosted selection in b-tag category 2, where it contributes roughly 50% of the background for $m_{t\bar{t}}^{\text{reco}} > 3$ TeV. The fraction in b-tag category 3, which is the purest channel, is at most 6% for $m_{t\bar{t}}^{\text{reco}} > 3$ TeV. In the resolved channel, the contribution of the W+jets background also grows with $m_{t\bar{t}}^{\text{reco}}$ and it contributes less than 1% in the b-tag category 3, while it has up to a 14% effect in b-tag category 2.

9 Results

The final discriminating observables used to search for a massive resonance are the $m_{t\bar{t}}^{\text{reco}}$ spectra from the two selections. After the reconstruction of the $t\bar{t}$ mass distribution, the data and expected background distributions are compared using BumpHunter [109], which is a hypothesis-testing tool that searches the data for local excesses or deficits compared to the expected background, taking the look-elsewhere effect [110] into account over the full mass spectrum in both the boosted (480 GeV to 6 TeV) and resolved (390 GeV to 2 TeV) channels. After accounting for the systematic uncertainties, no significant deviation from the total expected background is

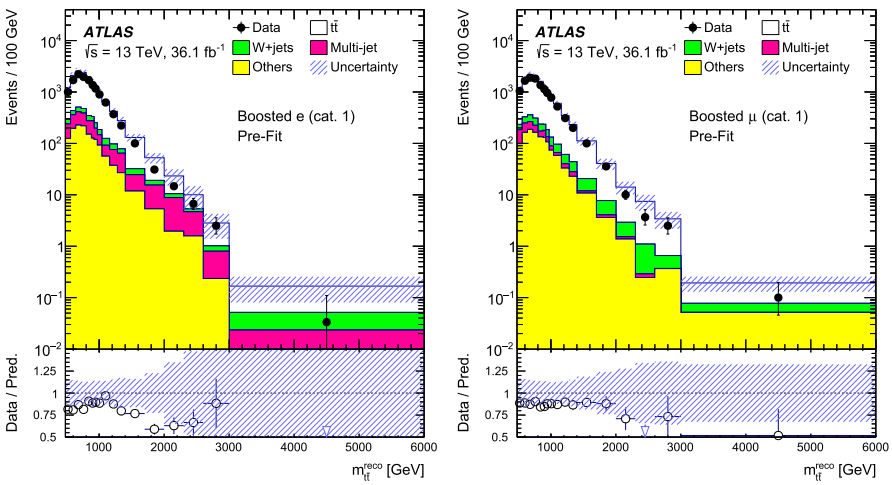

(a) e+jets b-tag category 1 **(b)** μ+jets b-tag category 1

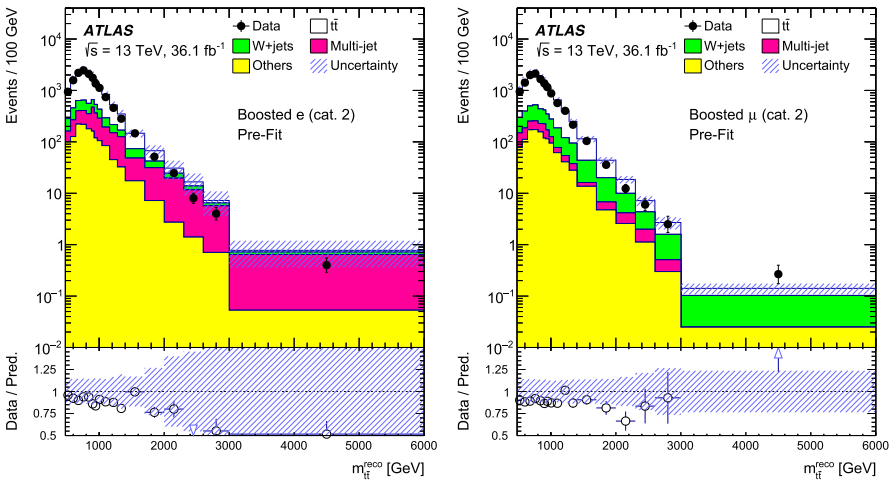

(c) e+jets b-tag category 2 **(d)** μ+jets b-tag category 2

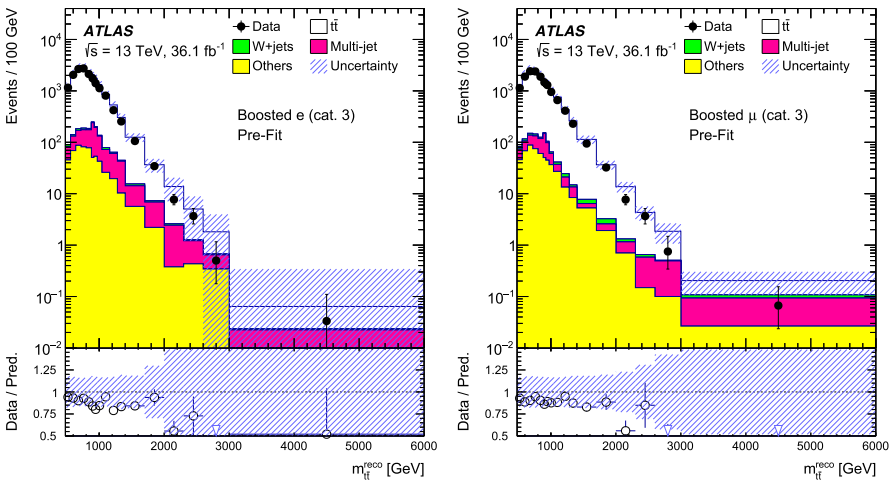

(e) e+jets b-tag category 3 **(f)** μ+jets b-tag category 3

Fig. 10 The $m_{t\bar{t}}^{\mathrm{reco}}$ distribution before the likelihood fit in the boosted selection. The SM background components are shown as stacked histograms. The shaded areas indicate the total systematic uncertainties. The ratio of the data to the total expectation from background processes is shown in the lower panel, open triangles indicate that the ratio point would appear outside the panel

Fig. 11 The $m_{t\bar{t}}^{\mathrm{reco}}$ distribution before the likelihood fit in the resolved selection. The SM background components are shown as stacked histograms. The shaded areas indicate the total systematic uncertainties. The ratio of the data to the total expectation from background processes is shown in the lower panel

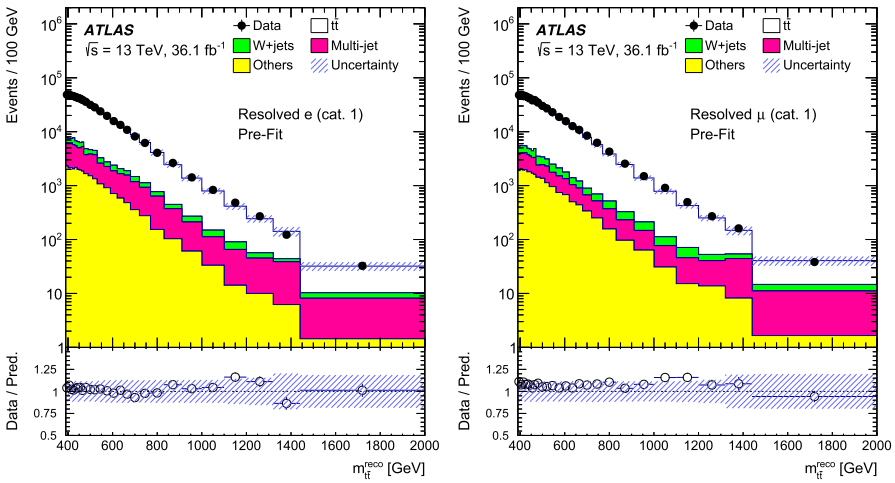

(a) e+jets b-tag category 1

(b) μ+jets b-tag category 1

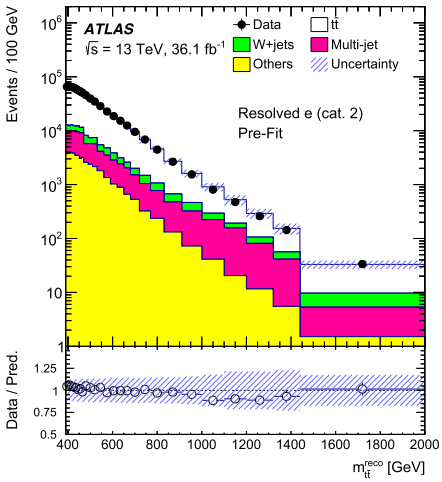

(c) e+jets b-tag category 2

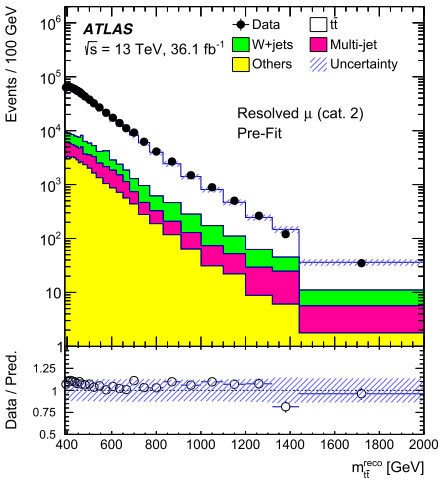

(d) μ+jets b-tag category 2

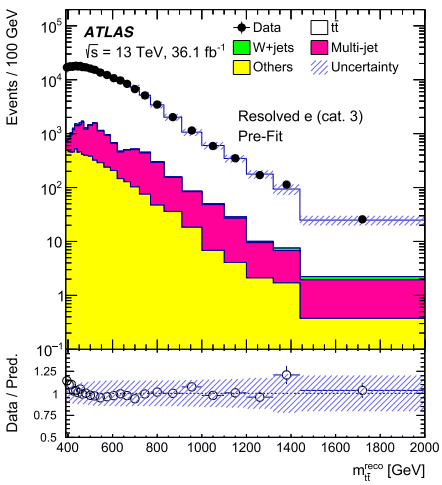

(e) e+jets b-tag category 3

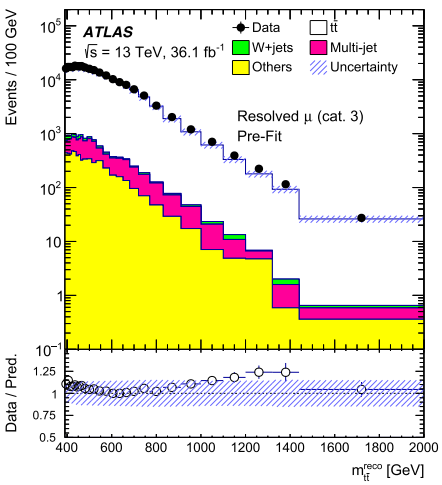

(f) μ+jets b-tag category 3

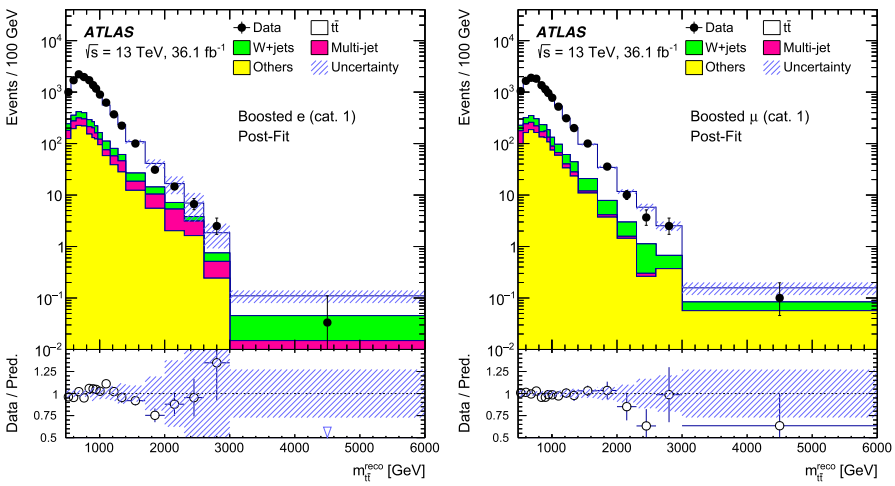

(a) e+jets b-tag category 1 **(b)** μ+jets b-tag category 1

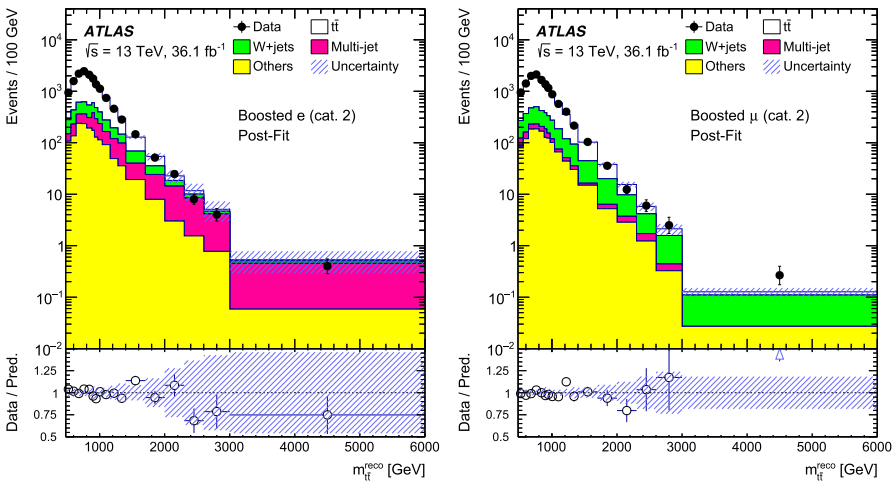

(c) e+jets b-tag category 2 **(d)** μ+jets b-tag category 2

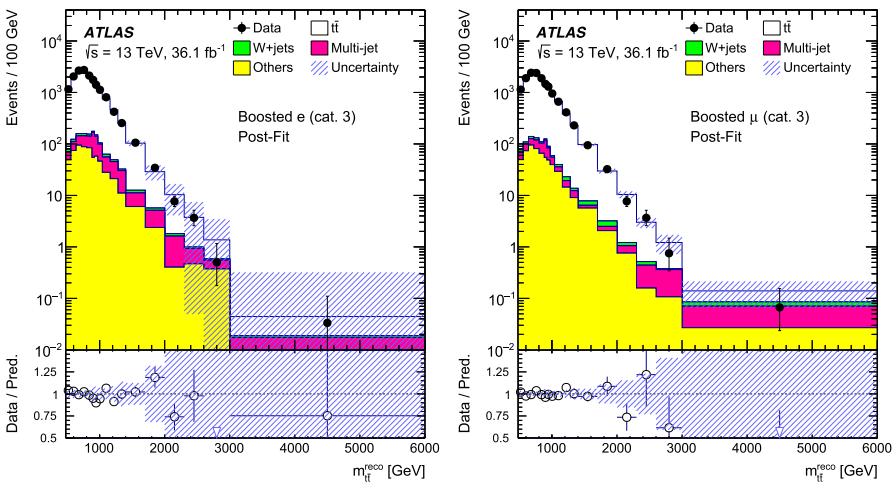

(e) e+jets b-tag category 3 **(f)** μ+jets b-tag category 3

Fig. 12 The $m_{t\bar{t}}^{\mathrm{reco}}$ distributions, after a likelihood fit under the background-only hypothesis, for the boosted selection. The SM background components are shown as stacked histograms. The shaded areas indicate the total systematic uncertainties. The ratio of the data to the final fitted expectation is shown in the lower panel, open triangles indicate that the ratio point would appear outside the panel

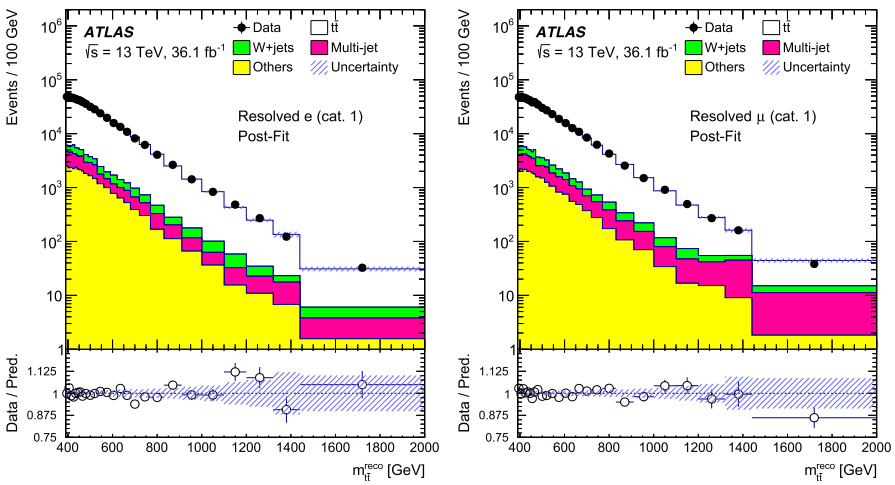

(a) e+jets b-tag category 1

(b) μ+jets b-tag category 1

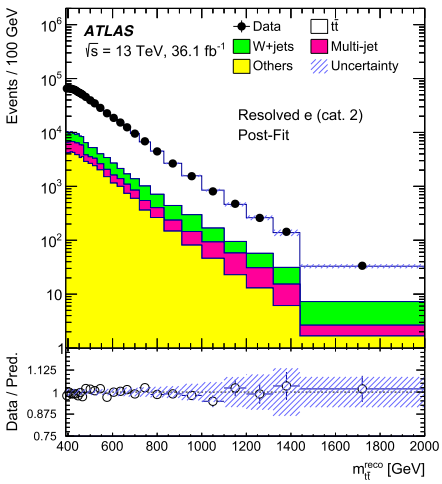

(c) e+jets b-tag category 2

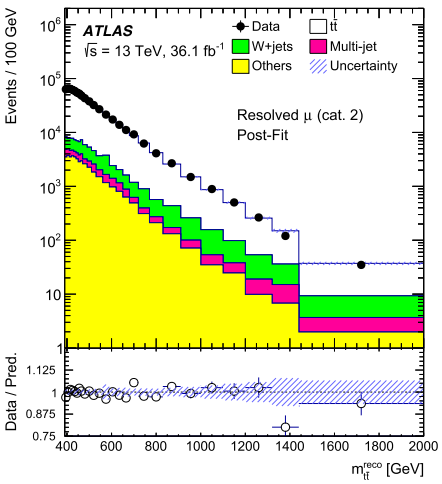

(d) μ+jets b-tag category 2

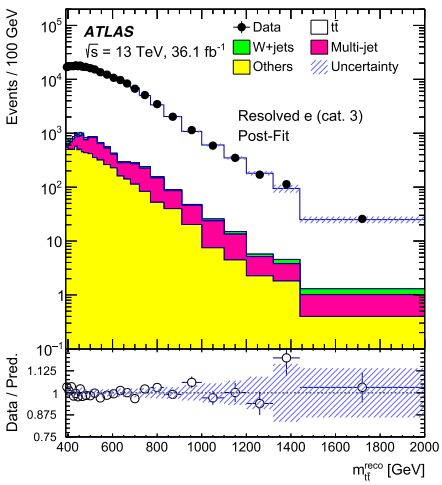

(e) e+jets b-tag category 3

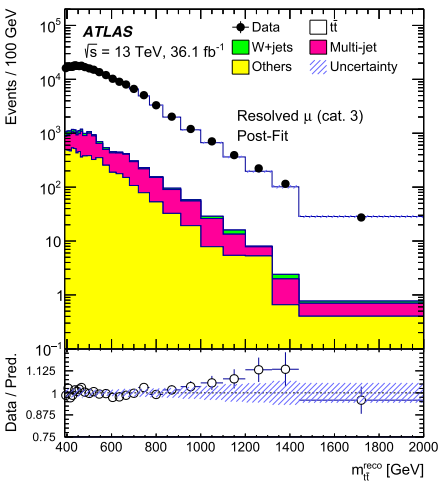

(f) μ+jets b-tag category 3

Fig. 13 The $m_{t\bar{t}}^{\mathrm{reco}}$ distributions, after a likelihood fit under the background-only hypothesis, for the resolved selection. The SM background components are shown as stacked histograms. The shaded areas indicate the total systematic uncertainties. The ratio of the data to the final fitted expectation is shown in the lower panel

Table 2 Data and expected background in all channels after the background-only fit is performed. The total systematic uncertainty in the expected background yields is also given. The $t\bar{t}$ normalisation is extracted from the fit in the boosted channels and its ratio to the pre-fit content is 0.93

Type	Yields			
	Boosted e	Boosted μ	Resolved e	Resolved μ
$t\bar{t}$	$28{,}500 \pm 500$	$26{,}000 \pm 400$	$231{,}100 \pm 1900$	$225{,}300 \pm 1700$
W+jets	2200 ± 240	2200 ± 180	9400 ± 1100	$10{,}300 \pm 800$
Multi-jet	2000 ± 400	780 ± 200	8200 ± 1400	7400 ± 1400
Others	2880 ± 230	2420 ± 180	$13{,}000 \pm 600$	$12{,}000 \pm 500$
Total	$35{,}600 \pm 500$	$31{,}300 \pm 300$	$262{,}200 \pm 1200$	$254{,}600 \pm 1100$
Data	35,612	31,188	261,554	254,277

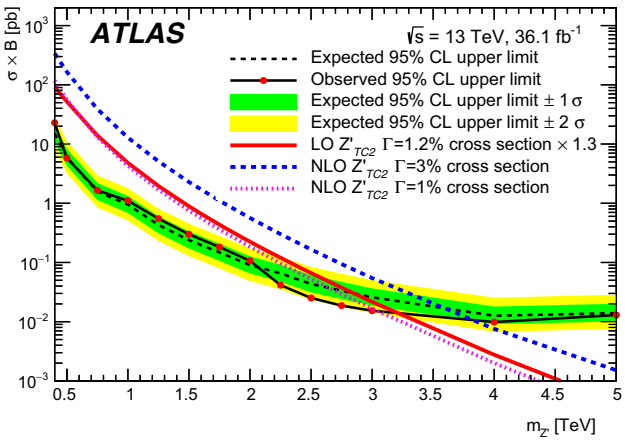

Fig. 14 The observed and expected cross-section 95% CL upper limits on the Z'_{TC2} signal. The theoretical predictions for the production cross-section times branching ratio of $Z'_{\mathrm{TC2}} \to t\bar{t}$ at the corresponding masses are also shown

found. Upper limits are set on the cross-section times branching ratio for each of the signal models using a combined profile likelihood-ratio test build using the 12 categories. The $\mathrm{CL_s}$ prescription [111] is used to derive one-sided 95% confidence level (CL) limits.

The statistical and systematic uncertainties in the expected distributions are included in this $\mathrm{CL_s}$ procedure as nuisance parameters in the likelihood fits. The nuisance parameters for the systematic uncertainties are constrained by a Gaussian probability density function with a width corresponding to the size of the uncertainty considered. Correlations between different channels and bins are taken into account. The product of the various probability density functions forms the likelihood function that is maximised in the fit by adjusting the free parameter, called the signal strength (a multiplicative factor applied to the signal expected cross-section), and the nuisance parameters. The expected $m_{t\bar{t}}^{\mathrm{reco}}$ distributions are compared to data in Figs. 12 and 13 after a fit of the nuisance parameters under the background-only hypothesis. The expected yields after the background-only fit are also shown in Table 2. It can be seen that the uncertainties are smaller than in Figs. 10 and 11.

Under the background-only hypothesis, a fit to data leads to a constraint of the jet energy resolution and the large-R jet energy scale nuisance parameters amongst the experimental uncertainties. The $t\bar{t}$ generator, radiation and modelling uncertainty nuisance parameters are also constrained, due to the large uncertainty in this background modelling. Amongst the most relevant uncertainties for the 3 TeV Z'_{TC2} model, the

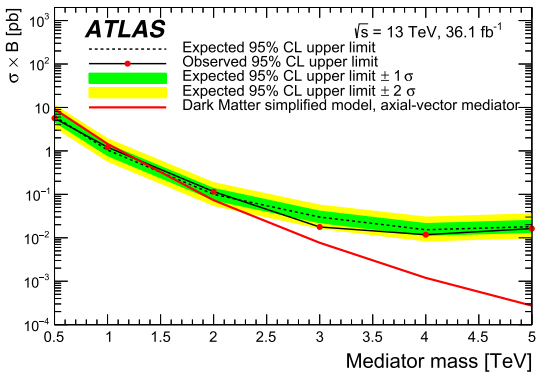

(a) Axial-vector mediator

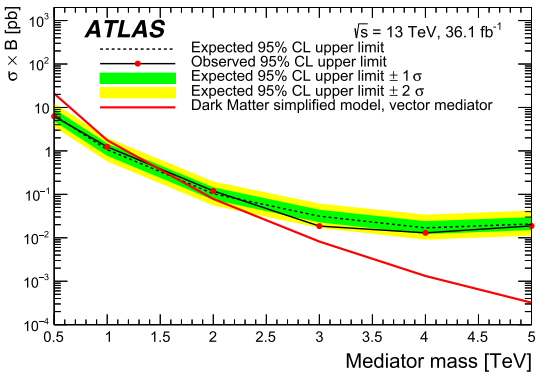

(b) Vector mediator

Fig. 15 The observed and expected cross-section 95% CL upper limits on the **a** $Z'_{\mathrm{DM,ax}}$ and **b** $Z'_{\mathrm{DM,vec}}$ signals. The theoretical predictions for the production cross-section times branching ratio of $Z'_{\mathrm{DM}} \to t\bar{t}$ at the corresponding masses are also shown

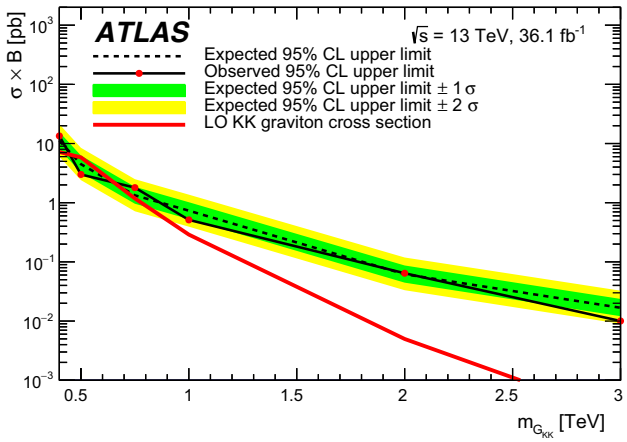

Fig. 16 The observed and expected cross-section 95% CL upper limits on the G_{KK} signal. The theoretical predictions for the production cross-section times branching ratio of $G_{\mathrm{KK}} \to t\bar{t}$ at the corresponding masses are also shown

$t\bar{t}$ radiation uncertainty nuisance parameter is constrained by a factor of three in the boosted channel and the parton shower uncertainty, by a factor of two.

The impact of the fitted nuisance parameters on the fitted signal strength is different at each candidate signal mass. In order to estimate the impact of a nuisance parameter in the fit of the signal strength, the nuisance parameter is fixed at its central value plus or minus its fit uncertainties, and the variation of the fitted signal strength is tested. For example, at a Z' mass of 3 TeV, the impact of an uncertainty on the best-fit value is computed by fixing the nuisance parameter θ to the one-standard-deviation range limits (positive or negative), and repeating the fit for a pseudodata sample with a 1 pb cross-section signal injected. The most significant uncertainties are related to the JES for large-R jets and affect the fitted signal strength by up to 5%.

The expected and observed limits on the studied signal models versus mass are presented in Figs. 14, 15, 16 and 17 and summarised in Table 3. The cross-section limits are extracted for each mass point, and are interpolated with straight lines in the regions between the mass points. For the Z'_{TC2} benchmark, upper limits on the production cross-sections vary from 25 to 0.02 pb for masses from 0.4 to 5 TeV. A Z'_{TC2} of width 1% is excluded for masses $m_{Z'_{\mathrm{TC2}}} < 3.0$ TeV while masses in the region $m_{Z'_{\mathrm{TC2}}} < 2.6$ TeV are expected to be excluded. The $Z'_{\mathrm{DM,ax}}$ considered in this search is excluded for masses in the region $m_{Z'_{\mathrm{DM,ax}}} < 1.2$ TeV, while masses in the region $m_{Z'_{\mathrm{DM,ax}}} < 1.4$ TeV are expected to be excluded. The $Z'_{\mathrm{DM,vec}}$ considered in this search is excluded for masses in the region $m_{Z'_{\mathrm{DM,vec}}} < 1.4$ TeV while masses in the region $m_{Z'_{\mathrm{DM,vec}}} < 1.6$ TeV are expected to be excluded. The Kaluza–Klein gravitons searched for in this analysis are excluded in the range $0.45 < m_{G_{\mathrm{KK}}} < 0.65$ TeV, which is also the expected exclusion region. A Kaluza–Klein gluon of width 30% is excluded for $m_{g_{\mathrm{KK}}} < 3.7$ TeV compared with an expected exclusion for $m_{g_{\mathrm{KK}}} < 3.2$ TeV. A Kaluza–Klein gluon of width 15% is excluded for $m_{g_{\mathrm{KK}}} < 3.8$ TeV compared with an expected exclusion for $m_{g_{\mathrm{KK}}} < 3.5$ TeV.

Table 3 Summary of the excluded mass ranges for the signals studied in this analysis

Summary of 95 % confidence level mass exclusion ranges on benchmark models		
Model	Observed excluded mass (TeV)	Expected excluded mass (TeV)
Z'_{TC2} (1% width)	< 3.0	< 2.6
$Z'_{\mathrm{DM,ax}}$	< 1.2	< 1.4
$Z'_{\mathrm{DM,vec}}$	< 1.4	< 1.6
G_{KK}	[0.45, 0.65]	[0.45, 0.65]
g_{KK} (15% width)	< 3.8	< 3.5
g_{KK} (30% width)	< 3.7	< 3.2

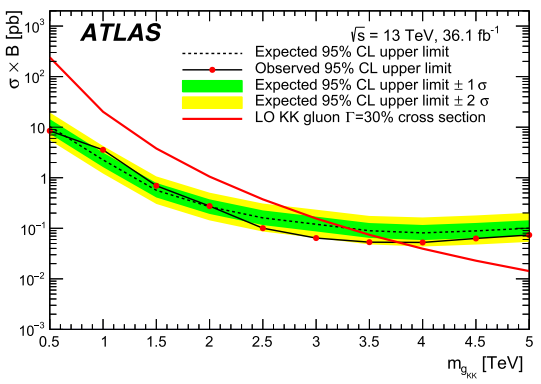

(a) 30% width

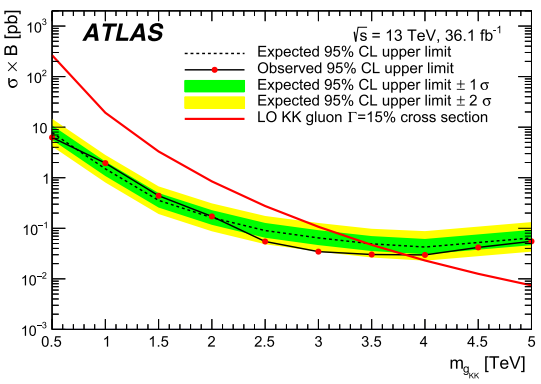

(b) 15% width

Fig. 17 The observed and expected cross-section 95% CL upper limits on the g_{KK} signal for resonance widths of **a** 30% and **b** 15%. The theoretical predictions for the production cross-section times branching ratio of $g_{\mathrm{KK}} \to t\bar{t}$ at the corresponding masses are also shown

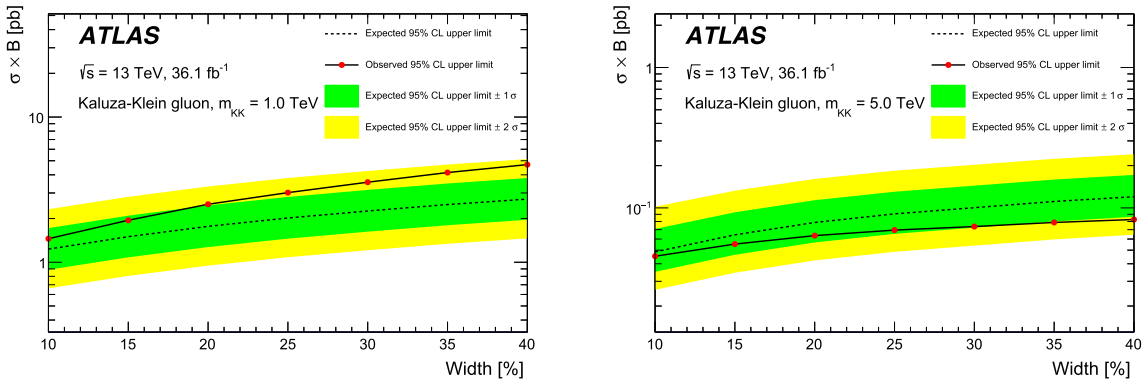

(a) $m_{g_{KK}} = 1$ TeV **(b)** $m_{g_{KK}} = 5$ TeV

Fig. 18 The observed and expected cross-section 95% CL upper limits on the g_{KK} signal as a function of the resonance width for masses of **a** 1 TeV, and **b** 5 TeV

Furthermore, for the Kaluza–Klein gluons, the search sensitivity as a function of resonance width was explored. Figure 18 shows the excluded cross-sections as a function of width for two different mass points. The cross-section limits deteriorate with increasing resonance width, as the signal peak is smeared out.

10 Summary

A search for heavy particles decaying into $t\bar{t}$ in the lepton-plus-jets decay channel with the ATLAS experiment at the LHC is presented. The search uses data corresponding to an integrated luminosity of 36.1 fb^{-1} of proton–proton collisions at a centre-of-mass energy of 13 TeV. No excess of events beyond the Standard Model predictions is observed in the $t\bar{t}$ invariant mass spectra. Upper limits on the cross-section times branching ratio are set for several heavy resonances in models of new physics. These results considerably extend the excluded regions for Z'_{TC2} and g_{KK} and represent the first mass ranges to be excluded, using the $t\bar{t}$ decay channel, for the dark-matter mediators $Z'_{DM,ax}$ and $Z'_{DM,vec}$, and for G_{KK}.

Acknowledgements We thank CERN for the very successful operation of the LHC, as well as the support staff from our institutions without whom ATLAS could not be operated efficiently. We acknowledge the support of ANPCyT, Argentina; YerPhI, Armenia; ARC, Australia; BMWFW and FWF, Austria; ANAS, Azerbaijan; SSTC, Belarus; CNPq and FAPESP, Brazil; NSERC, NRC and CFI, Canada; CERN; CONICYT, Chile; CAS, MOST and NSFC, China; COLCIENCIAS, Colombia; MSMT CR, MPO CR and VSC CR, Czech Republic; DNRF and DNSRC, Denmark; IN2P3-CNRS, CEA-DRF/IRFU, France; SRNSFG, Georgia; BMBF, HGF, and MPG, Germany; GSRT, Greece; RGC, Hong Kong SAR, China; ISF, I-CORE and Benoziyo Center, Israel; INFN, Italy; MEXT and JSPS, Japan; CNRST, Morocco; NWO, Netherlands; RCN, Norway; MNiSW and NCN, Poland; FCT, Portugal; MNE/IFA, Romania; MES of Russia and NRC KI, Russian Federation; JINR; MESTD, Serbia; MSSR, Slovakia; ARRS and MIZŠ, Slovenia; DST/NRF, South Africa; MINECO, Spain; SRC and Wallenberg Foundation, Sweden; SERI, SNSF and Cantons of Bern and Geneva, Switzerland; MOST, Taiwan; TAEK, Turkey; STFC, United Kingdom; DOE and NSF, United States of America. In addition, individual groups and members have received support from BCKDF, the Canada Council, CANARIE, CRC, Compute Canada, FQRNT, and the Ontario Innovation Trust, Canada; EPLANET, ERC, ERDF, FP7, Horizon 2020 and Marie Skłodowska-Curie Actions, European Union; Investissements d'Avenir Labex and Idex, ANR, Région Auvergne and Fondation Partager le Savoir, France; DFG and AvH Foundation, Germany; Herakleitos, Thales and Aristeia programmes co-financed by EU-ESF and the Greek NSRF; BSF, GIF and Minerva, Israel; BRF, Norway; CERCA Programme Generalitat de Catalunya, Generalitat Valenciana, Spain; the Royal Society and Leverhulme Trust, United Kingdom. The crucial computing support from all WLCG partners is acknowledged gratefully, in particular from CERN, the ATLAS Tier-1 facilities at TRIUMF (Canada), NDGF (Denmark, Norway, Sweden), CC-IN2P3 (France), KIT/GridKA (Germany), INFN-CNAF (Italy), NL-T1 (Netherlands), PIC (Spain), ASGC (Taiwan), RAL (UK) and BNL (USA), the Tier-2 facilities worldwide and large non-WLCG resource providers. Major contributors of computing resources are listed in Ref. [112].

Open Access This article is distributed under the terms of the Creative Commons Attribution 4.0 International License (http://creativecommons.org/licenses/by/4.0/), which permits unrestricted use, distribution, and reproduction in any medium, provided you give appropriate credit to the original author(s) and the source, provide a link to the Creative Commons license, and indicate if changes were made.
Funded by SCOAP[3].

References

1. ATLAS Collaboration, A search for $t\bar{t}$ resonances using lepton-plus-jets events in proton–proton collisions at $\sqrt{s} = 8$ TeV with the ATLAS detector. JHEP **08**, 148 (2015). arXiv:1505.07018 [hep-ex]
2. CMS Collaboration, Search for resonant $t\bar{t}$ production in proton-proton collisions at $\sqrt{s} = 8$ TeV. Phys. Rev. D **93**(1), 012001 (2015). arXiv:1506.03062 [hep-ex]
3. CMS Collaboration, Search for tt̄ resonances in highly boosted lepton+jets and fully hadronic final states in proton–proton colli-

sions at $\sqrt{s} = 13$ TeV. JHEP **07**, 001 (2017). arXiv:1704.03366 [hep-ex]
4. ATLAS Collaboration, Search for heavy Higgs bosons A/H decaying to a top quark pair in pp collisions at $\sqrt{s} = 8$TeV with the ATLAS detector. Phys. Rev. Lett. **119**(19), 191803 (2017). arXiv:1707.06025 [hep-ex]
5. C.T. Hill, S.J. Parke, Top production: sensitivity to new physics. Phys. Rev. D **49**, 4454–4462 (1994). arXiv:hep-ph/9312324
6. C.T. Hill, Topcolor assisted technicolor. Phys. Lett. B **345**, 483–489 (1995). arXiv:hep-ph/9411426
7. A. Albert et al., Recommendations of the LHC dark matter working group: comparing LHC searches for heavy mediators of dark matter production in visible and invisible decay channels. arXiv:1703.05703 [hep-ex]
8. R.M. Harris, C.T. Hill, S.J. Parke, Cross section for topcolor $Z'(t)$ decaying to $t\bar{t}$ (1999). arXiv:hep-ph/9911288
9. R.M. Harris, S. Jain, Cross sections for leptophobic topcolor Z' decaying to top-antitop. Eur. Phys. J. C **72**, 2072 (2012). arXiv:1112.4928 [hep-ph]
10. L. Randall, R. Sundrum, A large mass hierarchy from a small extra dimension. Phys. Rev. Lett. **83**, 3370–3373 (1999). arXiv:hep-ph/9905221
11. K. Agashe, H. Davoudiasl, G. Perez, A. Soni, Warped gravitons at the LHC and beyond. Phys. Rev. D **76**, 036006 (2007). arXiv:hep-ph/0701186
12. A.L. Fitzpatrick, J. Kaplan, L. Randall, L.T. Wang, Searching for the Kaluza–Klein graviton in bulk RS models. JHEP **09**, 013 (2007). arXiv:hep-ph/0701150
13. ATLAS Collaboration, Search for resonant diboson production in the $\ell\ell q\bar{q}$ final state in pp collisions at $\sqrt{s} = 8$ TeV with the ATLAS detector. Eur. Phys. J. C **75**, 69 (2015). arXiv:1409.6190 [hep-ex]
14. CMS Collaboration, Search for massive resonances decaying into pairs of boosted bosons in semi-leptonic final states at $\sqrt{s} = 8$ TeV. JHEP **08**, 174 (2014). arXiv:1405.3447 [hep-ex]
15. CMS Collaboration, Search for ZZ resonances in the $2\ell 2\nu$ final state in proton–proton collisions at 13 TeV. JHEP **03**, 003 (2018). arXiv:1711.04370 [hep-ex]
16. B. Lillie, L. Randall, L.T. Wang, The bulk RS KK-gluon at the LHC. JHEP **09**, 074 (2007). arXiv:hep-ph/0701166
17. S. Ask, J.H. Collins, J.R. Forshaw, K. Joshi, A.D. Pilkington, Identifying the colour of TeV-scale resonances. JHEP **01**, 018 (2012). arXiv:1108.2396 [hep-ph]
18. ATLAS Collaboration, Search for $t\bar{t}$ resonances in the lepton plus jets final state with ATLAS using 4.7 fb^{-1} of pp collisions at $\sqrt{s} = 7$ TeV. Phys. Rev. D **88**(1), 012004 (2013). arXiv:1305.2756 [hep-ex]
19. K. Agashe et al., LHC signals from warped extra dimensions. Phys. Rev. D **77**, 015003 (2008). arXiv:hep-ph/0612015
20. ATLAS Collaboration, The ATLAS experiment at the CERN large hadron collider. JINST **3**, S08003 (2008)
21. ATLAS Collaboration, ATLAS insertable B-layer technical design report . CERN-LHCC-2010-013; ATLAS-TDR-19 (2010). https://cds.cern.ch/record/1291633
22. S. Artz et al., Upgrade of the ATLAS central trigger for LHC run-2. JINST **10**(02), C02030 (2015)
23. ATLAS Collaboration, Performance of the ATLAS trigger system in 2015. Eur. Phys. J. C **77**, 317 (2017). arXiv:1611.09661 [hep-ex]
24. S. Frixione, P. Nason, G. Ridolfi, A positive-weight next-to-leading-order Monte Carlo for heavy flavour hadroproduction. JHEP **09**, 126 (2007). arXiv:0707.3088 [hep-ph]
25. E. Re, Single-top Wt-channel production matched with parton showers using the POWHEG method. Eur. Phys. J. C **71**, 1547 (2011). arXiv:1009.2450 [hep-ph]
26. S. Alioli, P. Nason, C. Oleari, E. Re, NLO single-top production matched with shower in POWHEG: s- and t-channel contributions. JHEP **09**, 111 (2009). arXiv:0907.4076 [hep-ph]. Erratum: Erratum: NLO single-top production matched with shower in POWHEG: s-and t-channel contributions, JHEP 02 (2010) 011
27. P. Nason, A new method for combining NLO QCD with shower Monte Carlo algorithms. JHEP **11**, 040 (2004). arXiv:hep-ph/0409146
28. S. Frixione, P. Nason, C. Oleari, Matching NLO QCD computations with parton shower simulations: the POWHEG method. JHEP **11**, 070 (2007). arXiv:0709.2092 [hep-ph]
29. S. Alioli, P. Nason, C. Oleari, E. Re, A general framework for implementing NLO calculations in shower Monte Carlo programs: the POWHEG BOX. JHEP **06**, 043 (2010). arXiv:1002.2581 [hep-ph]
30. H.L. Lai et al., New parton distributions for collider physics. Phys. Rev. D **82**, 074,024 (2010). arXiv:1007.2241 [hep-ph]
31. J. Gao et al., CT10 next-to-next-to-leading order global analysis of QCD. Phys. Rev. D **89**, 033,009 (2014). arXiv:1302.6246 [hep-ph]
32. S. Frixione et al., Single-top hadroproduction in association with a W boson. JHEP **07**, 029 (2008). arXiv:0805.3067 [hep-ph]
33. R. Frederix, E. Re, P. Torrielli, Single-top t-channel hadroproduction in the four-flavour scheme with POWHEG and aMC@NLO. JHEP **09**, 130 (2012). arXiv:1207.5391 [hep-ph]
34. P. Artoisenet, R. Frederix, O. Mattelaer, R. Rietkerk, Automatic spin-entangled decays of heavy resonances in Monte Carlo simulations. JHEP **03**, 015 (2013). arXiv:1212.3460 [hep-ph]
35. T. Sjöstrand, S. Mrenna, P.Z. Skands, PYTHIA 6.4 physics and manual. JHEP **05**, 26 (2006). arXiv:hep-ph/0603175
36. J. Pumplin et al., New generation of parton distributions with uncertainties from global QCD analysis. JHEP **07**, 012 (2002). arXiv:hep-ph/0201195
37. P.Z. Skands, Tuning Monte Carlo generators: the Perugia tunes. Phys. Rev. D **82**, 074,018 (2010). arXiv:1005.3457 [hep-ph]
38. D.J. Lange, The EvtGen particle decay simulation package. Nucl. Instrum. Methods A **462**, 152–155 (2001)
39. J. Kühn, A. Scharf, P. Uwer, Weak interactions in top-quark pair production at hadron colliders: an update. Phys. Rev. D **91**, 014,020 (2015). arXiv:1305.5773 [hep-ph]
40. T. Gleisberg et al., Event generation with SHERPA 1.1. JHEP **02**, 007 (2009). arXiv:1305.5773 [hep-ph]
41. T. Gleisberg, S. Höche, Comix, a new matrix element generator. JHEP **12**, 039 (2008). arXiv:0808.3674 [hep-ph]
42. F. Cascioli, P. Maierhofer, S. Pozzorini, Scattering amplitudes with open loops. Phys. Rev. Lett. **108**, 111,601 (2012). arXiv:1111.5206 [hep-ph]
43. S. Schumann, F. Krauss, A parton shower algorithm based on Catani–Seymour dipole factorisation. JHEP **03**, 038 (2008). arXiv:0709.1027 [hep-ph]
44. S. Höche, F. Krauss, M. Schönherr, F. Siegert, QCD matrix elements + parton showers: the NLO case. JHEP **04**, 027 (2013). arXiv:1207.5030 [hep-ph]
45. R.D. Ball et al., Parton distributions for the LHC run II. JHEP **04**, 040 (2015). arXiv:1410.8849 [hep-ph]
46. R. Gavin, Y. Li, F. Petriello, S. Quackenbush, W physics at the LHC with FEWZ 2.1. Comput. Phys. Commun. **184**, 208–214 (2013). arXiv:1201.5896 [hep-ph]
47. T. Sjöstrand, S. Mrenna, P.Z. Skands, A brief introduction to PYTHIA 8.1. Comput. Phys. Commun. **178**, 852–867 (2008). arXiv:0710.3820 [hep-ph]
48. R.D. Ball et al., Parton distributions with LHC data. Nucl. Phys. B **867**, 244–289 (2013). arXiv:1207.1303 [hep-ph]
49. ATLAS Collaboration, ATLAS Run 1 Pythia 8 tunes, ATL-PHYS-PUB-2014-021, 2014, https://cds.cern.ch/record/1966419

50. R. Bonciani, T. Jezo, M. Klasen, F. Lyonnet, I. Schienbein, Electroweak top-quark pair production at the LHC with Z' bosons to NLO QCD in POWHEG. JHEP **02**, 141 (2016). arXiv:1511.08185 [hep-ph]
51. J. Butterworth et al., PDF4LHC recommendations for LHC run II. J. Phys. G **43**, 023,001 (2016). arXiv:1510.03865 [hep-ph]
52. J. Alwall et al., The automated computation of tree-level and next-to-leading order differential cross sections, and their matching to parton shower simulations. JHEP **07**, 079 (2014). arXiv:1405.0301 [hep-ph]
53. ATLAS Collaboration, The ATLAS simulation infrastructure. Eur. Phys. J. C **70**, 823–874 (2010). arXiv:1005.4568 [physics.ins-det]
54. S. Agostinelli et al., GEANT4: a simulation toolkit. Nucl. Instrum. Methods A **506**, 250–303 (2003)
55. ATLAS Collaboration, The simulation principle and performance of the ATLAS fast calorimeter simulation FastCaloSim (2010). https://cds.cern.ch/record/1300517. Accessed Dec 2017
56. ATLAS Collaboration, Summary of ATLAS Pythia 8 tunes. ATL-PHYS-PUB-2012-003 (2012). https://cds.cern.ch/record/1474107
57. A. Martin, W. Stirling, R. Thorne, G. Watt, Parton distributions for the LHC. Eur. Phys. J. C **63**, 189–285 (2009). arXiv:0901.0002 [hep-ph]
58. ATLAS Collaboration, Topological cell clustering in the ATLAS calorimeters and its performance in LHC run 1. Eur. Phys. J. C **77**, 490 (2017). arXiv:1603.02934 [hep-ex]
59. M. Cacciari, G.P. Salam, G. Soyez, The Anti-k_t jet clustering algorithm. JHEP **04**, 063 (2008). arXiv:0802.1189 [hep-ph]
60. ATLAS Collaboration, Jet energy measurement with the ATLAS detector in proton–proton collisions at $\sqrt{s} = 7$ TeV. Eur. Phys. J. C **73**(3), 2304 (2013). arXiv:1112.6426 [hep-ex]
61. ATLAS Collaboration, Jet calibration and systematic uncertainties for jets reconstructed in the ATLAS detector at $\sqrt{s} = 13$ TeV. ATL-PHYS-PUB-2015-015 (2015). https://cds.cern.ch/record/2037613
62. ATLAS Collaboration, Tagging and suppression of pileup jets with the ATLAS detector. ATLAS-CONF-2014-018 (2014). https://cds.cern.ch/record/1700870
63. ATLAS Collaboration, Topological cell clustering in the ATLAS calorimeters and its performance in LHC Run 1. Eur. Phys. J. C **77**, 490 (2017). arXiv:1603.02934 [hep-ex]
64. D. Krohn, J. Thaler, L.T. Wang, Jet trimming. JHEP **02**, 084 (2010). arXiv:0912.1342 [hep-ph]
65. ATLAS Collaboration, Performance of jet substructure techniques for large-R jets in proton–proton collisions at $\sqrt{s} = 7$ TeV using the ATLAS detector. JHEP **09**, 076 (2013). arXiv:1306.4945 [hep-ex]
66. S. Catani, Y.L. Dokshitzer, M. Olsson, G. Turnock, B. Webber, New clustering algorithm for multi-jet cross-sections in e^+e^- annihilation. Phys. Lett. B **269**, 432–438 (1991)
67. S.D. Ellis, D.E. Soper, Successive combination jet algorithm for hadron collisions. Phys. Rev. D **48**, 3160–3166 (1993). arXiv:hep-ph/9305266
68. S. Catani, Y.L. Dokshitzer, M. Seymour, B. Webber, Longitudinally invariant K_t clustering algorithms for hadron hadron collisions. Nucl. Phys. B **406**, 187–224 (1993)
69. ATLAS Collaboration, Performance of jet substructure techniques in early $\sqrt{s} = 13$ TeV pp collisions with the ATLAS detector. ATLAS-CONF-2015-035 (2015). https://cds.cern.ch/record/2041462
70. ATLAS Collaboration, Jet mass reconstruction with the ATLAS Detector in early run 2 data. ATLAS-CONF-2016-035 (2016). https://cds.cern.ch/record/2200211
71. ATLAS Collaboration, Boosted hadronic top identification at ATLAS for early 13 TeV data. ATL-PHYS-PUB-2015-053 (2015). https://cds.cern.ch/record/2116351
72. J. Thaler, K. Van Tilburg, Identifying boosted objects with N-subjettiness. JHEP **03**, 015 (2011). arXiv:1011.2268 [hep-ph]
73. J. Thaler, K. Van Tilburg, Maximizing boosted top identification by minimizing N-subjettiness. JHEP **02**, 093 (2012). arXiv:1108.2701 [hep-ph]
74. ATLAS Collaboration, Expected performance of boosted Higgs ($\rightarrow b\bar{b}$) Boson identification with the ATLAS detector at $\sqrt{s} = 13$ TeV. ATL-PHYS-PUB-2015-035 (2015). https://cds.cern.ch/record/2042155
75. ATLAS Collaboration, Expected performance of the ATLAS b-tagging algorithms in run-2. ATL-PHYS-PUB-2015-022 (2015). https://cds.cern.ch/record/2037697
76. M. Cacciari, G.P. Salam, Dispelling the N^3 myth for the k_t jet-finder. Phys. Lett. B **641**, 57–61 (2006). arXiv:hep-ph/0512210
77. M. Cacciari, G.P. Salam, G. Soyez, FastJet user manual. Eur. Phys. J. **C72**, 1896 (2012). arXiv:1111.6097 [hep-ph]
78. ATLAS Collaboration, Electron efficiency measurements with the ATLAS detector using the 2012 LHC proton–proton collision data. ATLAS-CONF-2014-032 (2014). https://cds.cern.ch/record/1706245
79. ATLAS Collaboration, Performance of missing transverse momentum reconstruction with the ATLAS detector in the first proton–proton collisions at $\sqrt{s} = 13$ TeV. ATL-PHYS-PUB-2015-027 (2015). https://cds.cern.ch/record/2037904
80. K.A. Olive et al., Particle Data Group, Review of particle physics. Chin. Phys. C **38**, 090,001 (2014)
81. ATLAS Collaboration, Measurement of the top quark pair production cross-section with ATLAS in the single lepton channel. Phys. Lett. B **711**, 244–263 (2012). arXiv:1201.1889 [hep-ex]
82. ATLAS Collaboration. Measurement of the charge asymmetry in top quark pair production in pp collisions at $\sqrt{s} = 7$ TeV using the ATLAS detector. Eur. Phys. J. C **72**, 2039 (2012). arXiv:1203.4211 [hep-ex]
83. ATLAS Collaboration, Measurements of top quark pair relative differential cross-sections with ATLAS in pp collisions at $\sqrt{s} = 7$ TeV. Eur. Phys. J. C **73**, 2261 (2013). arXiv:1207.5644 [hep-ex]
84. ATLAS Collaboration, Luminosity determination in pp collisions at $\sqrt{s} = 8$ TeV using the ATLAS detector at the LHC. Eur. Phys. J. C **76**(12), 653 (2016). arXiv:1608.03953 [hep-ex]
85. ATLAS Collaboration, Search for the Standard Model Higgs and Z Boson decays to $J/\psi\gamma$: HL-LHC projections. ATL-PHYS-PUB-2015-043 (2015). https://cds.cern.ch/record/2054550
86. ATLAS Collaboration, Muon reconstruction performance of the ATLAS detector in proton–proton collision data at $\sqrt{s}$ =13 TeV. Eur. Phys. J. C **76**(5), 292 (2016). arXiv:1603.05598 [hep-ex]
87. ATLAS Collaboration, Jet energy scale measurements and their systematic uncertainties in proton–proton collisions at $\sqrt{s} = 13$ TeV with the ATLAS detector. Phys. Rev. D **96**, 072,002 (2017). arXiv:1703.09665 [hep-ex]
88. ATLAS Collaboration, Performance of b-jet identification in the ATLAS experiment. JINST **11**, P04,008 (2016). arXiv:1512.01094 [hep-ex]
89. ATLAS Collaboration, Optimisation of the ATLAS b-tagging performance for the 2016 LHC Run. ATL-PHYS-PUB-2016-012 (2016). https://cds.cern.ch/record/2160731
90. ATLAS Collaboration, Identification of high transverse momentum top quarks in pp collisions at $\sqrt{s} = 8$ TeV with the ATLAS detector. JHEP **06**, 093 (2016). arXiv:1603.03127 [hep-ex]
91. M. Cacciari, M. Czakon, M. Mangano, A. Mitov, P. Nason, Top-pair production at hadron colliders with next-to-next-to-leading logarithmic soft-gluon resummation. Phys. Lett. B **710**, 612–622 (2012). arXiv:1111.5869 [hep-ph]
92. M. Beneke, P. Falgari, S. Klein, C. Schwinn, Hadronic top-quark pair production with NNLL threshold resummation. Nucl. Phys. B **855**, 695–741 (2012). arXiv:1109.1536 [hep-ph]

93. P. Baernreuther, M. Czakon, A. Mitov, Percent Level precision physics at the tevatron: first genuine NNLO QCD Corrections to $q\bar{q} \to t\bar{t} + X$. Phys. Rev. Lett. **109**, 132,001 (2012). arXiv:1204.5201 [hep-ph]
94. M. Czakon, A. Mitov, NNLO corrections to top-pair production at hadron colliders: the all-fermionic scattering channels. JHEP **12**, 054 (2012). arXiv:1207.0236 [hep-ph]
95. M. Czakon, A. Mitov, NNLO corrections to top pair production at hadron colliders: the quark-gluon reaction. JHEP **01**, 080 (2013). arXiv:1210.6832 [hep-ph]
96. M. Czakon, P. Fiedler, A. Mitov, The total top quark pair production cross-section at hadron colliders through $\mathcal{O}(\alpha_S^4)$. Phys. Rev. Lett. **110**, 252,004 (2013). arXiv:1303.6254 [hep-ph]
97. M. Czakon, A. Mitov, Top++: a program for the calculation of the top-pair cross-section at hadron colliders. Comput. Phys. Commun. **185**, 2930 (2014). arXiv:1112.5675 [hep-ph]
98. M. Botje et al., The PDF4LHC working group interim recommendations (2011). arXiv:1101.0538 [hep-ph]
99. A. Martin, W. Stirling, R. Thorne, G. Watt, Uncertainties on α_S in global PDF analyses and implications for predicted hadronic cross sections. Eur. Phys. J. C **64**, 653–680 (2009). arXiv:0905.3531 [hep-ph]
100. M. Bahr et al., Herwig++ physics and manual. Eur. Phys. J. C **58**, 639–707 (2008). arXiv:0803.0883 [hep-ph]
101. J. Bellm et al., Herwig 7.0/Herwig++ 3.0 release note. Eur. Phys. J. **C76**(4), 196 (2016). arXiv:1512.01178 [hep-ph]
102. ATLAS Collaboration, Measurement of $t\bar{t}$ production with a veto on additional central jet activity in pp collisions at $\sqrt{s} = 7$ TeV using the ATLAS detector. Eur. Phys. J. C **72**, 2043 (2012). arXiv:1203.5015 [hep-ex]
103. ATLAS Collaboration, Measurement of the $t\bar{t}$ production cross-section as a function of jet multiplicity and jet transverse momentum in 7 TeV proton–proton collisions with the ATLAS detector. JHEP **01**, 020 (2015). arXiv:1407.0891 [hep-ex]
104. ATLAS Collaboration, Comparison of Monte Carlo generator predictions to ATLAS measurements of top pair production at 7 TeV. ATL-PHYS-PUB-2015-002 (2015). https://cds.cern.ch/record/1981319
105. M. Czakon, D. Heymes, A. Mitov, Dynamical scales for multi-TeV top-pair production at the LHC. JHEP **04**, 071 (2017). arXiv:1606.03350 [hep-ph]
106. N. Kidonakis, Two-loop soft anomalous dimensions for single top quark associated production with a W^- or H^-. Phys. Rev. D **82**, 054,018 (2010). arXiv:1005.4451 [hep-ph]
107. N. Kidonakis, NNLL resummation for s-channel single top quark production. Phys. Rev. D **81**, 054,028 (2010). arXiv:1001.5034 [hep-ph]
108. N. Kidonakis, Next-to-next-to-leading-order collinear and soft gluon corrections for t-channel single top quark production. Phys. Rev. D **83**, 091,503 (2011). arXiv:1103.2792 [hep-ph]
109. G. Choudalakis, On hypothesis testing, trials factor, hypertests and the BumpHunter (2011). arXiv:1101.0390 [physics.data-an]
110. L. Lyons, Open statistical issues in particle physics. Ann. Appl. Stat. **2**, 887–915 (2008). arXiv:0811.1663 [Stat.AP]
111. A.L. Read, Presentation of search results: the CL_s technique. J. Phys. G **28**, 2693–2704 (2002)
112. ATLAS Collaboration, ATLAS computing acknowledgements. ATL-GEN-PUB-2016-002. https://cds.cern.ch/record/2202407

ATLAS Collaboration

M. Aaboud[34d], G. Aad[99], B. Abbott[124], O. Abdinov[13,*], B. Abeloos[128], S. H. Abidi[164], O. S. AbouZeid[143], N. L. Abraham[153], H. Abramowicz[158], H. Abreu[157], Y. Abulaiti[6], B. S. Acharya[67a,67b,l], S. Adachi[160], L. Adamczyk[41a], J. Adelman[119], M. Adersberger[112], A. Adiguzel[12c], T. Adye[140], A. A. Affolder[143], Y. Afik[157], C. Agheorghiesei[27c], J. A. Aguilar-Saavedra[135f,135a], F. Ahmadov[80,ai], G. Aielli[74a,74b], S. Akatsuka[83], T. P. A. Åkesson[95], E. Akilli[55], A. V. Akimov[108], G. L. Alberghi[23b,23a], J. Albert[174], P. Albicocco[52], M. J. Alconada Verzini[86], S. Alderweireldt[117], M. Aleksa[35], I. N. Aleksandrov[80], C. Alexa[27b], G. Alexander[158], T. Alexopoulos[10], M. Alhroob[124], B. Ali[137], M. Aliev[68a,68b], G. Alimonti[69a], J. Alison[36], S. P. Alkire[145], C. Allaire[128], B. M. M. Allbrooke[153], B. W. Allen[127], P. P. Allport[21], A. Aloisio[70a,70b], A. Alonso[39], F. Alonso[86], C. Alpigiani[145], A. A. Alshehri[58], M. I. Alstaty[99], B. Alvarez Gonzalez[35], D. Álvarez Piqueras[172], M. G. Alviggi[70a,70b], B. T. Amadio[18], Y. Amaral Coutinho[141a], L. Ambroz[131], C. Amelung[26], D. Amidei[103], S. P. Amor Dos Santos[135a,135c], S. Amoroso[35], C. S. Amrouche[55], C. Anastopoulos[146], L. S. Ancu[55], N. Andari[21], T. Andeen[11], C. F. Anders[62b], J. K. Anders[20], K. J. Anderson[36], A. Andreazza[69a,69b], V. Andrei[62a], S. Angelidakis[37], I. Angelozzi[118], A. Angerami[38], A. V. Anisenkov[120b,120a], A. Annovi[72a], C. Antel[62a], M. T. Anthony[146], M. Antonelli[52], D. J. A. Antrim[169], F. Anulli[73a], M. Aoki[81], L. Aperio Bella[35], G. Arabidze[104], Y. Arai[81], J. P. Araque[135a], V. Araujo Ferraz[141a], R. Araujo Pereira[141a], A. T. H. Arce[49], R. E. Ardell[91], F. A. Arduh[86], J-F. Arguin[107], S. Argyropoulos[78], A. J. Armbruster[35], L. J. Armitage[90], O. Arnaez[164], H. Arnold[118], M. Arratia[31], O. Arslan[24], A. Artamonov[109,*], G. Artoni[131], S. Artz[97], S. Asai[160], N. Asbah[46], A. Ashkenazi[158], E. M. Asimakopoulou[170], L. Asquith[153], K. Assamagan[29], R. Astalos[28a], R. J. Atkin[32a], M. Atkinson[171], N. B. Atlay[148], K. Augsten[137], G. Avolio[35], R. Avramidou[61a], B. Axen[18], M. K. Ayoub[15a], G. Azuelos[107,av], A. E. Baas[62a], M. J. Baca[21], H. Bachacou[142], K. Bachas[68a,68b], M. Backes[131], P. Bagnaia[73a,73b], M. Bahmani[42], H. Bahrasemani[149], A. J. Bailey[172], J. T. Baines[140], M. Bajic[39], O. K. Baker[181], P. J. Bakker[118], D. Bakshi Gupta[93], E. M. Baldin[120b,120a], P. Balek[178], F. Balli[142], W. K. Balunas[132], E. Banas[42], A. Bandyopadhyay[24], Sw. Banerjee[179,i], A. A. E. Bannoura[180], L. Barak[158], W. M. Barbe[37], E. L. Barberio[102], D. Barberis[56b,56a], M. Barbero[99], T. Barillari[113], M-S. Barisits[35], J. T. Barkeloo[127], T. Barklow[150], N. Barlow[31], R. Barnea[157], S. L. Barnes[61c], B. M. Barnett[140], R. M. Barnett[18], Z. Barnovska-Blenessy[61a], A. Baroncelli[75a], G. Barone[26], A. J. Barr[131], L. Barranco Navarro[172], F. Barreiro[96], J. Barreiro Guimarães da Costa[15a],

R. Bartoldus[150], A. E. Barton[87], P. Bartos[28a], A. Basalaev[133], A. Bassalat[128], R. L. Bates[58], S. J. Batista[164], S. Batlamous[34e], J. R. Batley[31], M. Battaglia[143], M. Bauce[73a,73b], F. Bauer[142], K. T. Bauer[169], H. S. Bawa[150,j], J. B. Beacham[122], M. D. Beattie[87], T. Beau[94], P. H. Beauchemin[167], P. Bechtle[24], H. C. Beck[54], H. P. Beck[20,r], K. Becker[53], M. Becker[97], C. Becot[121], A. Beddall[12d], A. J. Beddall[12a], V. A. Bednyakov[80], M. Bedognetti[118], C. P. Bee[152], T. A. Beermann[35], M. Begalli[141a], M. Begel[29], A. Behera[152], J. K. Behr[46], A. S. Bell[92], G. Bella[158], L. Bellagamba[23b], A. Bellerive[33], M. Bellomo[157], K. Belotskiy[110], N. L. Belyaev[110], O. Benary[158,*], D. Benchekroun[34a], M. Bender[112], N. Benekos[10], Y. Benhammou[158], E. Benhar Noccioli[181], J. Benitez[78], D. P. Benjamin[49], M. Benoit[55], J. R. Bensinger[26], S. Bentvelsen[118], L. Beresford[131], M. Beretta[52], D. Berge[46], E. Bergeaas Kuutmann[170], N. Berger[5], L. J. Bergsten[26], J. Beringer[18], S. Berlendis[59], N. R. Bernard[100], G. Bernardi[94], C. Bernius[150], F. U. Bernlochner[24], T. Berry[91], P. Berta[97], C. Bertella[15a], G. Bertoli[45a,45b], I. A. Bertram[87], G. J. Besjes[39], O. Bessidskaia Bylund[45a,45b], M. Bessner[46], N. Besson[142], A. Bethani[98], S. Bethke[113], A. Betti[24], A. J. Bevan[90], J. Beyer[113], R. M. Bianchi[134], O. Biebel[112], D. Biedermann[19], R. Bielski[98], K. Bierwagen[97], N. V. Biesuz[72a,72b], M. Biglietti[75a], T. R. V. Billoud[107], M. Bindi[54], A. Bingul[12d], C. Bini[73a,73b], S. Biondi[23b,23a], T. Bisanz[54], J. P. Biswal[158], C. Bittrich[48], D. M. Bjergaard[49], J. E. Black[150], K. M. Black[25], R. E. Blair[6], T. Blazek[28a], I. Bloch[46], C. Blocker[26], A. Blue[58], U. Blumenschein[90], Dr. Blunier[144a], G. J. Bobbink[118], V. S. Bobrovnikov[120b,120a], S. S. Bocchetta[95], A. Bocci[49], D. Boerner[180], D. Bogavac[112], A. G. Bogdanchikov[120b,120a], C. Bohm[45a], V. Boisvert[91], P. Bokan[170,aa], T. Bold[41a], A. S. Boldyrev[111], A. E. Bolz[62b], M. Bomben[94], M. Bona[90], J. S. B. Bonilla[127], M. Boonekamp[142], A. Borisov[139], G. Borissov[87], J. Bortfeldt[35], D. Bortoletto[131], V. Bortolotto[74a,74b], D. Boscherini[23b], M. Bosman[14], J. D. Bossio Sola[30], J. Boudreau[134], E. V. Bouhova-Thacker[87], D. Boumediene[37], C. Bourdarios[128], S. K. Boutle[58], A. Boveia[122], J. Boyd[35], I. R. Boyko[80], A. J. Bozson[91], J. Bracinik[21], N. Brahimi[99], A. Brandt[8], G. Brandt[180], O. Brandt[62a], F. Braren[46], U. Bratzler[161], B. Brau[100], J. E. Brau[127], W. D. Breaden Madden[58], K. Brendlinger[46], A. J. Brennan[102], L. Brenner[46], R. Brenner[170], S. Bressler[178], B. Brickwedde[97], D. L. Briglin[21], D. Britton[58], D. Britzger[62b], I. Brock[24], R. Brock[104], G. Brooijmans[38], T. Brooks[91], W. K. Brooks[144b], E. Brost[119], J. H Broughton[21], P. A. Bruckman de Renstrom[42], D. Bruncko[28b], A. Bruni[23b], G. Bruni[23b], L. S. Bruni[118], S. Bruno[74a,74b], B.H. Brunt[31], M. Bruschi[23b], N. Bruscino[134], P. Bryant[36], L. Bryngemark[46], T. Buanes[17], Q. Buat[35], P. Buchholz[148], A. G. Buckley[58], I. A. Budagov[80], F. Buehrer[53], M. K. Bugge[130], O. Bulekov[110], D. Bullock[8], T. J. Burch[119], S. Burdin[88], C. D. Burgard[118], A. M. Burger[5], B. Burghgrave[119], K. Burka[42], S. Burke[140], I. Burmeister[47], J. T. P. Burr[131], D. Büscher[53], V. Büscher[97], E. Buschmann[54], P. Bussey[58], J. M. Butler[25], C. M. Buttar[58], J. M. Butterworth[92], P. Butti[35], W. Buttinger[35], A. Buzatu[155], A. R. Buzykaev[120b,120a], G. Cabras[23b,23a], S. Cabrera Urbán[172], D. Caforio[137], H. Cai[171], V. M. M. Cairo[2], O. Cakir[4a], N. Calace[55], P. Calafiura[18], A. Calandri[99], G. Calderini[94], P. Calfayan[66], G. Callea[40b,40a], L. P. Caloba[141a], S. Calvente Lopez[96], D. Calvet[37], S. Calvet[37], T. P. Calvet[152], M. Calvetti[72a,72b], R. Camacho Toro[94], S. Camarda[35], P. Camarri[74a,74b], D. Cameron[130], R. Caminal Armadans[100], C. Camincher[35], S. Campana[35], M. Campanelli[92], A. Camplani[69a,69b], A. Campoverde[148], V. Canale[70a,70b], M. Cano Bret[61c], J. Cantero[125], T. Cao[158], Y. Cao[171], M. D. M. Capeans Garrido[35], I. Caprini[27b], M. Caprini[27b], M. Capua[40b,40a], R. M. Carbone[38], R. Cardarelli[74a], F. Cardillo[53], I. Carli[138], T. Carli[35], G. Carlino[70a], B. T. Carlson[134], L. Carminati[69a,69b], R. M. D. Carney[45a,45b], S. Caron[117], E. Carquin[144b], S. Carrá[69a,69b], G. D. Carrillo-Montoya[35], D. Casadei[32b], M. P. Casado[14,e], A. F. Casha[164], M. Casolino[14], D. W. Casper[169], R. Castelijn[118], V. Castillo Gimenez[172], N. F. Castro[135a,135e], A. Catinaccio[35], J. R. Catmore[130], A. Cattai[35], J. Caudron[24], V. Cavaliere[29], E. Cavallaro[14], D. Cavalli[69a], M. Cavalli-Sforza[14], V. Cavasinni[72a,72b], E. Celebi[12b], F. Ceradini[75a,75b], L. Cerda Alberich[172], A. S. Cerqueira[141b], A. Cerri[153], L. Cerrito[74a,74b], F. Cerutti[18], A. Cervelli[23b,23a], S. A. Cetin[12b], A. Chafaq[34a], DC Chakraborty[119], S. K. Chan[60], W. S. Chan[118], Y. L. Chan[64a], P. Chang[171], J. D. Chapman[31], D. G. Charlton[21], C. C. Chau[33], C. A. Chavez Barajas[153], S. Che[122], A. Chegwidden[104], S. Chekanov[6], S. V. Chekulaev[165a], G. A. Chelkov[80,au], M. A. Chelstowska[35], C. Chen[61a], C. Chen[79], H. Chen[29], J. Chen[61a], J. Chen[38], S. Chen[15b], S. Chen[132], X. Chen[15c,at], Y. Chen[82], Y. -H. Chen[46], H. C. Cheng[103], H. J. Cheng[15d], A. Cheplakov[80], E. Cheremushkina[139], R. Cherkaoui El Moursli[34e], E. Cheu[7], K. Cheung[65], L. Chevalier[142], V. Chiarella[52], G. Chiarelli[72a], G. Chiodini[68a], A. S. Chisholm[35], A. Chitan[27b], I. Chiu[160], Y. H. Chiu[174], M. V. Chizhov[80], K. Choi[66], A. R. Chomont[128], S. Chouridou[159], Y. S. Chow[118], V. Christodoulou[92], M. C. Chu[64a], J. Chudoba[136], A. J. Chuinard[101], J. J. Chwastowski[42], L. Chytka[126], D. Cinca[47], V. Cindro[89], I. A. Cioară[24], A. Ciocio[18], F. Cirotto[70a,70b], Z. H. Citron[178], M. Citterio[69a], A. Clark[55], M. R. Clark[38], P. J. Clark[50], C. Clement[45a,45b], Y. Coadou[99], M. Cobal[67a,67c], A. Coccaro[56b,56a], J. Cochran[79], A. E. C. Coimbra[178], L. Colasurdo[117], B. Cole[38], A. P. Colijn[118], J. Collot[59], P. Conde Muiño[135a,135b], E. Coniavitis[53], S. H. Connell[32b], I. A. Connelly[98], S. Constantinescu[27b], F. Conventi[70a,aw], A. M. Cooper-Sarkar[131], F. Cormier[173], K. J. R. Cormier[164], M. Corradi[73a,73b], E. E. Corrigan[95], F. Corriveau[101,ag], A. Cortes-Gonzalez[35], M. J. Costa[172], D. Costanzo[146], G. Cottin[31], G. Cowan[91], B. E. Cox[98], J. Crane[98], K. Cranmer[121], S. J. Crawley[58], R. A. Creager[132], G. Cree[33], S. Crépé-Renaudin[59], F. Crescioli[94], M. Cristinziani[24], V. Croft[121], G. Crosetti[40b,40a], A. Cueto[96], T. Cuhadar Donszelmann[146], A. R. Cukierman[150], M. Curatolo[52], J. Cúth[97],

S. Czekierda[42], P. Czodrowski[35], M. J. Da Cunha Sargedas De Sousa[61b,135b], C. Da Via[98], W. Dabrowski[41a], T. Dado[28a,aa], S. Dahbi[34e], T. Dai[103], F. Dallaire[107], C. Dallapiccola[100], M. Dam[39], G. D'amen[23b,23a], J. R. Dandoy[132], M. F. Daneri[30], N. P. Dang[179,i], N.D Dann[98], M. Danninger[173], V. Dao[35], G. Darbo[56b], S. Darmora[8], O. Dartsi[5], A. Dattagupta[127], T. Daubney[46], S. D'Auria[58], W. Davey[24], C. David[46], T. Davidek[138], D. R. Davis[49], E. Dawe[102], I. Dawson[146], K. De[8], R. de Asmundis[70a], A. De Benedetti[124], S. De Castro[23b,23a], S. De Cecco[73a,73b], N. De Groot[117], P. de Jong[118], H. De la Torre[104], F. De Lorenzi[79], A. De Maria[54,s], D. De Pedis[73a], A. De Salvo[73a], U. De Sanctis[74a,74b], A. De Santo[153], K. De Vasconcelos Corga[99], J. B. De Vivie De Regie[128], C. Debenedetti[143], D. V. Dedovich[80], N. Dehghanian[3], M. Del Gaudio[40b,40a], J. Del Peso[96], D. Delgove[128], F. Deliot[142], C. M. Delitzsch[7], M. Della Pietra[70a,70b], D. della Volpe[55], A. Dell'Acqua[35], L. Dell'Asta[25], M. Delmastro[5], C. Delporte[128], P. A. Delsart[59], D. A. DeMarco[164], S. Demers[181], M. Demichev[80], S. P. Denisov[139], D. Denysiuk[118], L. D'Eramo[94], D. Derendarz[42], J. E. Derkaoui[34d], F. Derue[94], P. Dervan[88], K. Desch[24], C. Deterre[46], K. Dette[164], M. R. Devesa[30], P. O. Deviveiros[35], A. Dewhurst[140], S. Dhaliwal[26], F. A. Di Bello[55], A. Di Ciaccio[74a,74b], L. Di Ciaccio[5], W. K. Di Clemente[132], C. Di Donato[70a,70b], A. Di Girolamo[35], B. Di Micco[75a,75b], R. Di Nardo[35], K. F. Di Petrillo[60], A. Di Simone[53], R. Di Sipio[164], D. Di Valentino[33], C. Diaconu[99], M. Diamond[164], F. A. Dias[39], T. Dias do Vale[135a], M. A. Diaz[144a], J. Dickinson[18], E. B. Diehl[103], J. Dietrich[19], S. Díez Cornell[46], A. Dimitrievska[18], J. Dingfelder[24], F. Dittus[35], F. Djama[99], T. Djobava[156b], J. I. Djuvsland[62a], M. A. B. do Vale[141c], M. Dobre[27b], D. Dodsworth[26], C. Doglioni[95], J. Dolejsi[138], Z. Dolezal[138], M. Donadelli[141d], J. Donini[37], A. D'onofrio[90], M. D'Onofrio[88], J. Dopke[140], A. Doria[70a], M. T. Dova[86], A. T. Doyle[58], E. Drechsler[54], E. Dreyer[149], T. Dreyer[54], M. Dris[10], Y. Du[61b], J. Duarte-Campderros[158], F. Dubinin[108], A. Dubreuil[55], E. Duchovni[178], G. Duckeck[112], A. Ducourthial[94], O. A. Ducu[107,z], D. Duda[118], A. Dudarev[35], A. Chr. Dudder[97], E. M. Duffield[18], L. Duflot[128], M. Dührssen[35], C. Dülsen[180], M. Dumancic[178], A. E. Dumitriu[27b,d], A. K. Duncan[58], M. Dunford[62a], A. Duperrin[99], H. Duran Yildiz[4a], M. Düren[57], A. Durglishvili[156b], D. Duschinger[48], B. Dutta[46], D. Duvnjak[1], M. Dyndal[46], B. S. Dziedzic[42], C. Eckardt[46], K. M. Ecker[113], R. C. Edgar[103], T. Eifert[35], G. Eigen[17], K. Einsweiler[18], T. Ekelof[170], M. El Kacimi[34c], R. El Kosseifi[99], V. Ellajosyula[99], M. Ellert[170], F. Ellinghaus[180], A. A. Elliot[174], N. Ellis[35], J. Elmsheuser[29], M. Elsing[35], D. Emeliyanov[140], Y. Enari[160], J. S. Ennis[176], M. B. Epland[49], J. Erdmann[47], A. Ereditato[20], S. Errede[171], M. Escalier[128], C. Escobar[172], B. Esposito[52], O. Estrada Pastor[172], A. I. Etienvre[142], E. Etzion[158], H. Evans[66], A. Ezhilov[133], M. Ezzi[34e], F. Fabbri[23b,23a], L. Fabbri[23b,23a], V. Fabiani[117], G. Facini[92], R. M. Faisca Rodrigues Pereira[135a], R. M. Fakhrutdinov[139], S. Falciano[73a], P. J. Falke[5], S. Falke[5], J. Faltova[138], Y. Fang[15a], M. Fanti[69a,69b], A. Farbin[8], A. Farilla[75a], E. M. Farina[71a,71b], T. Farooque[104], S. Farrell[18], S. M. Farrington[176], P. Farthouat[35], F. Fassi[34e], P. Fassnacht[35], D. Fassouliotis[9], M. Faucci Giannelli[50], A. Favareto[56b,56a], W. J. Fawcett[55], L. Fayard[128], O. L. Fedin[133,n], W. Fedorko[173], M. Feickert[43], S. Feigl[130], L. Feligioni[99], C. Feng[61b], E. J. Feng[35], M. Feng[49], M. J. Fenton[58], A. B. Fenyuk[139], L. Feremenga[8], J. Ferrando[46], A. Ferrari[170], P. Ferrari[118], R. Ferrari[71a], D. E. Ferreira de Lima[62b], A. Ferrer[172], D. Ferrere[55], C. Ferretti[103], F. Fiedler[97], A. Filipčič[89], F. Filthaut[117], M. Fincke-Keeler[174], K. D. Finelli[25], M. C. N. Fiolhais[135a,135c,a], L. Fiorini[172], C. Fischer[14], W. C. Fisher[104], N. Flaschel[46], I. Fleck[148], P. Fleischmann[103], R. R. M. Fletcher[132], T. Flick[180], B. M. Flierl[112], L. M. Flores[132], L. R. Flores Castillo[64a], N. Fomin[17], G. T. Forcolin[98], A. Formica[142], F. A. Förster[14], A. C. Forti[98], A. G. Foster[21], D. Fournier[128], H. Fox[87], S. Fracchia[146], P. Francavilla[72a,72b], M. Franchini[23b,23a], S. Franchino[62a], D. Francis[35], L. Franconi[130], M. Franklin[60], M. Frate[169], M. Fraternali[71a,71b], D. Freeborn[92], S. M. Fressard-Batraneanu[35], B. Freund[107], W. S. Freund[141a], D. Froidevaux[35], J. A. Frost[131], C. Fukunaga[161], T. Fusayasu[114], J. Fuster[172], O. Gabizon[157], A. Gabrielli[23b,23a], A. Gabrielli[18], G. P. Gach[41a], S. Gadatsch[55], P. Gadow[113], G. Gagliardi[56b,56a], L. G. Gagnon[107], C. Galea[27b], B. Galhardo[135a,135c], E. J. Gallas[131], B. J. Gallop[140], P. Gallus[137], G. Galster[39], R. Gamboa Goni[90], K. K. Gan[122], S. Ganguly[178], Y. Gao[88], Y. S. Gao[150,j], C. García[172], J. E. García Navarro[172], J. A. García Pascual[15a], M. Garcia-Sciveres[18], R. W. Gardner[36], N. Garelli[150], V. Garonne[130], K. Gasnikova[46], A. Gaudiello[56b,56a], G. Gaudio[71a], I. L. Gavrilenko[108], A. Gavrilyuk[109], C. Gay[173], G. Gaycken[24], E. N. Gazis[10], C. N. P. Gee[140], J. Geisen[54], M. Geisen[97], M. P. Geisler[62a], K. Gellerstedt[45a,45b], C. Gemme[56b], M. H. Genest[59], C. Geng[103], S. Gentile[73a,73b], C. Gentsos[159], S. George[91], D. Gerbaudo[14], G. Gessner[47], S. Ghasemi[148], M. Ghneimat[24], B. Giacobbe[23b], S. Giagu[73a,73b], N. Giangiacomi[23b,23a], P. Giannetti[72a], S. M. Gibson[91], M. Gignac[143], D. Gillberg[33], G. Gilles[180], D. M. Gingrich[3,av], M. P. Giordani[67a,67c], F. M. Giorgi[23b], P. F. Giraud[142], P. Giromini[60], G. Giugliarelli[67a,67c], D. Giugni[69a], F. Giuli[131], M. Giulini[62b], S. Gkaitatzis[159], I. Gkialas[9,h], E. L. Gkougkousis[14], P. Gkountoumis[10], L. K. Gladilin[111], C. Glasman[96], J. Glatzer[14], P. C. F. Glaysher[46], A. Glazov[46], M. Goblirsch-Kolb[26], J. Godlewski[42], S. Goldfarb[102], T. Golling[55], D. Golubkov[139], A. Gomes[135a,135b,135d], R. Goŋcalo[135a], R. Goncalves Gama[141b], G. Gonella[53], L. Gonella[21], A. Gongadze[80], F. Gonnella[21], J. L. Gonski[60], S. González de la Hoz[172], S. Gonzalez-Sevilla[55], L. Goossens[35], P. A. Gorbounov[109], H. A. Gordon[29], B. Gorini[35], E. Gorini[68a,68b], A. Gorišek[89], A. T. Goshaw[49], C. Gössling[47], M. I. Gostkin[80], C. A. Gottardo[24], C. R. Goudet[128], D. Goujdami[34c], A. G. Goussiou[145], N. Govender[32b,b], C. Goy[5], E. Gozani[157], I. Grabowska-Bold[41a], P. O. J. Gradin[170],

E. C. Graham[88], J. Gramling[169], E. Gramstad[130], S. Grancagnolo[19], V. Gratchev[133], P. M. Gravila[27f], C. Gray[58], H. M. Gray[18], Z. D. Greenwood[93,al], C. Grefe[24], K. Gregersen[92], I. M. Gregor[46], P. Grenier[150], K. Grevtsov[46], J. Griffiths[8], A. A. Grillo[143], K. Grimm[150], S. Grinstein[14,ab], Ph. Gris[37], J.-F. Grivaz[128], S. Groh[97], E. Gross[178], J. Grosse-Knetter[54], G. C. Grossi[93], Z. J. Grout[92], C. Grud[103], A. Grummer[116], L. Guan[103], W. Guan[179], J. Guenther[35], A. Guerguichon[128], F. Guescini[165a], D. Guest[169], R. Gugel[53], B. Gui[122], T. Guillemin[5], S. Guindon[35], U. Gul[58], C. Gumpert[35], J. Guo[61c], W. Guo[103], Y. Guo[61a,p], Z. Guo[99], R. Gupta[43], S. Gurbuz[12c], G. Gustavino[124], B. J. Gutelman[157], P. Gutierrez[124], C. Gutschow[92], C. Guyot[142], M. P. Guzik[41a], C. Gwenlan[131], C. B. Gwilliam[88], A. Haas[121], C. Haber[18], H. K. Hadavand[8], N. Haddad[34e], A. Hadef[61a], S. Hageböck[24], M. Hagihara[166], H. Hakobyan[182,*], M. Haleem[175], J. Haley[125], G. Halladjian[104], G. D. Hallewell[99], K. Hamacher[180], P. Hamal[126], K. Hamano[174], A. Hamilton[32a], G. N. Hamity[146], K. Han[61a,ak], L. Han[61a], S. Han[15d], K. Hanagaki[81,x], M. Hance[143], D. M. Handl[112], B. Haney[132], R. Hankache[94], P. Hanke[62a], E. Hansen[95], J. B. Hansen[39], J. D. Hansen[39], M. C. Hansen[24], P. H. Hansen[39], K. Hara[166], A. S. Hard[179], T. Harenberg[180], S. Harkusha[105], P. F. Harrison[176], N. M. Hartmann[112], Y. Hasegawa[147], A. Hasib[50], S. Hassani[142], S. Haug[20], R. Hauser[104], L. Hauswald[48], L. B. Havener[38], M. Havranek[137], C. M. Hawkes[21], R. J. Hawkings[35], D. Hayden[104], C. Hayes[152], C. P. Hays[131], J. M. Hays[90], H. S. Hayward[88], S. J. Haywood[140], M. P. Heath[50], V. Hedberg[95], L. Heelan[8], S. Heer[24], K. K. Heidegger[53], J. Heilman[33], S. Heim[46], T. Heim[18], B. Heinemann[46,u], J. J. Heinrich[112], L. Heinrich[121], C. Heinz[57], J. Hejbal[136], L. Helary[35], A. Held[173], S. Hellesund[130], S. Hellman[45a,45b], C. Helsens[35], R. C. W. Henderson[87], Y. Heng[179], S. Henkelmann[173], A. M. Henriques Correia[35], G. H. Herbert[19], H. Herde[26], V. Herget[175], Y. Hernández Jiménez[32c], H. Herr[97], G. Herten[53], R. Hertenberger[112], L. Hervas[35], T. C. Herwig[132], G. G. Hesketh[92], N. P. Hessey[165a], J. W. Hetherly[43], S. Higashino[81], E. Higón-Rodriguez[172], K. Hildebrand[36], E. Hill[174], J. C. Hill[31], K. H. Hiller[46], S. J. Hillier[21], M. Hils[48], I. Hinchliffe[18], M. Hirose[129], D. Hirschbuehl[180], B. Hiti[89], O. Hladik[136], D. R. Hlaluku[32c], X. Hoad[50], J. Hobbs[152], N. Hod[165a], M. C. Hodgkinson[146], A. Hoecker[35], M. R. Hoeferkamp[116], F. Hoenig[112], D. Hohn[24], D. Hohov[128], T. R. Holmes[36], M. Holzbock[112], M. Homann[47], S. Honda[166], T. Honda[81], T. M. Hong[134], A. Hönle[113], B. H. Hooberman[171], W. H. Hopkins[127], Y. Horii[115], P. Horn[48], A. J. Horton[149], L. A. Horyn[36], J-Y. Hostachy[59], A. Hostiuc[145], S. Hou[155], A. Hoummada[34a], J. Howarth[98], J. Hoya[86], M. Hrabovsky[126], J. Hrdinka[35], I. Hristova[19], J. Hrivnac[128], A. Hrynevich[106], T. Hryn'ova[5], P. J. Hsu[65], S.-C. Hsu[145], Q. Hu[29], S. Hu[61c], Y. Huang[15a], Z. Hubacek[137], F. Hubaut[99], M. Huebner[24], F. Huegging[24], T. B. Huffman[131], E. W. Hughes[38], M. Huhtinen[35], R. F. H. Hunter[33], P. Huo[152], A. M. Hupe[33], N. Huseynov[80,ai], J. Huston[104], J. Huth[60], R. Hyneman[103], G. Iacobucci[55], G. Iakovidis[29], I. Ibragimov[148], L. Iconomidou-Fayard[128], Z. Idrissi[34e], P. Iengo[35], R. Ignazzi[39], O. Igonkina[118,ad], R. Iguchi[160], T. Iizawa[177], Y. Ikegami[81], M. Ikeno[81], D. Iliadis[159], N. Ilic[150], F. Iltzsche[48], G. Introzzi[71a,71b], M. Iodice[75a], K. Iordanidou[38], V. Ippolito[73a,73b], M. F. Isacson[170], N. Ishijima[129], M. Ishino[160], M. Ishitsuka[162], C. Issever[131], S. Istin[12c,ap], F. Ito[166], J. M. Iturbe Ponce[64a], R. Iuppa[76a,76b], A. Ivina[178], H. Iwasaki[81], J. M. Izen[44], V. Izzo[70a], S. Jabbar[3], P. Jacka[136], P. Jackson[1], R. M. Jacobs[24], V. Jain[2], G. Jäkel[180], K. B. Jakobi[97], K. Jakobs[53], S. Jakobsen[77], T. Jakoubek[136], D. O. Jamin[125], D. K. Jana[93], R. Jansky[55], J. Janssen[24], M. Janus[54], P. A. Janus[41a], G. Jarlskog[95], N. Javadov[80,ai], T. Javůrek[53], M. Javurkova[53], F. Jeanneau[142], L. Jeanty[18], J. Jejelava[56a,aj], A. Jelinskas[176], P. Jenni[53,c], J. Jeong[46], C. Jeske[176], S. Jézéquel[5], H. Ji[179], J. Jia[152], H. Jiang[79], Y. Jiang[61a], Z. Jiang[150], S. Jiggins[53], F. A. Jimenez Morales[37], J. Jimenez Pena[172], S. Jin[15b], A. Jinaru[27b], O. Jinnouchi[162], H. Jivan[32c], P. Johansson[146], K. A. Johns[7], C. A. Johnson[66], W. J. Johnson[145], K. Jon-And[45a,45b], R. W. L. Jones[87], S. D. Jones[153], S. Jones[7], T. J. Jones[88], J. Jongmanns[62a], P. M. Jorge[135a,135b], J. Jovicevic[165a], X. Ju[179], J. J. Junggeburth[113], A. Juste Rozas[14,ab], A. Kaczmarska[42], M. Kado[128], H. Kagan[122], M. Kagan[150], T. Kaji[177], E. Kajomovitz[157], C. W. Kalderon[95], A. Kaluza[97], S. Kama[43], A. Kamenshchikov[139], L. Kanjir[89], Y. Kano[160], V. A. Kantserov[110], J. Kanzaki[81], B. Kaplan[121], L. S. Kaplan[179], D. Kar[32c], M. J. Kareem[165b], E. Karentzos[10], S. N. Karpov[80], Z. M. Karpova[80], V. Kartvelishvili[87], A. N. Karyukhin[139], K. Kasahara[166], L. Kashif[179], R. D. Kass[122], A. Kastanas[151], Y. Kataoka[160], C. Kato[160], J. Katzy[46], K. Kawade[82], K. Kawagoe[85], T. Kawamoto[160], G. Kawamura[54], E. F. Kay[88], V. F. Kazanin[120b,120a], R. Keeler[174], R. Kehoe[43], J. S. Keller[33], E. Kellermann[95], J. J. Kempster[21], J Kendrick[21], O. Kepka[136], S. Kersten[180], B. P. Kerševan[89], R. A. Keyes[101], M. Khader[171], F. Khalil-zada[13], A. Khanov[125], A. G. Kharlamov[120b,120a], T. Kharlamova[120b,120a], A. Khodinov[163], T. J. Khoo[55], V. Khovanskiy[109,*], E. Khramov[80], J. Khubua[156b,v], S. Kido[82], M. Kiehn[55], C. R. Kilby[91], S. H. Kim[166], Y. K. Kim[36], N. Kimura[67a,67c], O. M. Kind[19], B. T. King[88], D. Kirchmeier[48], J. Kirk[140], A. E. Kiryunin[113], T. Kishimoto[160], D. Kisielewska[41a], V. Kitali[46], O. Kivernyk[5], E. Kladiva[28b], T. Klapdor-Kleingrothaus[53], M. H. Klein[103], M. Klein[88], U. Klein[88], K. Kleinknecht[97], P. Klimek[119], A. Klimentov[29], R. Klingenberg[47,*], T. Klingl[24], T. Klioutchnikova[35], F. F. Klitzner[112], P. Kluit[118], S. Kluth[113], E. Kneringer[77], E. B. F. G. Knoops[99], A. Knue[53], A. Kobayashi[160], D. Kobayashi[85], T. Kobayashi[160], M. Kobel[48], M. Kocian[150], P. Kodys[138], T. Koffas[33], E. Koffeman[118], N. M. Köhler[113], T. Koi[150], M. Kolb[62b], I. Koletsou[5], T. Kondo[81], N. Kondrashova[61c], K. Köneke[53], A. C. König[117], T. Kono[81], R. Konoplich[121,am], N. Konstantinidis[92], B. Konya[95], R. Kopeliansky[66], S. Koperny[41a], K. Korcyl[42], K. Kordas[159], A. Korn[92], I. Korolkov[14], E. V. Korolkova[146], O. Kortner[113],

S. Kortner[113], T. Kosek[138], V. V. Kostyukhin[24], A. Kotwal[49], A. Koulouris[10], A. Kourkoumeli-Charalampidi[71a,71b], C. Kourkoumelis[9], E. Kourlitis[146], V. Kouskoura[29], A. B. Kowalewska[42], R. Kowalewski[174], T. Z. Kowalski[41a], C. Kozakai[160], W. Kozanecki[142], A. S. Kozhin[139], V. A. Kramarenko[111], G. Kramberger[89], D. Krasnopevtsev[110], M. W. Krasny[94], A. Krasznahorkay[35], D. Krauss[113], J. A. Kremer[41a], J. Kretzschmar[88], P. Krieger[164], K. Krizka[18], K. Kroeninger[47], H. Kroha[113], J. Kroll[136], J. Kroll[132], J. Krstic[16], U. Kruchonak[80], H. Krüger[24], N. Krumnack[79], M. C. Kruse[49], T. Kubota[102], S. Kuday[4b], J. T. Kuechler[180], S. Kuehn[35], A. Kugel[62a], F. Kuger[175], T. Kuhl[46], V. Kukhtin[80], R. Kukla[99], Y. Kulchitsky[105], S. Kuleshov[144b], Y. P. Kulinich[171], M. Kuna[59], T. Kunigo[83], A. Kupco[136], T. Kupfer[47], O. Kuprash[158], H. Kurashige[82], L. L. Kurchaninov[165a], Y. A. Kurochkin[105], M. G. Kurth[15d], E. S. Kuwertz[174], M. Kuze[162], J. Kvita[126], T. Kwan[174], A. La Rosa[113], J. L. La Rosa Navarro[141d], L. La Rotonda[40b,40a], F. La Ruffa[40b,40a], C. Lacasta[172], F. Lacava[73a,73b], J. Lacey[46], D. P. J. Lack[98], H. Lacker[19], D. Lacour[94], E. Ladygin[80], R. Lafaye[5], B. Laforge[94], T. Lagouri[32c], S. Lai[54], S. Lammers[66], W. Lampl[7], E. Lancon[29], U. Landgraf[53], M. P. J. Landon[90], M. C. Lanfermann[55], V. S. Lang[46], J. C. Lange[14], R. J. Langenberg[35], A. J. Lankford[169], F. Lanni[29], K. Lantzsch[24], A. Lanza[71a], A. Lapertosa[56b,56a], S. Laplace[94], J. F. Laporte[142], T. Lari[69a], F. Lasagni Manghi[23b,23a], M. Lassnig[35], T. S. Lau[64a], A. Laudrain[128], A. T. Law[143], P. Laycock[88], M. Lazzaroni[69a,69b], B. Le[102], O. Le Dortz[94], E. Le Guirriec[99], E. P. Le Quilleuc[142], M. LeBlanc[7], T. LeCompte[6], F. Ledroit-Guillon[59], C. A. Lee[29], G. R. Lee[144a], L. Lee[60], S. C. Lee[155], B. Lefebvre[101], M. Lefebvre[174], F. Legger[112], C. Leggett[18], G. Lehmann Miotto[35], W. A. Leight[46], A. Leisos[159,y], M. A. L. Leite[141d], R. Leitner[138], D. Lellouch[178], B. Lemmer[54], K. J. C. Leney[92], T. Lenz[24], B. Lenzi[35], R. Leone[7], S. Leone[72a], C. Leonidopoulos[50], G. Lerner[153], C. Leroy[107], R. Les[164], A. A. J. Lesage[142], C. G. Lester[31], M. Levchenko[133], J. Levêque[5], D. Levin[103], L. J. Levinson[178], D. Lewis[90], B. Li[103], C. -Q. Li[61a], H. Li[61b], L. Li[61c], Q. Li[15d], Q. Li[61a], S. Li[61d,61c], X. Li[61c], Y. Li[148], Z. Liang[15a], B. Liberti[74a], A. Liblong[164], K. Lie[64c], S. Liem[118], A. Limosani[154], C. Y. Lin[31], K. Lin[104], S. C. Lin[168], T. H. Lin[97], R. A. Linck[66], B. E. Lindquist[152], A. L. Lionti[55], E. Lipeles[132], A. Lipniacka[17], M. Lisovyi[62b], T. M. Liss[171,as], A. Lister[173], A. M. Litke[143], J. D. Little[8], B. Liu[79], B.L Liu[6], H. Liu[29], H. Liu[103], J. B. Liu[61a], J. K. K. Liu[131], K. Liu[94], M. Liu[61a], P. Liu[18], Y. Liu[61a], Y. L. Liu[61a], M. Livan[71a,71b], A. Lleres[59], J. Llorente Merino[15a], S. L. Lloyd[90], C. Y. Lo[64b], F. Lo Sterzo[43], E. M. Lobodzinska[46], P. Loch[7], F. K. Loebinger[98], A. Loesle[53], K. M. Loew[26], T. Lohse[19], K. Lohwasser[146], M. Lokajicek[136], B. A. Long[25], J. D. Long[171], R. E. Long[87], L. Longo[68a,68b], K. A. Looper[122], J. A. Lopez[144b], I. Lopez Paz[14], A. Lopez Solis[94], J. Lorenz[112], N. Lorenzo Martinez[5], M. Losada[22], P. J. Lösel[112], X. Lou[46], X. Lou[15a], A. Lounis[128], J. Love[6], P. A. Love[87], H. Lu[64a], N. Lu[103], Y. J. Lu[65], H. J. Lubatti[145], C. Luci[73a,73b], A. Lucotte[59], C. Luedtke[53], F. Luehring[66], I. Luise[94], W. Lukas[77], L. Luminari[73a], B. Lund-Jensen[151], M. S. Lutz[100], P. M. Luzi[94], D. Lynn[29], R. Lysak[136], E. Lytken[95], F. Lyu[15a], V. Lyubushkin[80], H. Ma[29], L. L. Ma[61b], Y. Ma[61b], G. Maccarrone[52], A. Macchiolo[113], C. M. Macdonald[146], J. Machado Miguens[132], D. Madaffari[172], R. Madar[37], W. F. Mader[48], A. Madsen[46], N. Madysa[48], J. Maeda[82], S. Maeland[17], T. Maeno[29], A. S. Maevskiy[111], V. Magerl[53], C. Maidantchik[141a], T. Maier[112], A. Maio[135a,135b,135d], O. Majersky[28a], S. Majewski[127], Y. Makida[81], N. Makovec[128], B. Malaescu[94], Pa. Malecki[42], V. P. Maleev[133], F. Malek[59], U. Mallik[78], D. Malon[6], C. Malone[31], S. Maltezos[10], S. Malyukov[35], J. Mamuzic[172], G. Mancini[52], I. Mandić[89], J. Maneira[135a,135b], L. Manhaes de Andrade Filho[141b], J. Manjarres Ramos[48], K. H. Mankinen[95], A. Mann[112], A. Manousos[77], B. Mansoulie[142], J. D. Mansour[15a], M. Mantoani[54], S. Manzoni[69a,69b], G. Marceca[30], L. March[55], L. Marchese[131], G. Marchiori[94], M. Marcisovsky[136], C. A. Marin Tobon[35], M. Marjanovic[37], D. E. Marley[103], F. Marroquim[141a], Z. Marshall[18], M. U. F Martensson[170], S. Marti-Garcia[172], C. B. Martin[122], T. A. Martin[176], V. J. Martin[50], B. Martin dit Latour[17], M. Martinez[14,ab], V. I. Martinez Outschoorn[100], S. Martin-Haugh[140], V. S. Martoiu[27b], A. C. Martyniuk[92], A. Marzin[35], L. Masetti[97], T. Mashimo[160], R. Mashinistov[108], J. Masik[98], A. L. Maslennikov[120b,120a], L. H. Mason[102], L. Massa[74a,74b], P. Mastrandrea[5], A. Mastroberardino[40b,40a], T. Masubuchi[160], P. Mättig[180], J. Maurer[27b], B. Maček[89], S. J. Maxfield[88], D. A. Maximov[120b,120a], R. Mazini[155], I. Maznas[159], S. M. Mazza[143], N. C. Mc Fadden[116], G. Mc Goldrick[164], S. P. Mc Kee[103], A. McCarn[103], T. G. McCarthy[113], L. I. McClymont[92], E. F. McDonald[102], J. A. Mcfayden[35], G. Mchedlidze[54], M. A. McKay[43], K. D. McLean[174], S. J. McMahon[140], P. C. McNamara[102], C. J. McNicol[176], R. A. McPherson[174,ag], J. E. Mdhluli[32c], Z. A. Meadows[100], S. Meehan[145], T. Megy[53], S. Mehlhase[112], A. Mehta[88], T. Meideck[59], B. Meirose[44], D. Melini[172,f], B. R. Mellado Garcia[32c], J. D. Mellenthin[54], M. Melo[28a], F. Meloni[20], A. Melzer[24], S. B. Menary[98], L. Meng[88], X. T. Meng[103], A. Mengarelli[23b,23a], S. Menke[113], E. Meoni[40b,40a], S. Mergelmeyer[19], C. Merlassino[20], P. Mermod[55], L. Merola[70a,70b], C. Meroni[69a], F. S. Merritt[36], A. Messina[73a,73b], J. Metcalfe[6], A. S. Mete[169], C. Meyer[132], J. Meyer[157], J-P. Meyer[142], H. Meyer Zu Theenhausen[62a], F. Miano[153], R. P. Middleton[140], L. Mijović[50], G. Mikenberg[178], M. Mikestikova[136], M. Mikuž[89], M. Milesi[102], A. Milic[164], D. A. Millar[90], D. W. Miller[36], A. Milov[178], D. A. Milstead[45a,45b], A. A. Minaenko[139], I. A. Minashvili[156b], A. I. Mincer[121], B. Mindur[41a], M. Mineev[80], Y. Minegishi[160], Y. Ming[179], L. M. Mir[14], A. Mirto[68a,68b], K. P. Mistry[132], T. Mitani[177], J. Mitrevski[112], V. A. Mitsou[172], A. Miucci[20], P. S. Miyagawa[146], A. Mizukami[81], J. U. Mjörnmark[95], T. Mkrtchyan[182],

M. Mlynarikova[138], T. Moa[45a,45b], K. Mochizuki[107], P. Mogg[53], S. Mohapatra[38], S. Molander[45a,45b], R. Moles-Valls[24], M. C. Mondragon[104], K. Mönig[46], J. Monk[39], E. Monnier[99], A. Montalbano[149], J. Montejo Berlingen[35], F. Monticelli[86], S. Monzani[69a], R. W. Moore[3], N. Morange[128], D. Moreno[22], M. Moreno Llácer[35], P. Morettini[56b], M. Morgenstern[118], S. Morgenstern[35], D. Mori[149], T. Mori[160], M. Morii[60], M. Morinaga[177], V. Morisbak[130], A. K. Morley[35], G. Mornacchi[35], J. D. Morris[90], L. Morvaj[152], P. Moschovakos[10], M. Mosidze[156b], H. J. Moss[146], J. Moss[150,k], K. Motohashi[162], R. Mount[150], E. Mountricha[29], E. J. W. Moyse[100], S. Muanza[99], F. Mueller[113], J. Mueller[134], R. S. P. Mueller[112], D. Muenstermann[87], P. Mullen[58], G. A. Mullier[20], F. J. Munoz Sanchez[98], P. Murin[28b], W. J. Murray[176,140], H. Musheghyan[69a,69b], M. Muškinja[89], C. Mwewa[32a], A. G. Myagkov[139,an], J. Myers[127], M. Myska[137], B. P. Nachman[18], O. Nackenhorst[47], K. Nagai[131], R. Nagai[81,aq], K. Nagano[81], Y. Nagasaka[63], K. Nagata[166], M. Nagel[53], E. Nagy[99], A. M. Nairz[35], Y. Nakahama[115], K. Nakamura[81], T. Nakamura[160], I. Nakano[123], F. Napolitano[62a], R. F. Naranjo Garcia[46], R. Narayan[11], D. I. Narrias Villar[62a], I. Naryshkin[133], T. Naumann[46], G. Navarro[22], R. Nayyar[7], H. A. Neal[103], P. Yu. Nechaeva[108], T. J. Neep[142], A. Negri[71a,71b], M. Negrini[23b], S. Nektarijevic[117], C. Nellist[54], M. E. Nelson[131], S. Nemecek[136], P. Nemethy[121], M. Nessi[35,g], M. S. Neubauer[171], M. Neumann[180], P. R. Newman[21], T. Y. Ng[64c], Y. S. Ng[19], H. D. N. Nguyen[99], T. Nguyen Manh[107], E. Nibigira[37], R. B. Nickerson[131], R. Nicolaidou[142], J. Nielsen[143], N. Nikiforou[11], V. Nikolaenko[139,an], I. Nikolic-Audit[94], K. Nikolopoulos[21], P. Nilsson[29], Y. Ninomiya[81], A. Nisati[73a], N. Nishu[61c], R. Nisius[113], I. Nitsche[47], T. Nitta[177], T. Nobe[160], Y. Noguchi[83], M. Nomachi[129], I. Nomidis[33], M. A. Nomura[29], T. Nooney[90], M. Nordberg[35], N. Norjoharuddeen[131], T. Novak[89], O. Novgorodova[48], R. Novotny[137], M. Nozaki[81], L. Nozka[126], K. Ntekas[169], E. Nurse[92], F. Nuti[102], F. G. Oakham[33,av], H. Oberlack[113], T. Obermann[24], J. Ocariz[94], A. Ochi[82], I. Ochoa[38], J. P. Ochoa-Ricoux[144a], K. O'Connor[26], S. Oda[85], S. Odaka[81], A. Oh[98], S. H. Oh[49], C. C. Ohm[151], H. Oide[56b,56a], H. Okawa[166], Y. Okazaki[83], Y. Okumura[160], T. Okuyama[81], A. Olariu[27b], L. F. Oleiro Seabra[135a], S. A. Olivares Pino[144a], D. Oliveira Damazio[29], J. L. Oliver[1], M. J. R. Olsson[36], A. Olszewski[42], J. Olszowska[42], D. C. O'Neil[149], A. Onofre[135a,135e], K. Onogi[115], P. U. E. Onyisi[11,q], H. Oppen[130], M. J. Oreglia[36], Y. Oren[158], D. Orestano[75a,75b], E. C. Orgill[98], N. Orlando[64b], A. A. O'Rourke[46], R. S. Orr[164], B. Osculati[56b,56a,*], V. O'Shea[58], R. Ospanov[61a], G. Otero y Garzon[30], H. Otono[85], M. Ouchrif[34d], F. Ould-Saada[130], A. Ouraou[142], Q. Ouyang[15a], M. Owen[58], R. E. Owen[21], V. E. Ozcan[12c], N. Ozturk[8], J. Pacalt[126], H. A. Pacey[31], K. Pachal[149], A. Pacheco Pages[14], L. Pacheco Rodriguez[142], C. Padilla Aranda[14], S. Pagan Griso[18], M. Paganini[181], G. Palacino[66], S. Palazzo[40b,40a], S. Palestini[35], M. Palka[41b], D. Pallin[37], I. Panagoulias[10], C. E. Pandini[55], J. G. Panduro Vazquez[91], P. Pani[35], L. Paolozzi[55], Th. D. Papadopoulou[10], K. Papageorgiou[9,h], A. Paramonov[6], D. Paredes Hernandez[64b], B. Parida[61c], A. J. Parker[87], K. A. Parker[46], M. A. Parker[31], F. Parodi[56b,56a], J. A. Parsons[38], U. Parzefall[53], V. R. Pascuzzi[164], J.M.P Pasner[143], E. Pasqualucci[73a], S. Passaggio[56b], Fr. Pastore[91], P. Pasuwan[45a,45b], S. Pataraia[97], J. R. Pater[98], A. Pathak[179,i], T. Pauly[35], B. Pearson[113], M. Pedersen[130], S. Pedraza Lopez[172], R. Pedro[135a,135b], S. V. Peleganchuk[120b,120a], O. Penc[136], C. Peng[15d], H. Peng[61a], B. S. Peralva[141b], M. M. Perego[142], A. P. Pereira Peixoto[135a], D. V. Perepelitsa[29], F. Peri[19], L. Perini[69a,69b], H. Pernegger[35], S. Perrella[70a,70b], V. D. Peshekhonov[80,*], K. Peters[46], R. F. Y. Peters[98], B. A. Petersen[35], T. C. Petersen[39], E. Petit[59], A. Petridis[1], C. Petridou[159], P. Petroff[128], E. Petrolo[73a], M. Petrov[131], F. Petrucci[75a,75b], N. E. Pettersson[100], A. Peyaud[142], R. Pezoa[144b], T. Pham[102], F. H. Phillips[104], P. W. Phillips[140], G. Piacquadio[152], E. Pianori[18], A. Picazio[100], M. A. Pickering[131], R. Piegaia[30], J. E. Pilcher[36], A. D. Pilkington[98], M. Pinamonti[74a,74b], J. L. Pinfold[3], M. Pitt[178], M.-A. Pleier[29], V. Pleskot[138], E. Plotnikova[80], D. Pluth[79], P. Podberezko[120b,120a], R. Poettgen[95], R. Poggi[71a,71b], L. Poggioli[128], I. Pogrebnyak[104], D. Pohl[24], I. Pokharel[54], G. Polesello[71a], A. Poley[46], A. Policicchio[40b,40a], R. Polifka[35], A. Polini[23b], C. S. Pollard[46], V. Polychronakos[29], D. Ponomarenko[110], L. Pontecorvo[73a], G. A. Popeneciu[27d], D. M. Portillo Quintero[94], S. Pospisil[137], K. Potamianos[46], I. N. Potrap[80], C. J. Potter[31], H. Potti[11], T. Poulsen[95], J. Poveda[35], T. D. Powell[146], M. E. Pozo Astigarraga[35], P. Pralavorio[99], S. Prell[79], D. Price[98], M. Primavera[68a], S. Prince[101], N. Proklova[110], K. Prokofiev[64c], F. Prokoshin[144b], S. Protopopescu[29], J. Proudfoot[6], M. Przybycien[41a], A. Puri[171], P. Puzo[128], J. Qian[103], Y. Qin[98], A. Quadt[54], M. Queitsch-Maitland[46], A. Qureshi[1], P. Rados[102], F. Ragusa[69a,69b], G. Rahal[51], J. A. Raine[98], S. Rajagopalan[29], T. Rashid[128], S. Raspopov[5], M. G. Ratti[69a,69b], D. M. Rauch[46], F. Rauscher[112], S. Rave[97], B. Ravina[146], I. Ravinovich[178], J. H. Rawling[98], M. Raymond[35], A. L. Read[130], N. P. Readioff[59], M. Reale[68a,68b], D. M. Rebuzzi[71a,71b], A. Redelbach[175], G. Redlinger[29], R. Reece[143], R. G. Reed[32c], K. Reeves[44], L. Rehnisch[19], J. Reichert[132], A. Reiss[97], C. Rembser[35], H. Ren[15d], M. Rescigno[73a], S. Resconi[69a], E. D. Resseguie[132], S. Rettie[173], E. Reynolds[21], O. L. Rezanova[120b,120a], P. Reznicek[138], R. Richter[113], S. Richter[92], E. Richter-Was[41b], O. Ricken[24], M. Ridel[94], P. Rieck[113], C. J. Riegel[180], O. Rifki[46], M. Rijssenbeek[152], A. Rimoldi[71a,71b], M. Rimoldi[20], L. Rinaldi[23b], G. Ripellino[151], B. Ristić[87], E. Ritsch[35], I. Riu[14], J. C. Rivera Vergara[144a], F. Rizatdinova[125], E. Rizvi[90], C. Rizzi[14], R. T. Roberts[98], S. H. Robertson[101,ag], A. Robichaud-Veronneau[101], D. Robinson[31], J. E. M. Robinson[46], A. Robson[58], E. Rocco[97], C. Roda[72a,72b], Y. Rodina[99,ac], S. Rodriguez Bosca[172], A. Rodriguez Perez[14], D. Rodriguez Rodriguez[172], A. M. Rodríguez Vera[165b], S. Roe[35], C. S. Rogan[60], O. Røhne[130], R. Röhrig[113], C. P. A. Roland[66], J. Roloff[60],

A. Romaniouk[110], M. Romano[23b,23a], N. Rompotis[88], M. Ronzani[121], L. Roos[94], S. Rosati[73a], K. Rosbach[53], P. Rose[143], N.-A. Rosien[54], E. Rossi[70a,70b], L. P. Rossi[56b], L. Rossini[69a,69b], J. H. N. Rosten[31], R. Rosten[145], M. Rotaru[27b], J. Rothberg[145], D. Rousseau[128], D. Roy[32c], A. Rozanov[99], Y. Rozen[157], X. Ruan[32c], F. Rubbo[150], F. Rühr[53], A. Ruiz-Martinez[33], Z. Rurikova[53], N. A. Rusakovich[80], H. L. Russell[101], J. P. Rutherfoord[7], N. Ruthmann[35], E. M. Rüttinger[46], Y. F. Ryabov[125], M. Rybar[171], G. Rybkin[128], S. Ryu[6], A. Ryzhov[139], G. F. Rzehorz[54], P. Sabatini[54], G. Sabato[118], S. Sacerdoti[128], H. F-W. Sadrozinski[143], R. Sadykov[80], F. Safai Tehrani[73a], P. Saha[119], M. Sahinsoy[62a], M. Saimpert[46], M. Saito[160], T. Saito[160], H. Sakamoto[160], A. Sakharov[121,am], D. Salamani[55], G. Salamanna[75a,75b], J. E. Salazar Loyola[144b], D. Salek[118], P. H. Sales De Bruin[170], D. Salihagic[113], A. Salnikov[150], J. Salt[172], D. Salvatore[40b,40a], F. Salvatore[153], A. Salvucci[64a,64b,64c], A. Salzburger[35], D. Sammel[53], D. Sampsonidis[159], D. Sampsonidou[159], J. Sánchez[172], A. Sanchez Pineda[67a,67c], H. Sandaker[130], C. O. Sander[46], M. Sandhoff[180], C. Sandoval[22], D. P. C. Sankey[140], M. Sannino[56b,56a], Y. Sano[115], A. Sansoni[52], C. Santoni[37], H. Santos[135a], I. Santoyo Castillo[153], A. Sapronov[80], J. G. Saraiva[135a,135d], O. Sasaki[81], K. Sato[166], E. Sauvan[5], P. Savard[164,av], N. Savic[113], R. Sawada[160], C. Sawyer[140], L. Sawyer[93,al], C. Sbarra[23a], A. Sbrizzi[23b,23a], T. Scanlon[92], D. A. Scannicchio[169], J. Schaarschmidt[145], P. Schacht[113], B. M. Schachtner[112], D. Schaefer[36], L. Schaefer[132], J. Schaeffer[97], S. Schaepe[35], U. Schäfer[97], A. C. Schaffer[128], D. Schaile[112], R. D. Schamberger[152], N. Scharmberg[98], V. A. Schegelsky[133], D. Scheirich[138], F. Schenck[19], M. Schernau[169], C. Schiavi[56b,56a], S. Schier[143], L. K. Schildgen[24], Z. M. Schillaci[26], E. J. Schioppa[35], M. Schioppa[40b,40a], K. E. Schleicher[53], S. Schlenker[35], K. R. Schmidt-Sommerfeld[113], K. Schmieden[35], C. Schmitt[97], S. Schmitt[46], S. Schmitz[97], U. Schnoor[53], L. Schoeffel[142], A. Schoening[62b], E. Schopf[24], M. Schott[97], J. F. P. Schouwenberg[117], J. Schovancova[35], S. Schramm[55], N. Schuh[97], A. Schulte[97], H.-C. Schultz-Coulon[62a], M. Schumacher[53], B. A. Schumm[143], Ph. Schune[142], A. Schwartzman[150], T. A. Schwarz[103], H. Schweiger[98], Ph. Schwemling[142], R. Schwienhorst[104], A. Sciandra[24], G. Sciolla[26], M. Scornajenghi[40b,40a], F. Scuri[72a], F. Scutti[102], L. M. Scyboz[113], J. Searcy[103], C. D. Sebastiani[73a,73b], P. Seema[24], S. C. Seidel[116], A. Seiden[143], T. Seiss[36], J. M. Seixas[141a], G. Sekhniaidze[70a], K. Sekhon[103], S. J. Sekula[43], N. Semprini-Cesari[23b,23a], S. Sen[49], S. Senkin[37], C. Serfon[130], L. Serin[128], L. Serkin[67a,67b], M. Sessa[75a,75b], H. Severini[124], F. Sforza[167], A. Sfyrla[55], E. Shabalina[54], J. D. Shahinian[143], N. W. Shaikh[45a,45b], L. Y. Shan[15a], R. Shang[171], J. T. Shank[25], M. Shapiro[18], A. S. Sharma[1], A. Sharma[131], P. B. Shatalov[109], K. Shaw[67a,67b], S. M. Shaw[98], A. Shcherbakova[133], C. Y. Shehu[153], Y. Shen[124], N. Sherafati[33], A. D. Sherman[25], P. Sherwood[92], L. Shi[155,ar], S. Shimizu[82], C. O. Shimmin[181], M. Shimojima[114], I. P. J. Shipsey[131], S. Shirabe[85], M. Shiyakova[80,ae], J. Shlomi[178], A. Shmeleva[108], D. Shoaleh Saadi[107], M. J. Shochet[36], S. Shojaii[102], D. R. Shope[124], S. Shrestha[122], E. Shulga[110], P. Sicho[136], A. M. Sickles[171], P. E. Sidebo[151], E. Sideras Haddad[32c], O. Sidiropoulou[175], A. Sidoti[23b,23a], F. Siegert[48], Dj. Sijacki[16], J. Silva[135a,135d], M. Silva Jr.[179], S. B. Silverstein[45a], L. Simic[80], S. Simion[128], E. Simioni[97], M. Simon[97], P. Sinervo[164], N. B. Sinev[127], M. Sioli[23b,23a], G. Siragusa[175], I. Siral[103], S. Yu. Sivoklokov[111], J. Sjölin[45a,45b], M. B. Skinner[87], P. Skubic[124], M. Slater[21], T. Slavicek[137], M. Slawinska[42], K. Sliwa[167], R. Slovak[138], V. Smakhtin[178], B. H. Smart[5], J. Smiesko[28a], N. Smirnov[110], S. Yu. Smirnov[110], Y. Smirnov[110], L. N. Smirnova[111,t], O. Smirnova[95], J. W. Smith[54], M. N. K. Smith[38], R. W. Smith[38], M. Smizanska[87], K. Smolek[137], A. A. Snesarev[108], I. M. Snyder[127], S. Snyder[29], R. Sobie[174,ag], A. M. Soffa[169], A. Soffer[158], A. Søgaard[50], D. A. Soh[155], G. Sokhrannyi[89], C. A. Solans Sanchez[35], M. Solar[137], E. Yu. Soldatov[110], U. Soldevila[172], A. A. Solodkov[139], A. Soloshenko[80], O. V. Solovyanov[139], V. Solovyev[133], P. Sommer[146], H. Son[167], W. Song[140], A. Sopczak[137], F. Sopkova[28b], D. Sosa[62b], C. L. Sotiropoulou[72a,72b], S. Sottocornola[71a,71b], R. Soualah[67a,67c], A. M. Soukharev[120b,120a], D. South[46], B. C. Sowden[91], S. Spagnolo[68a,68b], M. Spalla[113], M. Spangenberg[176], F. Spanò[91], D. Sperlich[19], F. Spettel[113], T. M. Spieker[62a], R. Spighi[23b], G. Spigo[35], L. A. Spiller[102], M. Spousta[138], A. Stabile[69a,69b], R. Stamen[62a], S. Stamm[19], E. Stanecka[42], R. W. Stanek[6], C. Stanescu[75a], M. M. Stanitzki[46], B. S. Stapf[118], S. Stapnes[130], E. A. Starchenko[139], G. H. Stark[36], J. Stark[59], S. H Stark[39], P. Staroba[136], P. Starovoitov[62a], S. Stärz[35], R. Staszewski[42], M. Stegler[46], P. Steinberg[29], B. Stelzer[149], H. J. Stelzer[35], O. Stelzer-Chilton[165a], H. Stenzel[57], T. J. Stevenson[90], G. A. Stewart[58], M. C. Stockton[127], G. Stoicea[27b], P. Stolte[54], S. Stonjek[113], A. Straessner[48], J. Strandberg[151], S. Strandberg[45a,45b], M. Strauss[124], P. Strizenec[28b], R. Ströhmer[175], D. M. Strom[127], R. Stroynowski[43], A. Strubig[50], S. A. Stucci[29], B. Stugu[17], J. Stupak[124], N. A. Styles[46], D. Su[150], J. Su[134], S. Suchek[62a], Y. Sugaya[129], M. Suk[137], V. V. Sulin[108], D. M. S. Sultan[55], S. Sultansoy[4c], T. Sumida[83], S. Sun[103], X. Sun[3], K. Suruliz[153], C. J. E. Suster[154], M. R. Sutton[153], S. Suzuki[81], M. Svatos[136], M. Swiatlowski[36], S. P. Swift[2], A. Sydorenko[97], I. Sykora[28a], T. Sykora[138], D. Ta[97], K. Tackmann[46], J. Taenzer[158], A. Taffard[169], R. Tafirout[165a], E. Tahirovic[90], N. Taiblum[158], H. Takai[29], R. Takashima[84], E. H. Takasugi[113], K. Takeda[82], T. Takeshita[147], Y. Takubo[81], M. Talby[99], A. A. Talyshev[120b,120a], J. Tanaka[160], M. Tanaka[162], R. Tanaka[128], R. Tanioka[82], B. B. Tannenwald[122], S. Tapia Araya[144b], S. Tapprogge[97], A. Tarek Abouelfadl Mohamed[94], S. Tarem[157], G. Tarna[27b,d], G. F. Tartarelli[69a], P. Tas[138], M. Tasevsky[136], T. Tashiro[83], E. Tassi[40b,40a], A. Tavares Delgado[135a,135b], Y. Tayalati[34e], A. C. Taylor[116], A. J. Taylor[50], G. N. Taylor[102], P. T. E. Taylor[102], W. Taylor[165b], A. S. Tee[87], P. Teixeira-Dias[91],

D. Temple[149], H. Ten Kate[35], P. K. Teng[155], J. J. Teoh[129], F. Tepel[180], S. Terada[81], K. Terashi[160], J. Terron[96], S. Terzo[14], M. Testa[52], R. J. Teuscher[164,ag], S. J. Thais[181], T. Theveneaux-Pelzer[46], F. Thiele[39], J. P. Thomas[21], A. S. Thompson[58], P. D. Thompson[21], L. A. Thomsen[181], E. Thomson[132], Y. Tian[38], R. E. Ticse Torres[54], V. O. Tikhomirov[108,ao], Yu. A. Tikhonov[120b,120a], S. Timoshenko[110], P. Tipton[181], S. Tisserant[99], K. Todome[162], S. Todorova-Nova[5], S. Todt[48], J. Tojo[85], S. Tokár[28a], K. Tokushuku[81], E. Tolley[122], M. Tomoto[115], L. Tompkins[150,o], K. Toms[116], B. Tong[60], P. Tornambe[53], E. Torrence[127], H. Torres[48], E. Torró Pastor[145], C. Tosciri[131], J. Toth[99,af], F. Touchard[99], D. R. Tovey[146], C. J. Treado[121], T. Trefzger[175], F. Tresoldi[153], A. Tricoli[29], I. M. Trigger[165a], S. Trincaz-Duvoid[94], M. F. Tripiana[14], W. Trischuk[164], B. Trocmé[59], A. Trofymov[128], C. Troncon[69a], M. Trovatelli[174], F. Trovato[153], L. Truong[32b], M. Trzebinski[42], A. Trzupek[42], F. Tsai[46], J.C-L. Tseng[131], P. V. Tsiareshka[105], N. Tsirintanis[9], V. Tsiskaridze[152], E. G. Tskhadadze[156a], I. I. Tsukerman[109], V. Tsulaia[18], S. Tsuno[81], D. Tsybychev[152], Y. Tu[64b], A. Tudorache[27b], V. Tudorache[27b], T. T. Tulbure[27a], A. N. Tuna[60], S. Turchikhin[80], D. Turgeman[178], I. Turk Cakir[4b,w], R. Turra[69a], P. M. Tuts[38], E. Tzovara[97], G. Ucchielli[23b,23a], I. Ueda[81], M. Ughetto[45a,45b], F. Ukegawa[166], G. Unal[35], A. Undrus[29], G. Unel[169], F. C. Ungaro[102], Y. Unno[81], K. Uno[160], J. Urban[28b], P. Urquijo[102], P. Urrejola[97], G. Usai[8], J. Usui[81], L. Vacavant[99], V. Vacek[137], B. Vachon[101], K. O. H. Vadla[130], A. Vaidya[92], C. Valderanis[112], E. Valdes Santurio[45a,45b], M. Valente[55], S. Valentinetti[23b,23a], A. Valero[172], L. Valéry[46], R. A. Vallance[21], A. Vallier[5], J. A. Valls Ferrer[172], T. R. Van Daalen[14], W. Van Den Wollenberg[118], H. van der Graaf[118], P. van Gemmeren[6], J. Van Nieuwkoop[149], I. van Vulpen[118], M. C. van Woerden[118], M. Vanadia[74a,74b], W. Vandelli[35], A. Vaniachine[163], P. Vankov[118], R. Vari[73a], E. W. Varnes[7], C. Varni[56b,56a], T. Varol[43], D. Varouchas[128], A. Vartapetian[8], K. E. Varvell[154], G. A. Vasquez[144b], J. G. Vasquez[181], F. Vazeille[37], D. Vazquez Furelos[14], T. Vazquez Schroeder[101], J. Veatch[54], V. Vecchio[75a,75b], L. M. Veloce[164], F. Veloso[135a,135c], S. Veneziano[73a], A. Ventura[68a,68b], M. Venturi[174], N. Venturi[35], V. Vercesi[71a], M. Verducci[75a,75b], W. Verkerke[118], A. T. Vermeulen[118], J. C. Vermeulen[118], M. C. Vetterli[149,av], N. Viaux Maira[144b], O. Viazlo[95], I. Vichou[171,*], T. Vickey[146], O. E. Vickey Boeriu[146], G. H. A. Viehhauser[131], S. Viel[18], L. Vigani[131], M. Villa[23b,23a], M. Villaplana Perez[69a,69b], E. Vilucchi[52], M. G. Vincter[33], V. B. Vinogradov[80], A. Vishwakarma[46], C. Vittori[23b,23a], I. Vivarelli[153], S. Vlachos[10], M. Vogel[180], P. Vokac[137], G. Volpi[14], S. E. von Buddenbrock[32c], E. von Toerne[24], V. Vorobel[138], K. Vorobev[110], M. Vos[172], J. H. Vossebeld[88], N. Vranjes[16], M. Vranjes Milosavljevic[16], V. Vrba[137], M. Vreeswijk[118], T. Šfiligoj[89], R. Vuillermet[35], I. Vukotic[36], T. Ženiš[28a], L. Živković[16], P. Wagner[24], W. Wagner[180], J. Wagner-Kuhr[112], H. Wahlberg[86], S. Wahrmund[48], K. Wakamiya[82], J. Walder[87], R. Walker[112], W. Walkowiak[148], V. Wallangen[45a,45b], A. M. Wang[60], C. Wang[61b,d], F. Wang[179], H. Wang[18], H. Wang[3], J. Wang[154], J. Wang[62b], P. Wang[43], Q. Wang[124], R.-J. Wang[94], R. Wang[61a], R. Wang[6], S. M. Wang[155], W. Wang[155,m], W. Wang[61a,ah], Y. Wang[61a], Z. Wang[61c], C. Wanotayaroj[46], A. Warburton[101], C. P. Ward[31], D. R. Wardrope[92], A. Washbrook[50], P. M. Watkins[21], A. T. Watson[21], M. F. Watson[21], G. Watts[145], S. Watts[98], B. M. Waugh[92], A. F. Webb[11], S. Webb[97], C. Weber[181], M. S. Weber[20], S. A. Weber[62aa], J. S. Webster[6], A. R. Weidberg[131], B. Weinert[66], J. Weingarten[54], M. Weirich[97], C. Weiser[53], P. S. Wells[35], T. Wenaus[29], T. Wengler[35], S. Wenig[35], N. Wermes[24], M. D. Werner[79], P. Werner[35], M. Wessels[62a], T. D. Weston[20], K. Whalen[127], N. L. Whallon[145], A. M. Wharton[87], A. S. White[103], A. White[8], M. J. White[1], R. White[144b], D. Whiteson[169], B. W. Whitmore[87], F. J. Wickens[140], W. Wiedenmann[179], M. Wielers[140], C. Wiglesworth[39], L. A. M. Wiik-Fuchs[53], A. Wildauer[113], F. Wilk[98], H. G. Wilkens[35], H. H. Williams[132], S. Williams[31], C. Willis[104], S. Willocq[100], J. A. Wilson[21], I. Wingerter-Seez[5], E. Winkels[153], F. Winklmeier[127], O. J. Winston[153], B. T. Winter[24], M. Wittgen[150], M. Wobisch[93,al], A. Wolf[97], T. M. H. Wolf[118], R. Wolff[99], M. W. Wolter[42], H. Wolters[135a,135c], V. W. S. Wong[173], N. L. Woods[143], S. D. Worm[21], B. K. Wosiek[42], K. W. Woźniak[42], K. Wraight[58], M. Wu[36], S. L. Wu[179], X. Wu[55], Y. Wu[61a], T. R. Wyatt[98], B. M. Wynne[50], S. Xella[39], Z. Xi[103], L. Xia[176], D. Xu[15a], H. Xu[61a], L. Xu[29], T. Xu[142], W. Xu[103], B. Yabsley[154], S. Yacoob[32a], K. Yajima[129], D. P. Yallup[92], D. Yamaguchi[162], Y. Yamaguchi[162], A. Yamamoto[81], T. Yamanaka[160], F. Yamane[82], M. Yamatani[160], T. Yamazaki[160], Y. Yamazaki[82], Z. Yan[25], H. Yang[61c,61d], H. Yang[18], S. Yang[78], Y. Yang[160], Y. Yang[155], Z. Yang[17], W-M. Yao[18], Y. C. Yap[46], Y. Yasu[81], E. Yatsenko[5], J. Ye[43], S. Ye[29], I. Yeletskikh[80], E. Yigitbasi[25], E. Yildirim[97], K. Yorita[177], K. Yoshihara[132], C. J. S. Young[35], C. Young[150], J. Yu[8], J. Yu[79], X. Yue[62a], S. P. Y. Yuen[24], I. Yusuff[31,ax], B. Zabinski[42], G. Zacharis[10], E. Zaffaroni[55], R. Zaidan[14], A. M. Zaitsev[139,an], N. Zakharchuk[46], J. Zalieckas[17], S. Zambito[60], D. Zanzi[35], D. R. Zaripovas[58], C. Zeitnitz[180], G. Zemaityte[131], J. C. Zeng[171], Q. Zeng[150], O. Zenin[139], D. Zerwas[128], M. Zgubič[131], D. Zhang[103], D. Zhang[61b], F. Zhang[179], G. Zhang[61a,ah], H. Zhang[15b], J. Zhang[6], L. Zhang[53], L. Zhang[61a], M. Zhang[171], P. Zhang[15b], R. Zhang[61a,d], R. Zhang[24], X. Zhang[61b], Y. Zhang[15d], Z. Zhang[128], X. Zhao[43], Y. Zhao[61b,ak], Z. Zhao[61a], A. Zhemchugov[80], B. Zhou[103], C. Zhou[179], L. Zhou[43], M. Zhou[15d], M. Zhou[152], N. Zhou[61c], Y. Zhou[7], C. G. Zhu[61b], H. Zhu[61a], H. Zhu[15a], J. Zhu[103], Y. Zhu[61a], X. Zhuang[15a], K. Zhukov[108], V. Zhulanov[120b,120a], A. Zibell[175], D. Zieminska[66], N. I. Zimine[80], S. Zimmermann[53], Z. Zinonos[113], M. Zinser[97], M. Ziolkowski[148], G. Zobernig[179], A. Zoccoli[23b,23a], K. Zoch[54], T. G. Zorbas[146], R. Zou[36], M. zur Nedden[19], L. Zwalinski[35]

[1] Department of Physics, University of Adelaide, Adelaide, Australia
[2] Physics Department, SUNY Albany, Albany, NY, USA
[3] Department of Physics, University of Alberta, Edmonton, AB, Canada
[4] [(a)]Department of Physics, Ankara University, Ankara, Turkey; [(b)]Istanbul Aydin University, Istanbul, Turkey; [(c)]Division of Physics, TOBB University of Economics and Technology, Ankara, Turkey
[5] LAPP, Université Grenoble Alpes, Université Savoie Mont Blanc, CNRS/IN2P3, Annecy, France
[6] High Energy Physics Division, Argonne National Laboratory, Argonne, IL, USA
[7] Department of Physics, University of Arizona, Tucson, AZ, USA
[8] Department of Physics, The University of Texas at Arlington, Arlington, TX, USA
[9] Physics Department, National and Kapodistrian University of Athens, Athens, Greece
[10] Physics Department, National Technical University of Athens, Zografou, Greece
[11] Department of Physics, The University of Texas at Austin, Austin, TX, USA
[12] [(a)]Faculty of Engineering and Natural Sciences, Bahcesehir University, Istanbul, Turkey; [(b)]Faculty of Engineering and Natural Sciences, Istanbul Bilgi University, Istanbul, Turkey; [(c)]Department of Physics, Bogazici University, Istanbul, Turkey; [(d)]Department of Physics Engineering, Gaziantep University, Gaziantep, Turkey
[13] Institute of Physics, Azerbaijan Academy of Sciences, Baku, Azerbaijan
[14] Institut de Física d'Altes Energies (IFAE), The Barcelona Institute of Science and Technology, Barcelona, Spain
[15] [(a)]Institute of High Energy Physics, Chinese Academy of Sciences, Beijing, China; [(b)]Department of Physics, Nanjing University, Jiangsu, China; [(c)]Physics Department, Tsinghua University, Beijing, China; [(d)]University of Chinese Academy of Science (UCAS), Beijing, China
[16] Institute of Physics, University of Belgrade, Belgrade, Serbia
[17] Department for Physics and Technology, University of Bergen, Bergen, Norway
[18] Physics Division, Lawrence Berkeley National Laboratory and University of California, Berkeley, CA, USA
[19] Department of Physics, Humboldt University, Berlin, Germany
[20] Albert Einstein Center for Fundamental Physics and Laboratory for High Energy Physics, University of Bern, Bern, Switzerland
[21] School of Physics and Astronomy, University of Birmingham, Birmingham, UK
[22] Centro de Investigaciones, Universidad Antonio Narino, Bogotá, Colombia
[23] [(a)]Dipartimento di Fisica e Astronomia, Università di Bologna, Bologna, Italy; [(b)]INFN Sezione di Bologna, Bologna, Italy
[24] Physikalisches Institut, University of Bonn, Bonn, Germany
[25] Department of Physics, Boston University, Boston, MA, USA
[26] Department of Physics, Brandeis University, Waltham, MA, USA
[27] [(a)]Transilvania University of Brasov, Brasov, Romania; [(b)]Horia Hulubei National Institute of Physics and Nuclear Engineering, Bucharest, Romania; [(c)]Department of Physics, Alexandru Ioan Cuza University of Iasi, Iasi, Romania; [(d)]Physics Department, National Institute for Research and Development of Isotopic and Molecular Technologies, Cluj-Napoca, Romania; [(e)]University Politehnica Bucharest, Bucharest, Romania; [(f)]West University in Timisoara, Timisoara, Romania
[28] [(a)]Faculty of Mathematics, Physics and Informatics, Comenius University, Bratislava, Slovak Republic; [(b)]Department of Subnuclear Physics, Institute of Experimental Physics of the Slovak Academy of Sciences, Kosice, Slovak Republic
[29] Physics Department, Brookhaven National Laboratory, Upton, NY, USA
[30] Departamento de Física, Universidad de Buenos Aires, Buenos Aires, Argentina
[31] Cavendish Laboratory, University of Cambridge, Cambridge, UK
[32] [(a)]Department of Physics, University of Cape Town, Cape Town, South Africa; [(b)]Department of Mechanical Engineering Science, University of Johannesburg, Johannesburg, South Africa; [(c)]School of Physics, University of the Witwatersrand, Johannesburg, South Africa
[33] Department of Physics, Carleton University, Ottawa, ON, Canada
[34] [(a)]Faculté des Sciences Ain Chock, Réseau Universitaire de Physique des Hautes Energies-Université Hassan II, Casablanca, Morocco; [(b)]Centre National de l'Energie des Sciences Techniques Nucleaires, Rabat, Morocco; [(c)]Faculté des Sciences Semlalia, Université Cadi Ayyad, LPHEA-Marrakech, Marrakech, Morocco; [(d)]Faculté des Sciences, Université Mohamed Premier and LPTPM, Oujda, Morocco; [(e)]Faculté des sciences, Université Mohammed V, Rabat, Morocco
[35] CERN, Geneva, Switzerland

[36] Enrico Fermi Institute, University of Chicago, Chicago, IL, USA
[37] LPC, Université Clermont Auvergne, CNRS/IN2P3, Clermont-Ferrand, France
[38] Nevis Laboratory, Columbia University, Irvington, NY, USA
[39] Niels Bohr Institute, University of Copenhagen, Kobenhavn, Denmark
[40] [(a)]Dipartimento di Fisica, Università della Calabria, Rende, Italy; [(b)]INFN Gruppo Collegato di Cosenza, Laboratori Nazionali di Frascati, Frascati, Italy
[41] [(a)]Faculty of Physics and Applied Computer Science, AGH University of Science and Technology, Kraków, Poland; [(b)]Marian Smoluchowski Institute of Physics, Jagiellonian University, Kraków, Poland
[42] Institute of Nuclear Physics Polish Academy of Sciences, Kraków, Poland
[43] Physics Department, Southern Methodist University, Dallas, TX, USAmerica
[44] Physics Department, University of Texas at Dallas, Richardson, TX, USA
[45] [(a)]Department of Physics, Stockholm University, Stockholm, Sweden; [(b)]The Oskar Klein Centre, Stockholm, Sweden
[46] DESY, Hamburg and Zeuthen, Germany
[47] Lehrstuhl für Experimentelle Physik IV, Technische Universität Dortmund, Dortmund, Germany
[48] Institut für Kern- und Teilchenphysik, Technische Universität Dresden, Dresden, Germany
[49] Department of Physics, Duke University, Durham, NC, USA
[50] SUPA-School of Physics and Astronomy, University of Edinburgh, Edinburgh, UK
[51] Centre de Calcul de l'Institut National de Physique Nucléaire et de Physique des Particules (IN2P3), Villeurbanne, France
[52] INFN e Laboratori Nazionali di Frascati, Frascati, Italy
[53] Fakultät für Mathematik und Physik, Albert-Ludwigs-Universität, Freiburg, Germany
[54] II Physikalisches Institut, Georg-August-Universität, Göttingen, Germany
[55] Departement de Physique Nucléaire et Corpusculaire, Université de Genève, Geneva, Switzerland
[56] [(a)]Dipartimento di Fisica, Università di Genova, Genoa, Italy; [(b)]INFN Sezione di Genova, Genoa, Italy
[57] II. Physikalisches Institut, Justus-Liebig-Universität Giessen, Giessen, Germany
[58] SUPA-School of Physics and Astronomy, University of Glasgow, Glasgow, UK
[59] LPSC, Université Grenoble Alpes, CNRS/IN2P3, Grenoble INP, Grenoble, France
[60] Laboratory for Particle Physics and Cosmology, Harvard University, Cambridge, MA, USA
[61] [(a)]Department of Modern Physics and State Key Laboratory of Particle Detection and Electronics, University of Science and Technology of China, Anhui, China; [(b)]School of Physics, Shandong University, Shandong, China; [(c)]School of Physics and Astronomy, Key Laboratory for Particle Physics, Astrophysics and Cosmology, Ministry of Education, Shanghai Key Laboratory for Particle Physics and Cosmology, Shanghai Jiao Tong University, Shanghai, China; [(d)]Tsung-Dao Lee Institute, Shanghai, China
[62] [(a)]Kirchhoff-Institut für Physik, Ruprecht-Karls-Universität Heidelberg, Heidelberg, Germany; [(b)]Physikalisches Institut, Ruprecht-Karls-Universität Heidelberg, Heidelberg, Germany
[63] Faculty of Applied Information Science, Hiroshima Institute of Technology, Hiroshima, Japan
[64] [(a)]Department of Physics, The Chinese University of Hong Kong, Shatin, N.T., Hong Kong; [(b)]Department of Physics, The University of Hong Kong, Hong Kong, China; [(c)]Department of Physics, Institute for Advanced Study, The Hong Kong University of Science and Technology, Clear Water Bay, Kowloon, Hong Kong, China
[65] Department of Physics, National Tsing Hua University, Hsinchu, Taiwan
[66] Department of Physics, Indiana University, Bloomington, IN, USA
[67] [(a)]INFN Gruppo Collegato di Udine, Sezione di Trieste, Udine, Italy; [(b)]ICTP, Trieste, Italy; [(c)]Dipartimento di Chimica, Fisica e Ambiente, Università di Udine, Udine, Italy
[68] [(a)]INFN Sezione di Lecce, Lecce, Italy; [(b)]Dipartimento di Matematica e Fisica, Università del Salento, Lecce, Italy
[69] [(a)]INFN Sezione di Milano, Milan, Italy; [(b)]Dipartimento di Fisica, Università di Milano, Milan, Italy
[70] [(a)]INFN Sezione di Napoli, Naples, Italy; [(b)]Dipartimento di Fisica, Università di Napoli, Naples, Italy
[71] [(a)]INFN Sezione di Pavia, Pavia, Italy; [(b)]Dipartimento di Fisica, Università di Pavia, Pavia, Italy
[72] [(a)]INFN Sezione di Pisa, Pisa, Italy; [(b)]Dipartimento di Fisica E. Fermi, Università di Pisa, Pisa, Italy
[73] [(a)]INFN Sezione di Roma, Rome, Italy; [(b)]Dipartimento di Fisica, Sapienza Università di Roma, Rome, Italy
[74] [(a)]INFN Sezione di Roma Tor Vergata, Rome, Italy; [(b)]Dipartimento di Fisica, Università di Roma Tor Vergata, Rome, Italy
[75] [(a)]INFN Sezione di Roma Tre, Rome, Italy; [(b)]Dipartimento di Matematica e Fisica, Università Roma Tre, Rome, Italy
[76] [(a)]INFN-TIFPA, Trento, Italy; [(b)]University of Trento, Trento, Italy

[77] Institut für Astro- und Teilchenphysik, Leopold-Franzens-Universität, Innsbruck, Austria
[78] University of Iowa, Iowa City, IA, USA
[79] Department of Physics and Astronomy, Iowa State University, Ames, IA, USA
[80] Joint Institute for Nuclear Research, JINR Dubna, Dubna, Russia
[81] KEK, High Energy Accelerator Research Organization, Tsukuba, Japan
[82] Graduate School of Science, Kobe University, Kobe, Japan
[83] Faculty of Science, Kyoto University, Kyoto, Japan
[84] Kyoto University of Education, Kyoto, Japan
[85] Research Center for Advanced Particle Physics and Department of Physics, Kyushu University, Fukuoka, Japan
[86] Instituto de Física La Plata, Universidad Nacional de La Plata and CONICET, La Plata, Argentina
[87] Physics Department, Lancaster University, Lancaster, UK
[88] Oliver Lodge Laboratory, University of Liverpool, Liverpool, UK
[89] Department of Experimental Particle Physics, Jožef Stefan Institute and Department of Physics, University of Ljubljana, Ljubljana, Slovenia
[90] School of Physics and Astronomy, Queen Mary University of London, London, UK
[91] Department of Physics, Royal Holloway University of London, Surrey, UK
[92] Department of Physics and Astronomy, University College London, London, UK
[93] Louisiana Tech University, Ruston, LA, USA
[94] Laboratoire de Physique Nucléaire et de Hautes Energies, UPMC and Université Paris-Diderot and CNRS/IN2P3, Paris, France
[95] Fysiska institutionen, Lunds universitet, Lund, Sweden
[96] Departamento de Fisica Teorica C-15 and CIAFF, Universidad Autonoma de Madrid, Madrid, Spain
[97] Institut für Physik, Universität Mainz, Mainz, Germany
[98] School of Physics and Astronomy, University of Manchester, Manchester, UK
[99] CPPM, Aix-Marseille Université and CNRS/IN2P3, Marseille, France
[100] Department of Physics, University of Massachusetts, Amherst, MA, USA
[101] Department of Physics, McGill University, Montreal, QC, Canada
[102] School of Physics, University of Melbourne, Melbourne, VIC, Australia
[103] Department of Physics, The University of Michigan, Ann Arbor, MI, USA
[104] Department of Physics and Astronomy, Michigan State University, East Lansing, MI, USA
[105] B.I. Stepanov Institute of Physics, National Academy of Sciences of Belarus, Minsk, Republic of Belarus
[106] Research Institute for Nuclear Problems of Byelorussian State University, Minsk, Republic of Belarus
[107] Group of Particle Physics, University of Montreal, Montreal, QC, Canada
[108] P.N. Lebedev Physical Institute of the Russian Academy of Sciences, Moscow, Russia
[109] Institute for Theoretical and Experimental Physics (ITEP), Moscow, Russia
[110] National Research Nuclear University MEPhI, Moscow, Russia
[111] D.V. Skobeltsyn Institute of Nuclear Physics, M.V. Lomonosov Moscow State University, Moscow, Russia
[112] Fakultät für Physik, Ludwig-Maximilians-Universität München, Munich, Germany
[113] Max-Planck-Institut für Physik (Werner-Heisenberg-Institut), Munich, Germany
[114] Nagasaki Institute of Applied Science, Nagasaki, Japan
[115] Graduate School of Science and Kobayashi-Maskawa Institute, Nagoya University, Nagoya, Japan
[116] Department of Physics and Astronomy, University of New Mexico, Albuquerque, NM, USA
[117] Institute for Mathematics, Astrophysics and Particle Physics, Radboud University Nijmegen/Nikhef, Nijmegen, The Netherlands
[118] Nikhef National Institute for Subatomic Physics, University of Amsterdam, Amsterdam, The Netherlands
[119] Department of Physics, Northern Illinois University, DeKalb, IL, USA
[120] [(a)]Budker Institute of Nuclear Physics, SB RAS, Novosibirsk, Russia; [(b)]Novosibirsk State University, Novosibirsk, Russia
[121] Department of Physics, New York University, New York, NY, USA
[122] Ohio State University, Columbus, OH, USA
[123] Faculty of Science, Okayama University, Okayama, Japan
[124] Homer L. Dodge Department of Physics and Astronomy, University of Oklahoma, Norman, OK, USA
[125] Department of Physics, Oklahoma State University, Stillwater, OK, USA

[126] Palacký University, RCPTM, Olomouc, Czech Republic
[127] Center for High Energy Physics, University of Oregon, Eugene, OR, USA
[128] LAL, Université Paris-Sud, CNRS/IN2P3, Université Paris-Saclay, Orsay, France
[129] Graduate School of Science, Osaka University, Osaka, Japan
[130] Department of Physics, University of Oslo, Oslo, Norway
[131] Department of Physics, Oxford University, Oxford, UK
[132] Department of Physics, University of Pennsylvania, Philadelphia, PA, USA
[133] Konstantinov Nuclear Physics Institute of National Research Centre "Kurchatov Institute", PNPI, St. Petersburg, Russia
[134] Department of Physics and Astronomy, University of Pittsburgh, Pittsburgh, PA, USA
[135] [(a)]Laboratório de Instrumentação e Física Experimental de Partículas-LIP, Lisbon, Portugal; [(b)]Faculdade de Ciências, Universidade de Lisboa, Lisbon, Portugal; [(c)]Department of Physics, University of Coimbra, Coimbra, Portugal; [(d)]Centro de Física Nuclear da Universidade de Lisboa, Lisbon, Portugal; [(e)]Departamento de Fisica, Universidade do Minho, Braga, Portugal; [(f)]Departamento de Fisica Teorica y del Cosmos, Universidad de Granada, Granada, Spain; [(g)]Dep Fisica and CEFITEC of Faculdade de Ciencias e Tecnologia, Universidade Nova de Lisboa, Caparica, Portugal
[136] Institute of Physics, Academy of Sciences of the Czech Republic, Praha, Czech Republic
[137] Czech Technical University in Prague, Praha, Czech Republic
[138] Faculty of Mathematics and Physics, Charles University, Prague, Czech Republic
[139] State Research Center Institute for High Energy Physics (Protvino), NRC KI, Protvino, Russia
[140] Particle Physics Department, Rutherford Appleton Laboratory, Didcot, UK
[141] [(a)]Universidade Federal do Rio De Janeiro COPPE/EE/IF, Rio de Janeiro, Brazil; [(b)]Electrical Circuits Department, Federal University of Juiz de Fora (UFJF), Juiz de Fora, Brazil; [(c)]Federal University of Sao Joao del Rei (UFSJ), Sao Joao del Rei, Brazil; [(d)]Instituto de Fisica, Universidade de Sao Paulo, Sao Paulo, Brazil
[142] Institut de Recherches sur les Lois Fondamentales de l'Univers, DSM/IRFU, CEA Saclay, Gif-sur-Yvette, France
[143] Santa Cruz Institute for Particle Physics, University of California Santa Cruz, Santa Cruz, CA, USA
[144] [(a)]Departamento de Física, Pontificia Universidad Católica de Chile, Santiago, Chile; [(b)]Departamento de Física, Universidad Técnica Federico Santa María, Valparaiso, Chile
[145] Department of Physics, University of Washington, Seattle, WA, USA
[146] Department of Physics and Astronomy, University of Sheffield, Sheffield, UK
[147] Department of Physics, Shinshu University, Nagano, Japan
[148] Department Physik, Universität Siegen, Siegen, Germany
[149] Department of Physics, Simon Fraser University, Burnaby, BC, Canada
[150] SLAC National Accelerator Laboratory, Stanford, CA, USA
[151] Physics Department, Royal Institute of Technology, Stockholm, Sweden
[152] Departments of Physics and Astronomy, Stony Brook University, Stony Brook, NY, USA
[153] Department of Physics and Astronomy, University of Sussex, Brighton, UK
[154] School of Physics, University of Sydney, Sydney, Australia
[155] Institute of Physics, Academia Sinica, Taipei, Taiwan
[156] [(a)]E. Andronikashvili Institute of Physics, Iv. Javakhishvili Tbilisi State University, Tbilisi, Georgia; [(b)]High Energy Physics Institute, Tbilisi State University, Tbilisi, Georgia
[157] Department of Physics, Technion: Israel Institute of Technology, Haifa, Israel
[158] Raymond and Beverly Sackler School of Physics and Astronomy, Tel Aviv University, Tel Aviv, Israel
[159] Department of Physics, Aristotle University of Thessaloniki, Thessaloníki, Greece
[160] International Center for Elementary Particle Physics and Department of Physics, The University of Tokyo, Tokyo, Japan
[161] Graduate School of Science and Technology, Tokyo Metropolitan University, Tokyo, Japan
[162] Department of Physics, Tokyo Institute of Technology, Tokyo, Japan
[163] Tomsk State University, Tomsk, Russia
[164] Department of Physics, University of Toronto, Toronto, ON, Canada
[165] [(a)]TRIUMF, Vancouver, BC, Canada; [(b)]Department of Physics and Astronomy, York University, Toronto, ON, Canada
[166] Division of Physics and Tomonaga Center for the History of the Universe, Faculty of Pure and Applied Sciences, University of Tsukuba, Tsukuba, Japan
[167] Department of Physics and Astronomy, Tufts University, Medford, MA, USA
[168] Academia Sinica Grid Computing, Institute of Physics, Academia Sinica, Taipei, Taiwan

[169] Department of Physics and Astronomy, University of California Irvine, Irvine, CA, USA
[170] Department of Physics and Astronomy, University of Uppsala, Uppsala, Sweden
[171] Department of Physics, University of Illinois, Urbana, IL, USA
[172] Instituto de Fisica Corpuscular (IFIC), Centro Mixto Universidad de Valencia-CSIC, Valencia, Spain
[173] Department of Physics, University of British Columbia, Vancouver, BC, Canada
[174] Department of Physics and Astronomy, University of Victoria, Victoria, BC, Canada
[175] Fakultät für Physik und Astronomie, Julius-Maximilians-Universität, Würzburg, Germany
[176] Department of Physics, University of Warwick, Coventry, UK
[177] Waseda University, Tokyo, Japan
[178] Department of Particle Physics, The Weizmann Institute of Science, Rehovot, Israel
[179] Department of Physics, University of Wisconsin, Madison, WI, USA
[180] Fakultät für Mathematik und Naturwissenschaften, Fachgruppe Physik, Bergische Universität Wuppertal, Wuppertal, Germany
[181] Department of Physics, Yale University, New Haven, CT, USA
[182] Yerevan Physics Institute, Yerevan, Armenia

[a] Also at Borough of Manhattan Community College, City University of New York, New York City, USA
[b] Also at Centre for High Performance Computing, CSIR Campus, Rosebank, Cape Town, South Africa
[c] Also at CERN, Geneva, Switzerland
[d] Also at CPPM, Aix-Marseille Université and CNRS/IN2P3, Marseille, France
[e] Also at Departament de Fisica de la Universitat Autonoma de Barcelona, Barcelona, Spain
[f] Also at Departamento de Fisica Teorica y del Cosmos, Universidad de Granada, Granada, Spain
[g] Also at Departement de Physique Nucléaire et Corpusculaire, Université de Genève, Geneva, Switzerland
[h] Also at Department of Financial and Management Engineering, University of the Aegean, Chios, Greece
[i] Also at Department of Physics and Astronomy, University of Louisville, Louisville, KY, USA
[j] Also at Department of Physics, California State University, Fresno, CA, USA
[k] Also at Department of Physics, California State University, Sacramento, CA, USA
[l] Also at Department of Physics, King's College London, London, UK
[m] Also at Department of Physics, Nanjing University, Jiangsu, China
[n] Also at Department of Physics, St. Petersburg State Polytechnical University, St. Petersburg, Russia
[o] Also at Department of Physics, Stanford University, Stanford, CA, USA
[p] Also at Department of Physics, The University of Michigan, Ann Arbor, MI, USA
[q] Also at Department of Physics, The University of Texas at Austin, Austin, TX, USA
[r] Also at Department of Physics, University of Fribourg, Fribourg, Switzerland
[s] Also at Dipartimento di Fisica E. Fermi, Università di Pisa, Pisa, Italy
[t] Also at Faculty of Physics, M.V.Lomonosov Moscow State University, Moscow, Russia
[u] Also at Fakultät für Mathematik und Physik, Albert-Ludwigs-Universität, Freiburg, Germany
[v] Also at Georgian Technical University (GTU), Tbilisi, Georgia
[w] Also at Faculty of Engineering, Giresun University, Giresun, Turkey
[x] Also at Graduate School of Science, Osaka University, Osaka, Japan
[y] Also at Hellenic Open University, Patras, Greece
[z] Also at Horia Hulubei National Institute of Physics and Nuclear Engineering, Măgurele, Romania
[aa] Also at II Physikalisches Institut, Georg-August-Universität, Göttingen, Germany
[ab] Also at Institucio Catalana de Recerca i Estudis Avancats, ICREA, Barcelona, Spain
[ac] Also at Institut de Física d'Altes Energies (IFAE), The Barcelona Institute of Science and Technology, Barcelona, Spain
[ad] Also at Institute for Mathematics, Astrophysics and Particle Physics, Radboud University Nijmegen/Nikhef, Nijmegen, The Netherlands.
[ae] Also at Institute for Nuclear Research and Nuclear Energy (INRNE) of the Bulgarian Academy of Sciences, Sofia, Bulgaria.
[af] Also at Institute for Particle and Nuclear Physics, Wigner Research Centre for Physics, Budapest, Hungary.
[ag] Also at Institute of Particle Physics (IPP), Canada
[ah] Also at Institute of Physics, Academia Sinica, Taipei, Taiwan

[ai] Also at Institute of Physics, Azerbaijan Academy of Sciences, Baku, Azerbaijan
[aj] Also at Institute of Theoretical Physics, Ilia State University, Tbilisi, Georgia
[ak] Also at LAL, Université Paris-Sud, CNRS/IN2P3, Université Paris-Saclay, Orsay, France
[al] Also at Louisiana Tech University, Ruston, LA, USA
[am] Also at Manhattan College, New York, NY, USA
[an] Also at Moscow Institute of Physics and Technology State University, Dolgoprudny, Russia
[ao] Also at National Research Nuclear University MEPhI, Moscow, Russia
[ap] Also at Near East University, Nicosia, North Cyprus, Mersin 10, Turkey
[aq] Also at Ochadai Academic Production, Ochanomizu University, Tokyo, Japan
[ar] Also at School of Physics, Sun Yat-sen University, Guangzhou, China
[as] Also at The City College of New York, New York, NY, USA
[at] Also at The Collaborative Innovation Center of Quantum Matter (CICQM), Beijing, China
[au] Also at Tomsk State University, Tomsk, and Moscow Institute of Physics and Technology State University, Dolgoprudny, Russia
[av] Also at TRIUMF, Vancouver, BC, Canada
[aw] Also at Universita di Napoli Parthenope, Napoli, Italy
[ax] Also at University of Malaya, Department of Physics, Kuala Lumpur, Malaysia
*Deceased